AD743071

.....contributing to man's
understanding of the environment world

SEISMIC ANALYSIS OF THE RULISON EXPLOSION

D. G. LAMBERT
R. O. AHNER
SEISMIC DATA LABORATORY

10 APRIL 1972

Prepared for
AIR FORCE TECHNICAL APPLICATIONS CENTER
Washington, D.C.

Under
Project VELA UNIFORM

Sponsored by
ADVANCED RESEARCH PROJECTS AGENCY
Nuclear Monitoring Research Office
ARPA Order No. 1714

DDC
RECEIVED
JUN 13 1972
C

TELEDYNE GEOTECH
ALEXANDRIA LABORATORIES

Reproduced by
NATIONAL TECHNICAL
INFORMATION SERVICE
Springfield, Va. 22151

APPROVED FOR PUBLIC RELEASE; DISTRIBUTION UNLIMITED.

Neither the Advanced Research Projects Agency nor the Air Force Technical Applications Center will be responsible for information contained herein which has been supplied by other organizations or contractors, and this document is subject to later revision as may be necessary. The views and conclusions presented are those of the authors and should not be interpreted as necessarily representing the official policies, either expressed or implied, of the Advanced Research Projects Agency, the Air Force Technical Applications Center, or the U S Government.

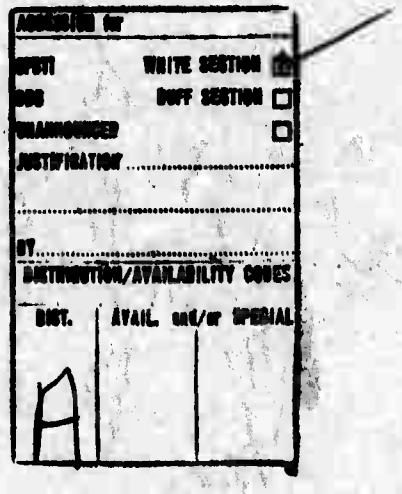

Unclassified
Security Classification

DOCUMENT CONTROL DATA - R&D

(Security classification of title, body of abstract and indexing annotation must be entered when the overall report is classified)

1. ORIGINATING ACTIVITY (Corporate author)
Teledyne Geotech
Alexandria, Virginia

2a. REPORT SECURITY CLASSIFICATION
Unclassified

2b. GROUP

3. REPORT TITLE
SEISMIC ANALYSIS OF THE RULISON EXPLOSION

4. DESCRIPTIVE NOTES (Type of report and inclusive dates)
Scientific

5. AUTHOR(S) (Last name, first name, initial)
Lambert, D.G.; Ahner, R.O.

6. REPORT DATE
10 April 1972

7a. TOTAL NO. OF PAGES
95

7b. NO. OF REFS
25

8a. CONTRACT OR GRANT NO.
F33657-72-C-0009

b. PROJECT NO.
VELA T/2706

ARPA Order No. 1714
ARPA Program Code No. 2F-10

9a. ORIGINATOR'S REPORT NUMBER(S)
255

9b. OTHER REPORT NO(S) (Any other numbers that may be assigned this report)

10. AVAILABILITY/LIMITATION NOTICES
APPROVED FOR PUBLIC RELEASE; DISTRIBUTION UNLIMITED.

11. SUPPLEMENTARY NOTES

12. SPONSORING MILITARY ACTIVITY
Advanced Research Projects Agency
Nuclear Monitoring Research Office
Washington, D.C.

13. ABSTRACT

RULISON was an underground nuclear explosion detonated to stimulate gas production as part of the PLOWSHARE program. The RULISON device was detonated at 21:00:00.1Z on 10 September 1969. It was detonated in Western Colorado, which represented a new source region, and was emplaced at a depth nearly double that of previous American explosions.

Our analysis includes study of seismograms from 18 LRSM, 2 VELA observatories, LASA, and 8 WWSS stations. When travel-times are compared to the Herrin 68 tables, interval velocities along an easterly profile generally agree with previously published findings. The most probable magnitude estimates based on amplitude data are: m_b (Gutenberg) = 4.62 and M_s (Gutenberg) = 3.99. Proposed identification criteria, developed mostly from NTS explosions and Western United States earthquakes were applied to RULISON and were compared when possible to a previous chemical explosion at CLIMAX, Colorado, and to a selected Colorado earthquake. The criteria include location, depth of focus, complexity, M_s vs m_b, energy relationships among phases, first motion, and radiation patterns.

Computed locations displaced the event from the true epicenter from 1 to 24 km depending upon the number of recording stations used and the source depth restrictions placed on the computations. Cepstral analyses produced a depth estimate of about 2.5 km for RULISON with reasonable velocity assumptions although the depth phase pP was not visible. For the 9 August 1967 earthquake cepstral analysis produced a depth estimate of 5.0 km. At present, however, we lack sufficient experience with earthquakes to say that cepstral peaks of the magnitude observed might occur for many of them. Thus, strictly speaking, the depth determination cannot be used as a discriminant. Complexities are not applicable to RULISON. M_s versus m_b and energy relationships among phases place RULISON in the explosion population; and show that there is less shear energy present for RULISON than for the 9 August 1967 Colorado earthquake. No rarefactional first motion was observed on RULISON or earthquake recordings. The long-period LQ/LR ratios can be explained by surface-wave radiation patterns from a compressional source accompanied by tectonic strain release of relative strength 0.6.

14. KEY WORDS

Travel Times
amplitude
magnitudes
location
energy relationships
depth of focus
complexity
radiation patterns
M_s versus m_b

Unclassified
Security Classification

SEISMIC ANALYSIS OF THE RULISON EXPLOSION

SEISMIC DATA LABORATORY REPORT NO. 255

AFTAC Project No.:	VELA T/2706
Project Title:	Seismic Data Laboratory
ARPA Order No.:	1714
ARPA Program Code No.:	2F-10
Name of Contractor:	TELEDYNE GEOTECH
Contract No.:	F33657-72-C-0009
Date of Contract:	01 July 1971
Amount of Contract:	$ 1,314,000
Contract Expiration Date:	30 June 1972
Project Manager:	Royal A. Hartenberger (703) 836-7647

P. O. Box 334, Alexandria, Virginia

APPROVED FOR PUBLIC RELEASE; DISTRIBUTION UNLIMITED.

SEISMIC ANALYSIS OF THE RULISON EXPLOSION

Abstract

RULISON was an underground nuclear explosion detonated to stimulate gas production as part of the PLOWSHARE program. The RULISON device was detonated at 21:00:00.1Z on 10 September 1969. It was detonated in Western Colorado, which represented a new source region, and was emplaced at a depth nearly double that of previous American explosions.

Our analysis includes study of seismograms from 18 LRSM, 2 VELA observatories, LASA, and 8 WWSS stations. When travel-times are compared to the Herrin 68 tables, interval velocities along an easterly profile generally agree with previously published findings. The most probable magnitude estimates based on amplitude data are:

m_b (Gutenberg) = 4.62 and M_s (Gutenberg) = 3.99.

Proposed identification criteria, developed mostly from NTS explosions and Western United States earthquakes were applied to RULISON and were compared when possible to a previous chemical explosion at CLIMAX, Colorado, and to a selected Colorado earthquake. The criteria include location, depth of focus, complexity, M_s vs m_b, energy relationships among phases, first motion, and radiation patterns.

Computed locations displaced the event from the true epicenter from 1 to 24 km depending upon the number of recording stations used and the source depth restrictions placed on the computations. Cepstral analyses produced a depth estimate of about 2.5 km for RULISON with reasonable velocity assumptions although the depth phase pP was not visible. For the 9 August 1967 earthquake cepstral analysis produced a depth estimate of 5.0km. At present, however, we lack sufficient experience with earthquakes to say that cepstral peaks of the magnitude observed might occur for many of them. Thus, strictly speaking, the depth determination cannot be used as a discriminant. Complexities are not applicable to RULISON.

M_s versus m_b and energy relationships among phases place RULISON in the explosion population; and show that there is less shear energy present for RULISON than for the 9 August 1967 Colorado earthquake. No rarefactional first motion was observed on RULISON or earthquake recordings. The long-period LQ/LR ratios can be explained by surface-wave radiation patterns from a compressional source accompanied by tectonic strain release of relative strength 0.6.

TABLE OF CONTENTS

TABLE OF CONTENTS (CONT'D.)

LIST OF FIGURES

LIST OF FIGURES (Cont'd.)

LIST OF TABLES

ANALYSIS OF THE RULISON EVENT

Introduction

The underground nuclear detonation RULISON was a part of the PLOWSHARE program to investigate gas stimulation. However, by virtue of its location, shot medium, and depth it provided an important set of new data relevant to underground nuclear test detection and identification. Its setting was in Western Colorado (39°21'21"N, 107°56'53"W), a completely new source region for investigation and comparison with the other source regions where underground nuclear detonations have occurred. The depth (8,431 feet) was approximately a factor of two greater than any previous underground nuclear explosion in the United States, and the shot medium (Mesa verde Sandstone) is different from previous shot media with the exception of GASBUGGY. Thus, the RULISON event provided an excellent opportunity to test the effectiveness of the proposed diagnostic criteria which were developed largely on the basis of NTS experience.

In this study we have made an evaluation of a selected set of RULISON seismic data and examined the applicability of each of the current purposed diagnostic criteria for identifying underground nuclear explosions. A more complete data analyses by the USC&GS is in preparation. In addition there was a large chemical explosion (CLIMAX) in the same general region available for comparison with RULISON.

The basic observational data are presented in a single section and saved permanently on magnetic tape at the Seismic Data Laboratory in order to provide a readily accessible data base for each aspect of this investigation as well as for future work. These data are then used in the detailed evaluation of location, source depth, and other diagnostic parameters for the RULISON event as compared to other underground nuclear detonations and earthquakes.

BASIC OBSERVATIONS AND MEASUREMENTS

Tabulated data

Epicenter data for the nuclear event RULISON are given in Table I. Data for 28 stations are presented in Table II. These include travel-times for observed short-period phases: P, Pg, and Lg. Maximum zero to peak amplitudes (A/T) and corresponding periods for short-period and long-period phases; and body-wave (m_b and m_e) magnitudes and surface-wave (M_s and M_s^c) magnitudes at those stations for which they could be computed.

The stations listed include 18 LRSM stations, 2 VELA observatories and 8 WWSS stations. The stations are listed in order of increasing distance from the RULISON epicenter. The geographic coordinates and elevations for these stations are given in Appendix 1. Figure 1, shows the event location and the LRSM and VELA station network.

Instrumentation

The LRSM, VELA and WWSS stations consist of three component short-period and long-period instrumentation. Pertinent recording information for these stations is given in Appendix 2. Relative magnification curves for all these networks are given in Appendix 3.

Reduced travel-times

Reduced travel-times are shown in Figure 2 relative to Herrin 68 times. We also show the Pn and P velocities which fit the data. These indicated velocities are used in conjunction with relative Pn and P amplitudes for magnitude estimates according to Evernden (1967) and are discussed in the magnitude section.

Amplitudes

Figures 3 through 7 are plots of maximum amplitude (zero to peak A/T) of Pn, P, Pg, Lg, LQ, and LR. For the short-period Pn and P phases, the maximum peak-to-peak excursion within the first few cycles of motion of the phase was measured, halved, and

divided by the period of the measured amplitude cycle to obtain zero-to-peak A/T. For both the short and long-period Pg, Lg, LQ, and LR phases the maximum peak-to-peak excursion visible on the record was measured, halved, and divided by the period to again obtain a zero-to-peak A/T value. Further, Lg and LQ measurements were made from the records of the horizontal instrument most nearly normal to the direction of the propagating wave.

The expected attenuation rates for Pn and P are indicated with the amplitudes on Figure 3. These are discussed in more detail in the Magnitude section. Attenuation rates of R^{-3} fitted visually for Pg and Lg data are shown in Figures 4 and 5. For LQ we visually fitted a slope of -1.66 through the data points, Figure 6. In Figure 7, LR amplitudes, we show two slopes of -1.16 and -1.66 for distances less than 15° and a slope of -1.66 for distances greater than 15°. These slopes are based on the surface wave magnitude estimates and are discussed in more detail in the Magnitude section.

In general, the Pg, Lg, and LQ amplitude data conform to the expected attenuation rates.

Magnitudes

Body-wave magnitudes are estimated in this report in two ways for stations in the distance range 2°-100°.

$m_b = \log A/T + B$ (Gutenberg and Richter 1956)

where

A = maximum zero to peak ground motion (millimicrons) of the Pn or P phase within the first three or four cycles,

T = apparent period of maximum ground motion (seconds),

B = distance correction factor.

The distance correction factors from 16° to 100° were taken from Gutenberg and Richter (1956). The VELA Seismological Center (VSC)

projected this curve back to 10° and assumed an inverse-cube relationship for the amplitude decay of the Pn wave from 10° to 2°. These factors are listed in Appendix 4.

Gutenberg and Richter's definition of body wave magnitude at teleseismic distances is accepted by practically all seismological organizations as the standard; however, Evernden (1967) shows that for distance less than 20° it is necessary to adjust the distance correction factor in their formulation for the Nevada Test Site. Evernden's formulas used in this report are as follows:

$$m_{7.9} = -7.55 + 1.21 \ (\log \ (A/T) + 3.04 \ \log\Delta)$$

$$m_{8.5} = -3.27 + \log \ (A/T) + 2 \ \log\Delta$$

where

Δ = distance in kilometers.

Application of these formulas are based on the appropriate velocites and relative amplitudes of P (Figures 2 and 3). In addition in Figure 3 we show what the amplitudes should be, for the various magnitude determinations relative to m_b (Gutenberg, $\Delta>16°$) = 4.62.

It should be noted that the Evernden formulation of $m_{8.1}$ was not used in these estimates. Even though the travel-times for LAO, TUC, and BP-CL show an apparent 8.1 km/sec velocity, these stations do not correspond to the appropriate region or path indicated by Evernden for this correction and; therefore, $m_{7.9}$ was used for the magnitude estimates. CR2NB could be either an $m_{8.1}$ or $m_{8.5}$ according to Figure 2; however, the amplitude shown in Figure 3 indicates that an $m_{8.5}$ would provide a better estimate with respect to the teleseismic magnitude estimate. The signals for LON and COR appear to travel at the 7.9 km/sec velocity but the amplitude at COR is large and consequently the $m_{8.5}$ is applied at this site. SJ-TX and WQ-IL show an apparent velocity of about 10.5 km/sec; however, the amplitudes indicate that $m_{8.5}$ provides the better magnitude estimates. We show all magnitude estimates in Table I and Figure 8.

On the basis of Figures 3 and 8, the best body-wave magnitude estimates are (Gutenberg $\Delta>16°$) m_b = 4.62 and the adjusted m_b = 4.59. However, due to the uncertainties, noted above, for applying Evernden's corrections, the most acceptable magnitude estimates is m_b (Gutenberg $\Delta>16°$) = 4.62.

Calculation of the surface-wave magnitude for RULISON is by the method of Gutenberg (1945) for all distances. In addition we computed M_s for distances less than 15° by a method of Von Seggern (1969).

$M_s = \log A_H + 1.656 \log + 1.818 + C + D$, Gutenberg (1945),

where

A_H = 0.5 peak to peak amplitude in microns at T = 20 seconds for the horizontal radial component of Rayleigh wave.

$1.656 \log\Delta$ = distance correction factor with Δ measured in degrees. This correction is limited to Δ between 15° and 130°.

C = Site correction factor.

D = Depth of source, azimuthal correction, etc.

For this study we set C and D equal to 0 and use the following relation adopted by Geotech (1964):

$M_s = \log (A_z/T) + 1.66 \log\Delta - 0.18$ where (A_z) = peak to peak amplitude in mμ and T = corresponding period in seconds for the vertical component of the Rayleigh wave and Δ = distance in degrees.

These two formulas are identical at T = 20 seconds. The Geotech formula does not consider ellipticity (A_H/A_Z); however, for periods of 15 to 17 seconds and an ellipticity of 0.8 the variance of M_s (Geotech) to M_s (Gutenberg) is $\pm$ 0.03 magnitude units. Since small magnitude events traversing continental paths have their maximum measurable amplitudes spanning this range of periods, the formula is compatible with Gutenberg's.

It is important to note that this magnitude estimate gives a magnitude of 0.18 less than the USC&GS and Bashams estimates. Their formulas are as follows:

USC&GS, $M_s = \log (A/T) + 1.66 \log\Delta + 3.3$

where

Δ = distance in degrees

and

A/T = amplitude, zero to peak in μ/sec;

Basham, $M_s = \log(A/T) + 1.66 \log\Delta + 0.3$

where

Δ = distance in degrees

and

A/T = amplitude, zero to peak in mμ/sec.

Since Gutenberg's formulation is for distances greater than 15°, we use a modified distance correction factor for surface waves for those less than 15° (Von Seggern, 1969) derived by the use of Rayleigh wave amplitude measurements from 29 Nevada Test Site explosions.

The formulation is as follows:

$M_s^C = \log(A/T) + 1.16 \log\Delta + 0.74.$

These estimates are tabulated in Table I and shown in Figure 9. Further, in Figure 7 we show the Rayleigh amplitudes and the expected amplitudes for $M_s^C = 4.18$, $M_s = 3.99$ (Δ>15°) and $M_s = 3.84$

for all stations; however, the scatter of the data makes it difficult to determine which slope best fits the data for distances less than 15°. From Figure 9, it is clear that M_s^c formulation over corrects and the Gutenberg M_s formulation applied to distances less than 15° under estimates the surface wave magnitude relative to those estimated at teleseismic distances. Therefore, we conclude that the best magnitude estimate is M_s (Gutenberg $\Delta>15°$) = 3.99.

The following table summarizes the magnitude estimates for RULISON. The word "Adjusted" preceding the magnitude symbol indicates the nearer station magnitudes are corrected using either Evernden or Von Seggern's formulas and are included in the average. The m_b or M_s for "all distances" includes in the average, the magnitudes determined by the use of VSC distance correction factors for m_b and Gutenbergs formula for M_s for distances less than 15°.

(All Distances)	m_b = 4.90 ± 0.62	for 27 stations,
(Gutenberg, $\Delta>16°$)	m_b = 4.62 ± 0.36	for 11 stations,
Adjusted	m_b = 4.59 ± 0.35	for 27 stations,
(All Distances)	M_s = 3.84 ± 0.39	for 26 stations,
(Gutenberg, $\Delta>15°$)	M_s = 3.99 ± 0.44	for 12 stations,
Adjusted	M_s = 4.09 ± 0.36	for 26 stations.

RULISON seismograms

Various profiles consisting of LRSM and VELA station seismograms for RULISON are shown in Appendix 8. Most of the indicated profiles are not profiles in terms of a continental linear array type due to the paucity of stations and lack of azimuthal alignment. However, the East profile consists of six LRSM stations (CR2NB, BY-IO, WQ-IL, GZ-OH, AS-PA, and PJ-PA) which are about equally spaced between 957 and 2757 kilometers and on an 80° azimuth from RULISON. Included also, is HN-ME even though this station is not exactly on the profile (Figure 1).

In Figure 10 we show the seismograms for the East profile which indicate a Pn velocity of 7.9 km/sec and later P velocities

of 8.4, 10.4, and 13.1 km/sec. These velocities appear reasonable when compared to the NE profile from BILBY, Archambeau et al (1969) and data from the Lake Superior study by Glover and Alexander (1970). Further the 8.4 km/sec lies between the 8.32 and 8.52 km/sec for the ESE and NNE profiles from GASBUGGY (Rasmussen and Lande, 1968). Thus the velocities seen along this profile are as expected.

Summary

For the RULISON event we have obtained the travel-time and amplitude data for 18 LRSM stations, 2 VELA observatories, LASA, and 8 WWSS stations. These are saved on magnetic tape at the Seismic Data Laboratory. In addition, the seismograms for the LRSM and VELA observatory stations were digitized and saved for subsequent analysis.

We conclude that the magnitude estimates most appropriate for RULISON are as follows:

(Gutenberg, $\Delta>16°$) $m_b = 4.62 \pm 0.36$ for 11 stations,

(Gutenberg, $\Delta>15°$) $M_s = 3.99 \pm 0.44$ for 12 stations.

IDENTIFICATION CRITERIA APPLIED TO RULISON

Introduction

One of the main objectives of the VELA program has been to develop seismological criteria for distinguishing between underground nuclear explosions and earthquakes. Prior to RULISON, considerable effort had been devoted to establishing diagnostic criteria making use primarily of Nevada Test Site (NTS) explosions, nearby earthquakes, and earthquakes from both Western United States and elsewhere. The RULISON explosion provided an excellent opportunity to determine the general applicability of these diagnostic criteria to a new source region. A chemical explosion was detonated in the same general region as RULISON on 23 May 1967 at Climax, Colorado; however, the seismic energy released was not sufficient to be detected at teleseismic distances thereby seriously limiting the application of the diagnostic criteria for that event. Wherever possible, these criteria have been applied to the CLIMAX explosion and to a selected Colorado earthquake as well as to RULISON. The earthquake occurred on 9 August 1967 and was located by USC&GS approximately 280 km east of RULISON. This earthquake was selected on the following basis from the Preliminary Determinations of Epicenters (USC&GS) listing, 1) magnitude approximately equal to that of RULISON, 2) a shallow event and, 3) location as near to RULISON epicenter as possible and fitting the above requirements. The 9 August 1967 earthquake, along with other Denver earthquakes at or near the Rocky Mountain Arsenal (RMA) well, is documented and discussed by Major and Simon, 1968. Further, the location used for this study was determined with depth restrained to 5 km and with travel-times from 43 WWSS and VELA stations, USC&GS Earthquake Data Report, 50-67. (See Appendix 5 for the event spatial and temporal parameters.)

Since we know the location, origin time, and size of RULISON it is important to show the degree to which RULISON revealed itself seismologically. Therefore, in this section we discuss the following diagnostic criteria as applied to RULISON: (1) location, (2) depth of focus, (3) complexity, (4) M_s versus m_b, (5) energy relationships among phases, (6) radiation patterns, and (7) other criteria.

Location

P-wave arrival times were read from all available VELA observatories and LRSM stations film seismograms, and from USC&GS WWSSN film chips. Where the film was not available, USC&GS arrival times reported in the "Earthquake Data Reports" were used in order to obtain a network of stations with the best distance range and azimuth aperture. Location according to Chiburis (1966) employing the Herrin 1968 travel-time tables was used for all the location determinations.

RULISON, when located using 66 stations with depth free to vary, shifted 6 km on an azimuth of 31° from the actual location with a depth estimate of 41 km. Using a subset of 33 stations having about the same azimuthal distribution, the event was mislocated about 10 km along an azimuth of 202° with depth estimated at 59 km.

Results of the cepstral analysis revealed the source at the expected depth. Accordingly, RULISON was relocated with depth restrained using the 66 station set, which produced an error of 1 km along an azimuth of 263°. In the case of the 33 station net, the epicenter shifted 24 km along an azimuth of 208° from the true epicenter.

The earthquake was located using all ten available arrival times and by restraining depth to the USC&GS determined value of 5 km. It shifted 27 km on an azimuth 10° from the input USC&GS location. The ten stations that recorded the earthquake also recorded RULISON. Using this ten station network, RULISON shifted 16 km on an azimuth of 38° from its true location. A comparison of location results is presented in Table III. The CLIMAX explosion was not located because there were no teleseismic data.

Thus, we see that location estimates for the RULISON event are highly variable (1 km to 24 km) depending on the recording stations and travel times used and the source depth restrictions placed on the computations.

It is desirable to determine the degree to which the

travel-times derived from one event are valid for use in locating another. Accordingly, travel time corrections were determined (Chiburis, 1968b) and the events were relocated with the network of ten common stations. Using the corrections determined from the earthquake, RULISON shifted 15 km on an azimuth of 172°, yielding no improvement in accuracy. We would expect a standard deviation of less than 0.5 seconds for a good solution with corrected travel times; however, the standard deviation of the travel time residuals was only reduced from 1.49 seconds for the uncorrected solution to 1.07 seconds for the corrected solution with a corresponding decrease in the standard 95% confidence ellipse from 4607 km^2 to 2396 km^2. Both ellipses comfortably contain the actual epicenter. The fact that the location did not improve is not surprising when one considers that the two events are separated by a distance of more than 275 km including the Rocky Mountains. Locating the earthquake with travel times determined from RULISON produced a shift to 14.42 km on an azimuth of 348.7°, which is nearly a mirror image, as expected, (Chiburis, 1969) of the shift obtained for RULISON with the earthquake travel time corrections. That the standard deviation of errors did not decrease significantly demonstrates that that the travel time corrections used are not appropriate. The conclusion is that RULISON and the Colorado earthquake are not in the same travel-time region. Although the area in the vicinity of RULISON is now calibrated for locating subsequent events, the area in the vicinity of the earthquake remains unknown regarding suitable corrections for accurate locations.

Depth of focus

Since the depth of focus for explosions is presently limited by drilling technology to shallow depths (less than 10 km), and since most earthquakes are known to occur at greater depths than this, depth determination is an important identification criterion. Events determined to be significantly deeper than a few kilometers can be classified as earthquakes. Determination of the focal depth is aided by the fact that many earthquakes have observable depth phases (pP, sP, etc.); explosions, however, are generally too

shallow to produce visually distinct depth phases on the seismogram. The RULISON event, for example showed no depth phase on the indivdual recordings.

For shallow events the pP and P phases overlap. However, if their waveforms are similar, the fact that an echo exists in the P coda may possibly be detected by the presense of periodic nulls in the P spectra. Cohen (1969) found nulls in P spectra for several explosions due to the interference of the pP and P phases. By computing the spectrum of the spectrum (the cepstrum), it was possible in some cases to estimate objectively the depth-phase delay time. The dot product of the cepstrum and the pseudo-autocorrelation functions shows the depth phase if present as a negative correlation peak.

RULISON and the 9 August 1967 earthquake are two shallow events which are deep enough to estimate their depths by the spectral null method. We would expect RULISON (2.6 km depth) to generate a pP phase 1.5 seconds (± 20% depending upon the overburden velocity) behind the P phase, with spectral nulls every 0.7 Hz. We would expect the earthquake at 5.0 km depth to generate a pP phase 2.8 seconds behind the P phase, and with spectral nulls every 0.4Hz.

The best evidence of regular spectral nulls and of the prominent negative dot-product correlation peaks are in the LASA data Figures 11a, 11b, and 11c. The data show Pn spectra (0 to 4 Hz) for RULISON recorded on the center seismometers of 18 LASA subarrays. The dot product of the pseudo-autocorrelation and the cepstrum accompanies each spectrum. The spectra are arranged in order of increasing distance from RULISON.

The sum spectrum (bottom, Figure 11c) gives the clearest indication of the spectral nulling occurring every 0.7 Hz interval. In addition, the negative correlation peak at 1.45 seconds is the most prominent feature on the dot product function. These results agree with the expected values for RULISON. Many of the individual spectra show some of the spectral nulls, but none of them as clearly as the summation spectra. In addition, many of the individual dot product functions show the negative correlation at the correct

delay but also display other more prominent positive and negative correlation peaks not associated with the expected depth phases.

LASA data for the 9 August 1967 earthquake is not available for comparison with these LASA results for RULISON.

Sum spectra from LRSM stations for both RULISON (17 stations at Pn and P distances) and the 9 August 1967 earthquake (15 stations at all distances) are shown in Figure 18. These spectra are log plots of the sums shown in Figures 12c and 13c. Spectral nulls, indicated for both events, are more prominent for the earthquake spectrum. Note, too, that since the earthquake is deeper, more spectral nulls are observed in the signal band of 0.5 Hz to 4.0 Hz.

Figures 12a, 12b, and 12c show individual and summation spectra and dot product traces for RULISON obtained from recordings at stations at all distances. The regular spectral nulls and negative dot-product correlation peaks are decidedly less prominent than those shown on the LASA data.

Figures 13a, 13b, and 13c show individual and sum spectra, and dot product traces from the 9 August 1967 earthquake for 15 LRSM stations at all distances. Again, these LRSM stations do not exhibit the regular spectral nulls and prominent negative correlation peaks as well as does the LASA data for RULISON.

Conclusions

1) Regular spectral nulls and negative correlation peaks were seen for both events where expected at several stations.

2) Not all stations show the regular spectral nulls and correlation peaks.

3) Nearly all stations showed other spectral nulls and negative correlation peaks besides those correlated with depth phases.

4) LASA data exhibited the clearest estimates of depth through the analysis of regular spectral nulls and dot-product correlation peaks.

5) This method requires summation spectra or correlations from several traces to cancel path and site effects. Multichannel

stations like LASA are helpful in this way since the structure varies across the array.

6) RULISON showed four spectral nulls across the short-period signal band (0 5 Hz to 3.0 Hz). A fewer number of nulls would make recognition of regular spectral nulling difficult. Thus, events with depths shallower than RULISON would be difficult to determine by any variation of this method.

8) The 9 August 1967 earthquake showed six regular nulls across the signal band. As a consequence, the depth phase for this event was easier to detect on LRSM station data than was RULISON's.

9) The method requires good signal-to-noise ratios.

Complexity

The generally agreed upon requirements for the satisfactory application of complexity as a diagnostic, (large teleseismic distances, good signal to noise ratios) could not be satisfied because of a lack of stations. However, the complexities for RULISON and the 9 August 1967 earthquake are shown in Figure 14 plotted as a function of distance. Both events have similar complexity values (F_c). However, for common stations; LC, KN, SJ, PG, and NP the earthquake has greater values of F_c except at NP where the noise for the quake is so high that one can hardly see the signal. Basically, the signal to noise ratio is inadequate to apply this criterion.

M_s versus m_b

Since body wave and surface wave magnitude estimates give some measure of the source type and/or depths by minimizing azimuthal and distance effects, the relative excitation of body and surface-wave energy is an important diagnostic in that most earthquakes have larger surface-wave magnitudes than explosions with comparable body-wave magnitude. RULISON by virtue of its new location and greater depth provided an opportunity to determine the effectiveness of this criterion as compared to nuclear explosions from the Nevada Test Site (NTS) and earthquakes from the Western United States.

Figure 15 shows surface-wave magnitudes with the Gutenberg formula applied to all distances, relative to Adjusted body-wave magnitudes (Adjusted m_b), Evernden (1967), for 39 Nevada Test Site (NTS) explosions. For comparison we also include twelve earthquakes from Western United States with magnitude estimates determined by Basham (1969) using the Canadian station network. Since the Canadian seismological network includes three stations at distances less than 15° from the Nevada Test region, we excluded 16 other earthquakes with an m_b determined by nine or less stations for the purpose of minimizing the near distant station effects. Therefore, Basham's m_b should be comparable to the Adjusted m_b.

If these earthquakes are representative of the area then they fall in a different population than the explosions. For 26 NTS explosions observed teleseismically, Basham obtained a least squares magnitude relationship of $M_s = 1.24\ m_b - 1.76$. We obtain $M_s = 1.21\ m_b - 1.89$ for 39 explosions including regional and near regional observations. Therefore, the latter $M_s::m_b$ relationship appears valid for NTS; however, the separation between our explosion and Basham's earthquake populations is enhanced. This is largely due to the differences in the M_s formulation (0.18) between Basham and Geotech (see Magnitude section). Also included in the figure, but not in the least squares determination, are the RULISON, GASBUGGY and CLIMAX explosions, the 23 January 1966 New Mexico and 9 August 1967 Colorado earthquakes.

As shown in Figure 15, M_s versus Adjusted m_b the three explosions, all from different source regions, fall into the NTS explosion population and the two earthquakes fall in the group of other earthquakes in Western United States. Thus had we not known in advance that these events were explosions, we would certainly have decided that they were suspicious on the basis of this criterion alone.

ARZ and ERZ (area under the Rayleigh wave and total energy contained in the Rayleigh wave), Turnbull and Lambert (1968), relative to body-wave magnitude are essentially measures of $M_s - m_b$. Figure 16 and 17 show ARZ and ERZ plotted versus (Gutenberg) magnitude (m_b) for earthquakes and explosions from different regions. The term (Gutenberg m_b) is not a true Gutenberg magnitude but includes data for distances less than 16° corrected according to VSC, (see Magnitude section). These figures are taken from the LONG SHOT report, Lambert et al (1970) and the event descriptions are listed in Appendix 5. The results place RULISON clearly in the explosion population.

Thus, on the basis of these results RULISON would fall in the general explosion population as defined by previous NTS (and other) explosions and earthquakes. This does not necessarily mean that we have identified RULISON as an explosion at this point but rather that it would not have been dismissed as being an earthquake.

Energy relationships among phases

The previous section (M_s versus m_b) shows that a difference in excitation of body and surface waves exists between RULISON and the 9 August 1967 Colorado earthquake. The purpose of this section is to examine these differences in more detail. Various authors have shown that more long-period energy is released by earthquakes than by explosions having equivalent m_b; however, the spectra of earthquakes seen at far-field are influenced by source orientation, depth, and distance (see Von Seggern and Lambert, 1969, for the bibliography and summary discussion). Therefore, we discuss (1) P-wave spectra, (2) Rayleigh-wave spectra, (3) spectral energy ratios, and (4) relative shear energy.

(1) P-wave spectra -

Figure 18, discussed in the Depth of Focus section is a log plot of the sum of 17 stations for RULISON and 15 stations for the 9 August 1967 earthquake shown in Figures 12c and 13c respectively. From this display the earthquake does show more long-period energy than the explosion. This is in qualitative agree- with most results of other works in the field of short-period spectral ratios.

(2) Rayleigh wave-spectra -

Rayleigh-wave energy spectra are computed by a sine-cosine Fourier transform for a signal velocity window of about 3.60 km/sec to 2.5 km/sec and a noise sample of equal length. The noise spectrum is subtracted from the signal spectrum. The resultant energy spectrum is then reduced to an amplitude spectrum which is further corrected for static magnification and system response. Figures 19a and 19b show Rayleigh-wave spectra of five common stations (KN-UT, LC-NM, SJ-TX, RK-ON, and NP-NT) for RULISON and 9 August 1967 earthquake. Fourteen additional RULISON spectra are shown in Appendix 6.

In Figure 20 we show summed and normalized energy spectra for these same five common stations for each event. This process of

summing Rayleigh-wave spectra smears out the spectrum because of frequency dependent attenuation with distance. Since the RULISON and earthquake epicenters are separated by a large distance (280 km) this method could also introduce large path effects. However, it is interesting to note that the spectral sums are very similar in shape between 0.02 and 0.076 cps. The earthquake does show more energy in the low (0.02 to 0.38 cps) and high (0.076 to .10 cps) frequency portions, however. This result is discussed more quantatively in the next section.

(3) Energy ratios -

Von Seggern and Lambert (1969) studied the Rayleigh wave spectral dependency as functions of magnitude, source type, and distance both theoretically and empirically. The theory indicates, for explosions, that the shape of the source spectra should not change with magnitude in the spectral band of interest (T = 10 to 50 seconds); thus, ratios of total energy between adjacent bands of frequency should not change with magnitude. However, due to different source types, layering response and depths, earthquake ratios can be greater than, less than, or equal to those of explosions. Empirical evidence supports these theoretical findings.

Mean ratios for RULISON, the 9 August 1967 Colorado earthquake and the 23 January 1966 New Mexico earthquake are computed as follows:

$$\bar{R}_i = \frac{1}{n} \sum_{m=1}^{n} \left[\int_{f_1}^{f_2} E_m(f)df \Big/ \int_{f_2}^{f_3} E_m(f)df \right]$$

where $\bar{R}_i$ equals the average energy ratio for n stations recording one event and E_m is the energy spectra at station m. For $\bar{R}_1$ we let

$f_1 = 1/T_1$ and $T_1 = 48$ seconds,

$f_2 = 1/T_2$ and $T_2 = 22$ seconds,

$f_3 = 1/T_3$ and $T_3 = 15$ seconds.

For $\bar{R}_2$, we change only T_3 from 15 to 10 seconds ($T_3 = 10$ seconds).

Figures 21 and 22 show $\bar{R}_1$ and $\bar{R}_2$ plotted versus Rayleigh-wave magnitude and the event descriptions are listed in Appendix 7. The Rayleigh-wave magnitude is determined from the spectra used in the above energy ratio analysis. For these estimates the maximum amplitude is picked from the spectra between T = 17 and 23 seconds and corrected according to Gutenberg M_s formulation applied to all distances. Therefore these magnitudes do not correspond to those determined from film analysis. It should be emphasized that, basically, the ratios are independent of magnitude, but only if the signal to noise ratio is high enough to allow a valid analysis.

In Figure 21, $\bar{R}_1$ (T_3 = 15 sec) determined from 19 stations for RULISON is clearly in the explosion population. Similar results for $\bar{R}_2$ (T_3 = 10 sec) are obtained in Figure 22.

$\bar{R}_1$ determined from 14 stations for the Colorado earthquake is greater than $\bar{R}_1$ for RULISON and places it in the earthquake-population while $\bar{R}_2$ for the earthquake places it in the mixed explosion-earthquake population. Similar results using 14 stations were obtained for the New Mexico earthquake. However, Von Seggern and Lambert (1969) indicate that for events with M_s greater than 3.0 and an average station network distance greater than 1000 km, $\bar{R}_1$ (T_3 = 15 sec) is more reliable as a diagnostic than $\bar{R}_2$ (T_3 = 10 sec). The average station network distances for these three events ranged from 1700 to 2000 km.

Therefore, for RULISON, $\bar{R}_1$ the preferred diagnostic, shows that the Rayleigh wave spectra in the T = 15 to 50 second band is similar to other explosions.

(4) Relative shear energy -

Earthquake source mechanisms by virture of their physical configuration should produce more shear energy than compressive source mechanisms such as explosions. Thus, we look at relative Lg and Love wave amplitudes for the 9 August 1967 earthquake and RULISON.

The average ratio of Lg earthquake amplitudes to Lg RULISON amplitudes is 6.62 and the average ratio of Love earthquake

amplitudes to Love RULISON amplitudes is 6.58.

Therefore the earthquake has more shear energy than RULISON, an equivalent magnitude explosion. However, additional data from many Colorado earthquakes will be needed to ascertain whether this is typical or atypical of this region. Moreover, there is no well accepted discriminant function for this ratio against which to test these two data points.

Radiation patterns

Various authors have shown that differences in radiation patterns between earthquakes and explosions should exist. Since path and site effects greatly influence body-wave amplitudes such that definitive radiation patterns are rarely possible, we look at only the direction of first motion for P.

For RULISON and the Colorado earthquake (9 August 1967) there appeared to be no distinct rarefactional first motion; however, the quality of the seismograms prevents any reliable determination of first motion. Thus, neither the earthquake nor RULISON, could be dismissed as an earthquake.

Studies by Toksoz et al (1965) and Toksoz and Clermont (1967) have shown that observations of non-circular radiation patterns of surface waves for the nuclear explosions, HARDHAT, HAYMAKER, SHOAL, and BILBY can be explained in terms of a compressional source accompanied by the release of tectonic strain.

For the theoretical aspects and procedural considerations of this study we reference Toksoz and Clermont (1967) and show formula 7 in the above paper.

$$\frac{|U_L|}{|U_{Rz}|} = \frac{F k_L^{\frac{1}{2}} A_L \cos 2\theta}{(1+F \sin 2\theta) A_R k_R^{\frac{1}{2}} (\dot{u}_o^*/\dot{w}_o)} \exp\left[-r(\gamma_L - \gamma_R)\right]$$

U_L = far-field displacement of Love waves,

U_{Rz} = far-field displacement of Rayleigh waves,

F = relative strength of the double-couple,

$\cos 2\theta$ = azimuthal dependence of the Love wave radiation for the double-couple,

$\sin 2\theta$ = azimuthal dependence of the Rayleigh wave radiation for the double-couple,

k_L, k_R = wave numbers for Love and Rayleigh waves,

r = radial distance,

γ_L, γ_R = Love and Rayleigh wave attenuation coefficients,

A_L, A_R = the medium response for Love and Rayleigh waves due to a vertical force,

u_o, w_o = the components of particle velocity at the surface.

We determined A_L, A_R, k_L, k_R, and $(\dot{u}_o^*/\dot{w}_o^*)$ using Harkrider's program (1964) for an average structure of the Western United States as given by Alexander (1963). These parameters were determined for a period (T) of 13.0 seconds since most of the observed peak amplitudes of the Love and Rayleigh waves for RULISON were near this value (Table II).

Figure 23 shows all possible data of U_L/U_R for RULISON and also the theoretical radiation pattern based on a strike plane of the double-couple system, $\theta = 24°$, and a relative strength (F) of the double-couple to explosion of 0.60.

The strike angle is normal to the strike of the tectonic features in the vicinity of the RULISON epicenter (Figure 24). Toksoz indicates that the relative strength (F) seemingly depends upon the properties of the source medium and cites the following:

(1) GNOME and SALMON (salt), SEDAN (loose aluvium); f = 0.0.

(2) HAYMAKER (allivium); F = 0.333.

(3) BILBY (tuff); F = 0.47.

(4) SHOAL at a relatively greater depth in granite; f = 0.90.

On this basis alone the F = 0.60 obtained for RULISON, perhaps appears greater than expected. It is possible that depth and the immediate stress field as well as medium would influence this value.

A further consideration of importance to the identification problem is a comparison of Love to Rayleigh wave amplitude ratios between RULISON and 9 August 1967 Colorado earthquake. Figure 25 shows the LQ/LR amplitude ratios for the Colorado earthquake. Even though we did not determine the earthquake double-couple parameters, it is evident that the differences are dramatic, as compared to RULISON both in radiation pattern and magnitude of ratios. The average LQ/LR amplitude ratio for RULISON is 0.52 and for the earthquake 3.48. Major and Simon (1968) indicate right lateral fault movement determined from RMA close-in strainmeter records for the 9 August 1967 earthquake. Further, the event originated at a depth of 5.0 km about 2.7 km north and 4.6 km west of the RMA well and propagated N70°W for a distance of about 10 km with a velocity of about 3.0 km/sec.

Thus, it is clear that the two events have distinctly different source mechanisms; however, additional data from many Colorado earthquakes will be needed to ascertain whether this earthquake is typical or atypical of this region.

Other criteria

Seismic events detected from aseismic regions and far from known nuclear test areas, are ones that would naturally be subjected to further study for the purpose of identification. For such events the presence or absence of aftershock activity would also be of considerable importance.

RULISON occurred in northern Colorado away from a known test region. The USC&GS, PDE listing was searched for events occuring in a 2° (latitude and longitude) area around the RULISON epicenter between 9 August 1966 and 1 January 1970. No seismic events were reported except RULISON (Figure 26). Further, from this listing and film analysis, no aftershocks were observed. In addition, the origin time, as determined from the location results, Table III,

is within 2.5 seconds of the 21:00:00.0Z hour. In contrast, a similar 2° area was studied for the 9 August 1967 earthquake and 14 events were reported. However, all but one of these events should also be considered suspicious because of the reported shallow depths (5 km) and close spatial grouping, near the RMA well. Table IV and Figure 27.

Thus, RULISON is located in an aseismic uncommon test region with an origin time of 21:00:00.0Z.

Summary and conclusions

The following table summarizes the results of applying the various discriminants discussed above to RULISON.

SUMMARY OF RULISON DIAGNOSTICS

Identification criterion	Characteristic of an explosion?	Comments
Depth of Focus	Yes (?)	Unconstrained location for RULISON gives a depth estimate of 41 km. No depth phases are observed however, cepstrum analysis gives a depth of about 2.5 km (actual: 2.57 km).
Complexity	No	Complexity is not applicable to the data available for RULISON.
$M_s::m_b$	Yes	Compared with observations for shallow quakes and explosions from western United States, RULISON clearly falls into the explosion population. RULISON ARZ and ERZ values also fall into the explosion population when compared to events from many different seismic regions.
Energy Relationships	Yes	P and Rayleigh-wave spectral estimates show more LP energy for the 9 August 1967 quake than for RULISON. LP spectral splitting shows that RULISON is similar to explosions from NTS and other regions. Earthquake Lg and LQ to RULISON Lg and LQ amplitudes, show more shear energy present for the 9 August 1970 quake than for RULISON.
First Motion	No	No distinct rarefactional first motions are observed for RULISON or the 9 Aug 67 earthquake; however, the quality of the seismograms prevent any reliable measure of first motion.
Radiation Patterns	Yes (?)	LQ/LR ratios for RULISON can be explained in terms of a compressional source accompanied by the release of tectonic strain.
Other Criteria	Yes (?)	RULISON is located in aseismic, uncommon test region with an origin time of 21:00:00.0Z.

REFERENCES

Alexander, S.S., 1963, Surface wave propagation in the western United States: Ph.D. thesis, California Institute of Technology, Pasadena, California.

Analyst's handbook, 1964, Report No. 64-51, Geotechnical Corp., Garland, Texas, 20 May.

Archambeau, C.B., Flinn, E.A., and Lambert, D.G., 1969, Fine structure of the upper mantle, Teledyne Geotech, Seismic Data Laboratory, Report No. 232.

Basham, P.W., Canadian magnitudes of earthquakes and nuclear explosions in southwestern North America, Geophys. J.R. Astr. Soc., v. 17, p. 1.

Chiburis, E.F., 1968a, Precision location of underground explosions using teleseismic networks and predetermined travel-time anomalies, Teledyne Geotech, Seismic Data Laboratory Report No. 214, 1 March.

Chiburis, E.F., 1968b, LASA travel time anomalies for 65 regions computed with the Herrin travel-time table, November 1966 version, Teledyne Geotech, Seismic Data Laboratory, Report No. 204.

Chiburis, E.F., 1966, Relative travel-time anomalies at LASA and the location of epicenters using "SHIFT", Teledyne Geotech, Seismic Data Laboratory Report No. 147.

Chiburis, E.F. and Ahner, R.O. 1969, A location and travel-time study of Aleutian Islands explosions and earthquakes, Teledyne Geotech, Seismic Data Laboratory Report No. 239.

Climax, 1964, Seismic Data Laboratory Report No. 106.

Cohen, T.J., 1969, Determination of source depth by spectral, pseudo-autocovariance and cepstral analysis, Teledyne Geotech, Seismic Data Laboratory Report No. 229.

Evernden, J.T., 1967, Magnitude determination at regional and near-regional distances in the United States, Bull. Seismol. Soc. Am., v. 57, p. 591.

Glover, P. and S.S. Alexander, 1970, A comparison of the Lake Superior and Nevada Test Site regions, Teledyne Geotech, Seismic Data Laboratory Report No. 243.

Gutenberg, B., 1945, Amplitudes of Surface waves and magnitudes of shallow earthquake, Bull. Seismol. Soc. Am., v. 35, p. 3.

Gutenberg, B., and Richter, C.F., 1956, Magnitude and energy of earthquakes, Ann. Geofis., v. 9, p. 1.

Harkrider, D.G., 1964, Surface waves in multi-layered elastic media, 1, Rayleigh and Love waves from buried courses in a multi-layered elastic half-space, Bull. Seism. Soc. Am., v. 54, p. 627-680.

Herrin, Eugene, 1968, Seismological table for P, Bull. Seismol. Soc. Am., v. 58, No. 4, p. 1196-1219.

King, Phillip B., 1959, The evolution of North America , Princeton University Press.

Lambert, D.G., Von Seggern, D.H., Alexander, S.S. and Galat, G.A., 1970, The LONG SHOT experiment, Vol. II, Comprehensive Analysis, Teledyne Geotech, Seismic Data Laboratory Report No. 234.

Major, M.W. and Simon, R.B., 1968, A seismic study of the Denver (Derby) earthquakes, in J.C. Hollister and R.J. Weimer, ed; Geophysical and geological studies of the relationships between the Denver earthquakes and the Rocky Mountain Arsenal Well, Part A: Colorado School of Mines Quarterly, v. 63, No. 1, p. 9-56.

Rasmussen, Darrell C. and Lande, Larry, 1968, Seismic analysis of the Gasbuggy explosion and an earthquake of similar magnitude and epicenter, Teledyne Geotech, Technical Report No. 68-15.

Toksoz, M.N., and Harkrider, D.G. and Ben-Menahem, A., 1965, determination of source parameters by amplitude equalization of seismic surface waves, 2, release of tectonic strain by underground nuclear explosions and mechanisms of earthquakes, J. Geophys. Res., v. 70, p. 907-922.

Toksoz, M. Nafi and Clermont, Kevin, 1967, Radiation of seismic waves from the Bilby explosion, Teledyne Geotech, Seismic Data Laboratory Report No. 183.

Turnbull, L.S. Jr., Lambert, D.G., Newton, C.A., 1968, Rayleigh wave discrimination techniques between underground explosions and earthquakes, Teledyne Geotech, Seismic Data Laboratory Report No. 211.

Von Seggern, D.H., 1969, Surface-wave amplitude-versus-distance relation in the western United States, Teledyne Geotech, Seismic Data Laboratory REport No. 249.

Von Seggern, D.H. and Lambert, D.G., 1969, Dependence of theoretical and observed Rayleigh-wave spectra on distance, magnitude, and source type, Teledyne Geotech, Seismic Data Laboratory Report No. 240.

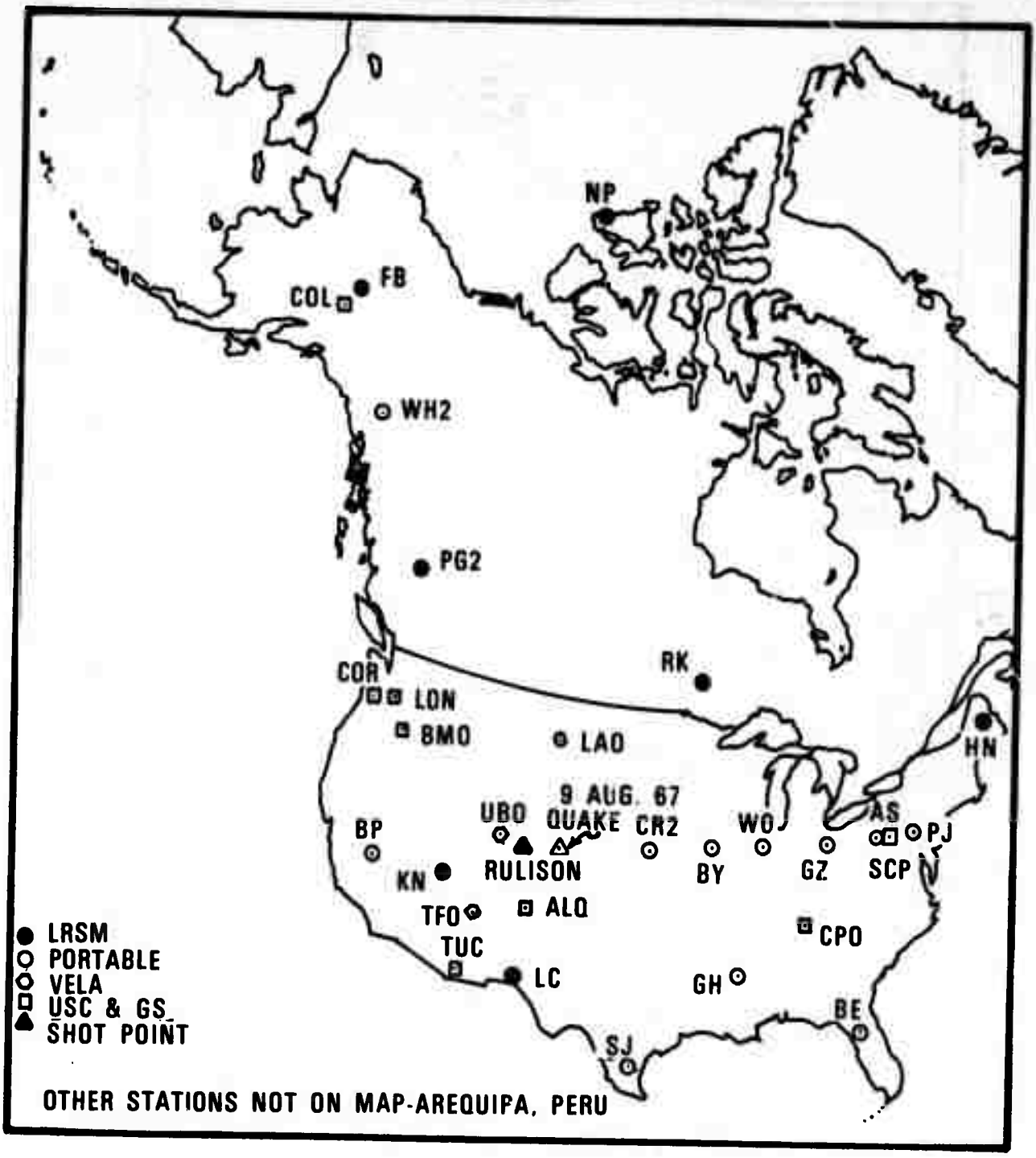

Figure 1. Station location map for RULISON.

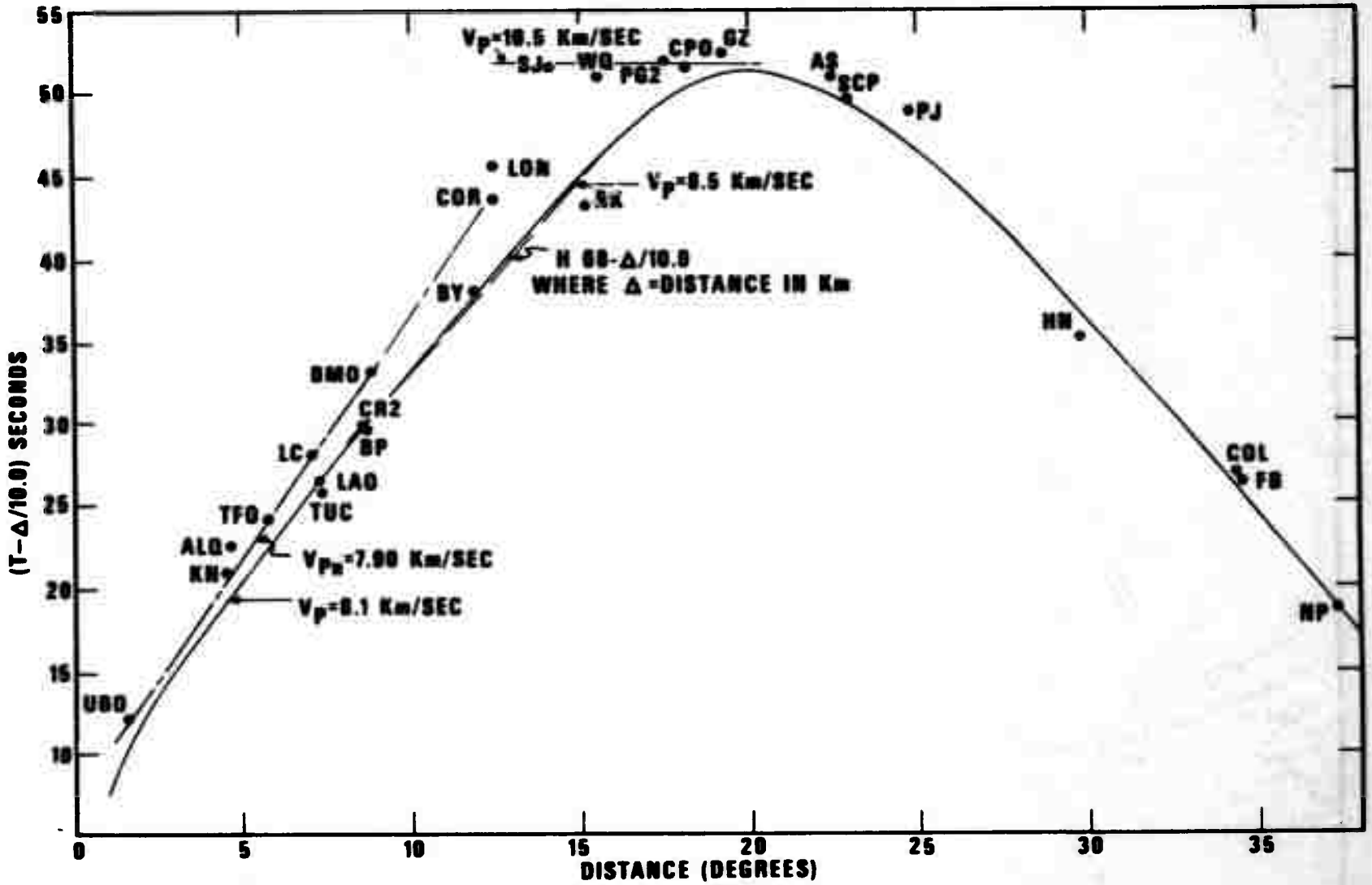

Figure 2. Reduced travel-times for RULISON.

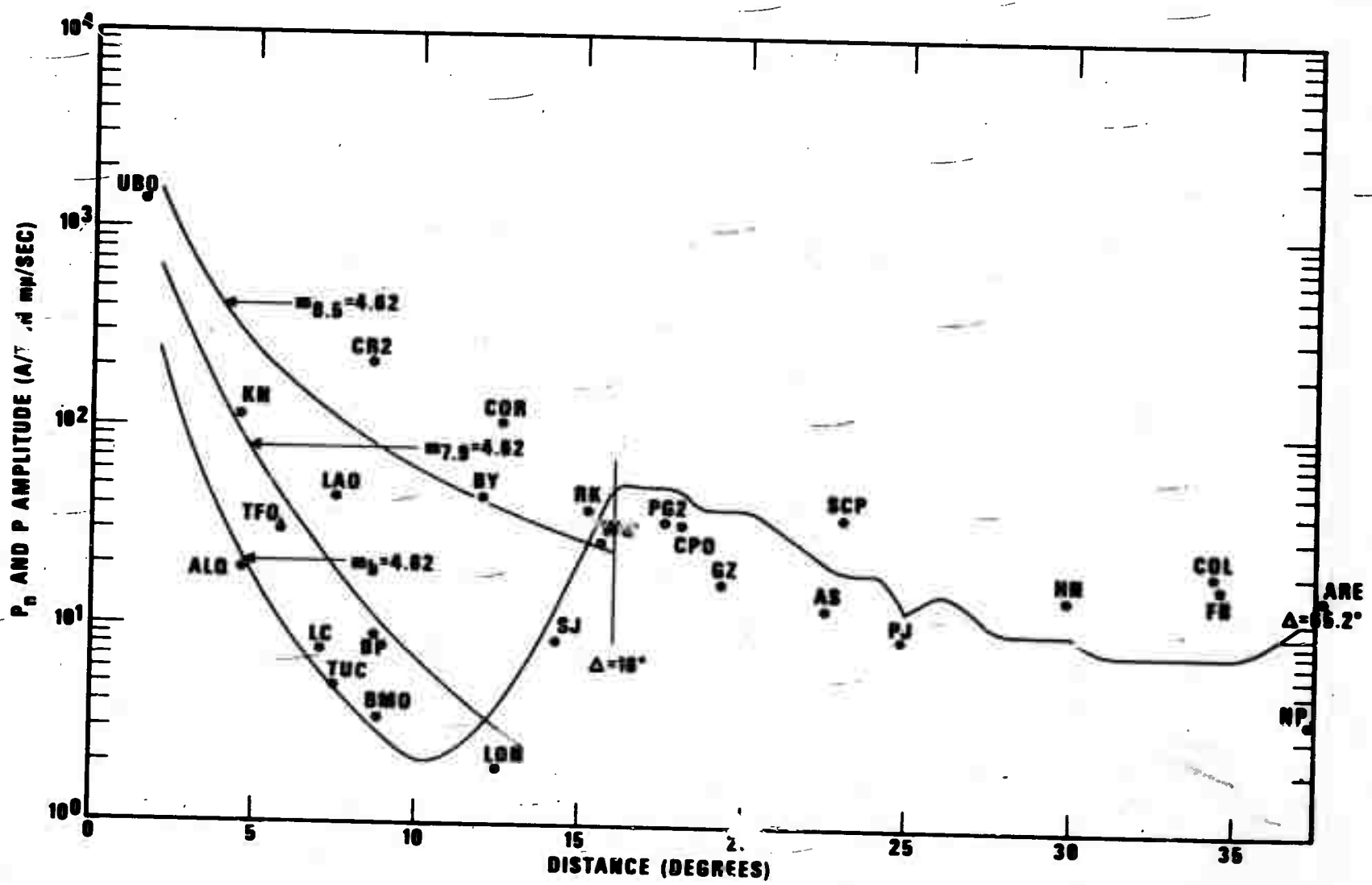

Figure 3. P_n and P amplitudes for RULISON.

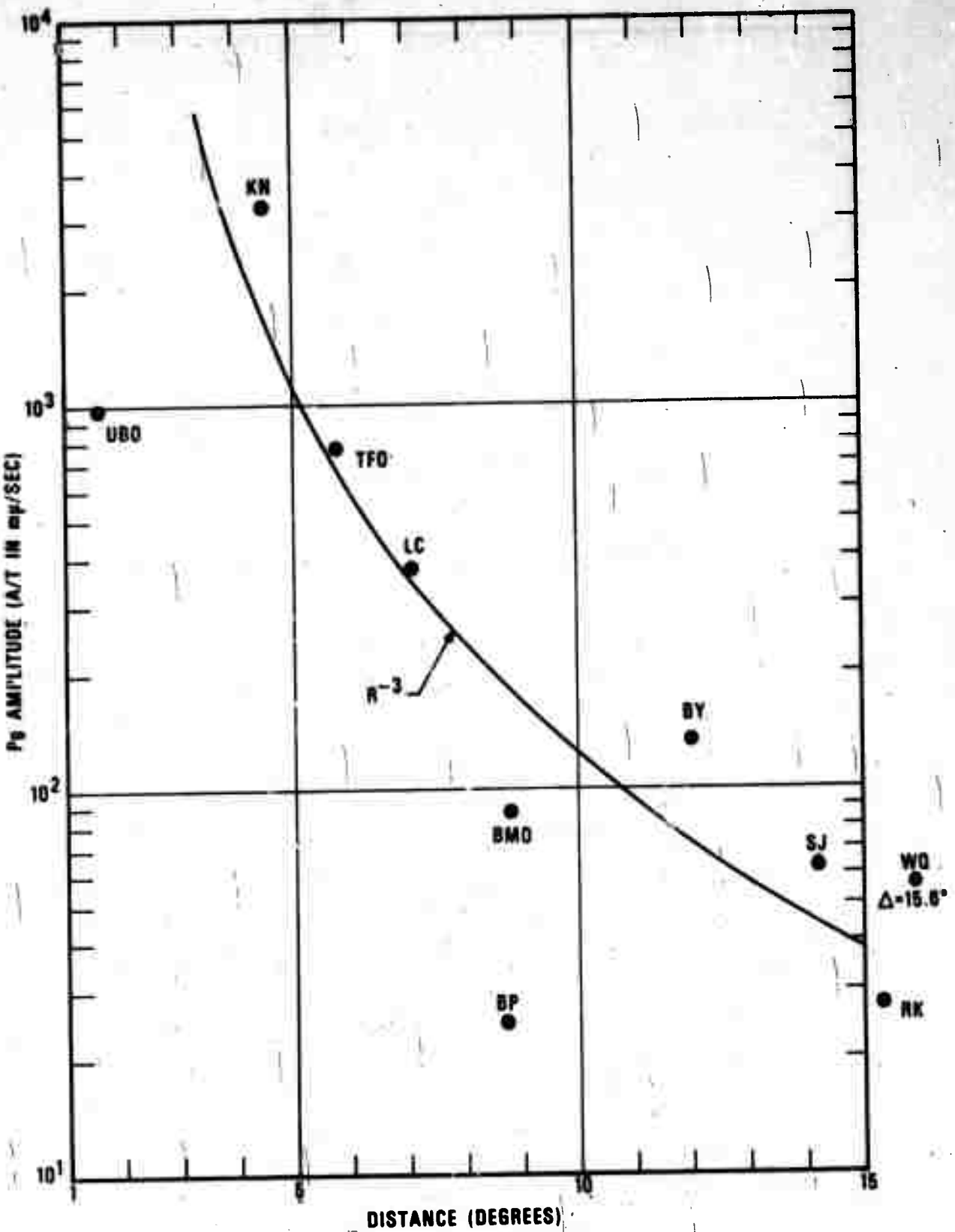

Figure 4. P_g amplitudes for RULISON.

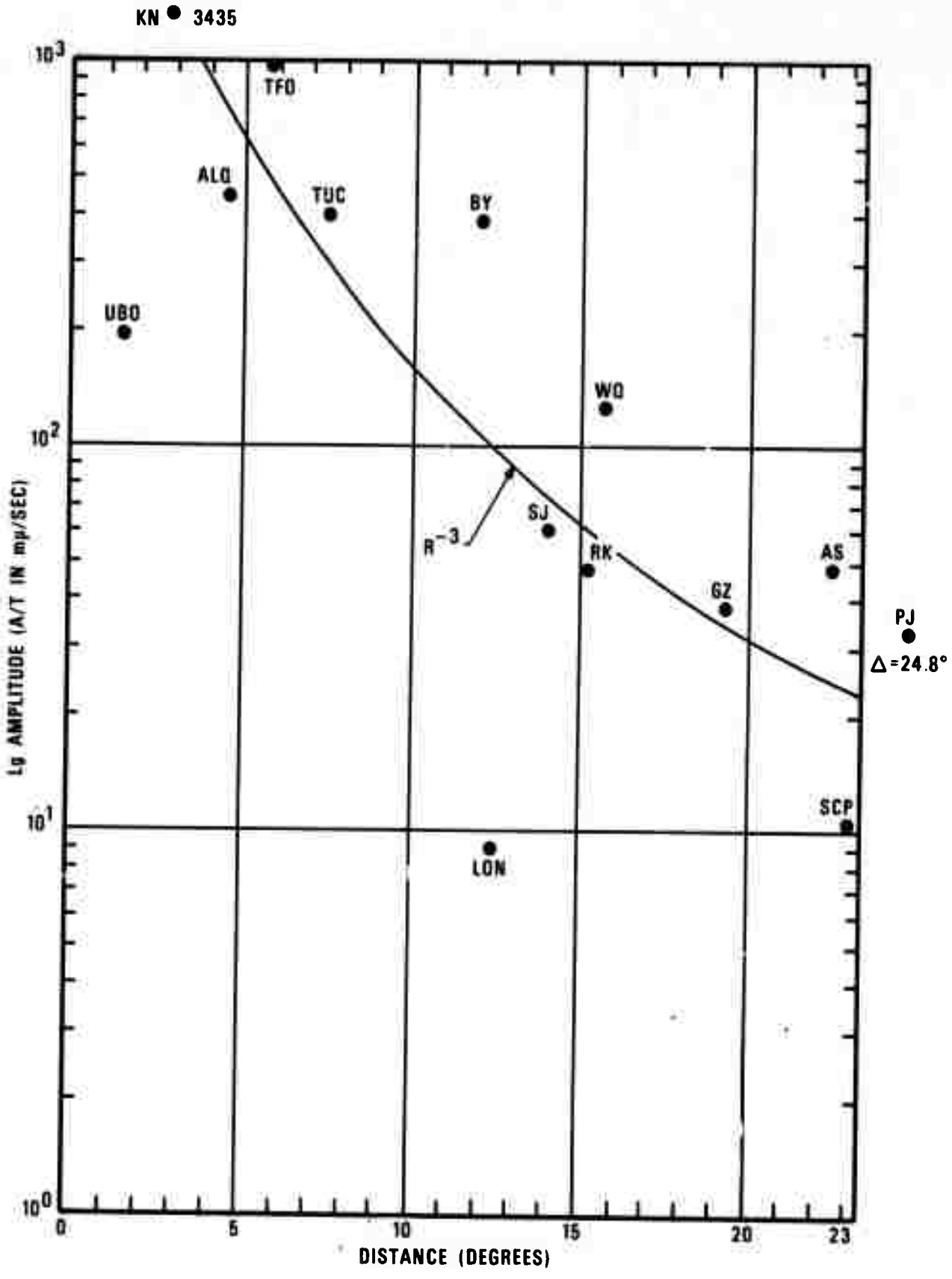

Figure 5. L_g amplitudes for RULISON.

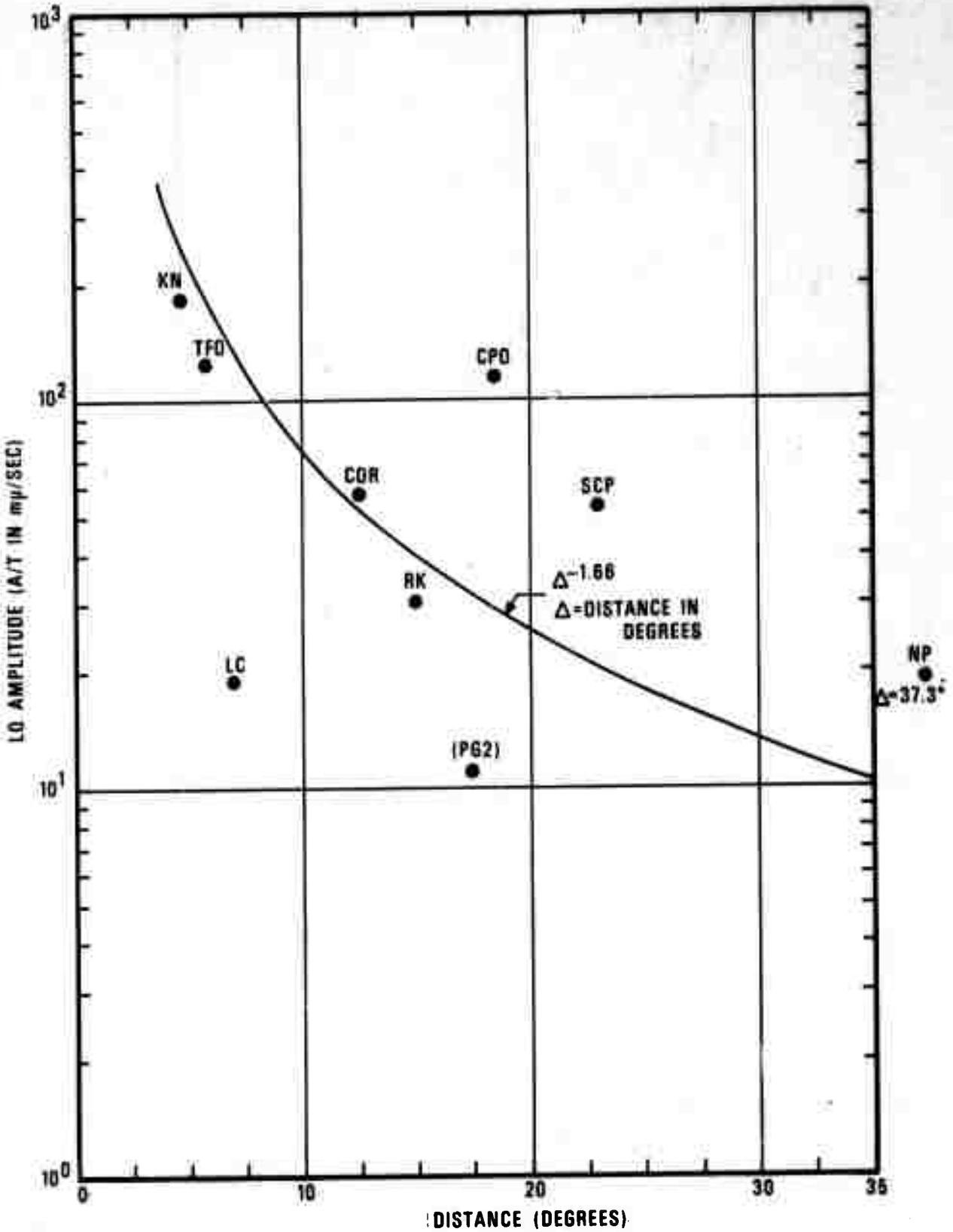

Figure 6. LQ amplitudes for RULISON.

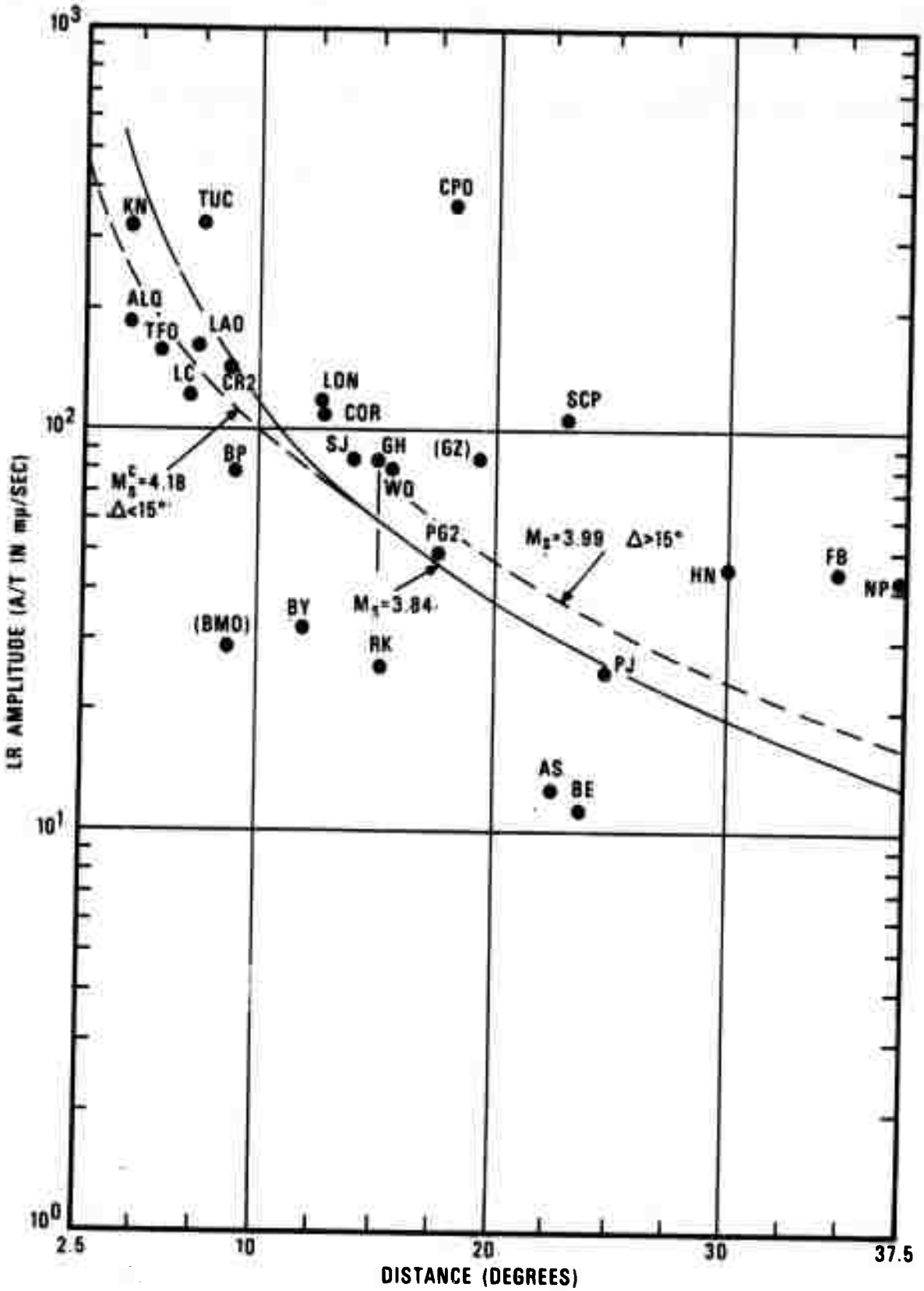

Figure 7. LR amplitudes for RULISON.

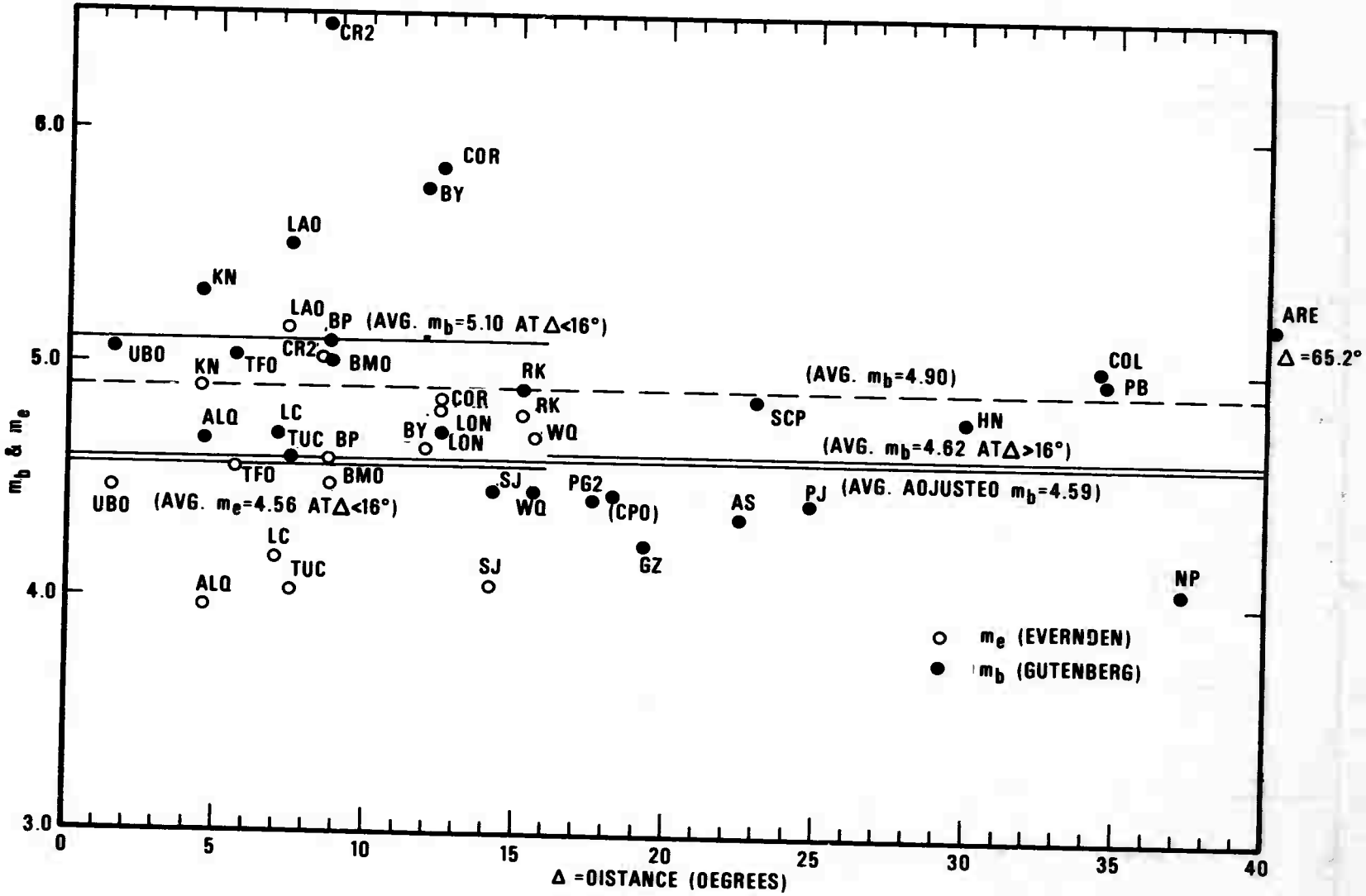

Figure 8. Body-wave magnitudes for RULISON.

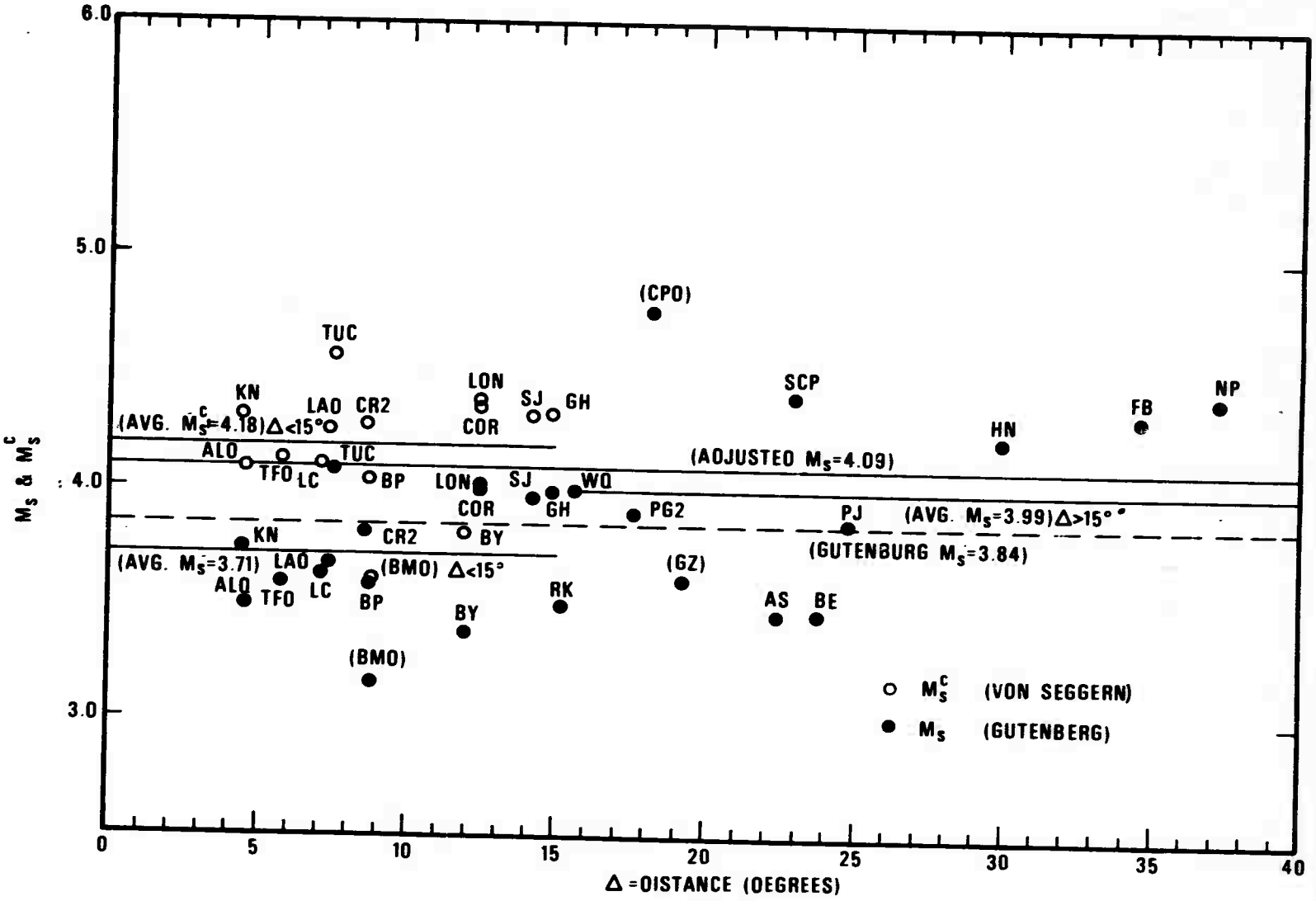

Figure 9. Surface-wave magnitudes for RULISON.

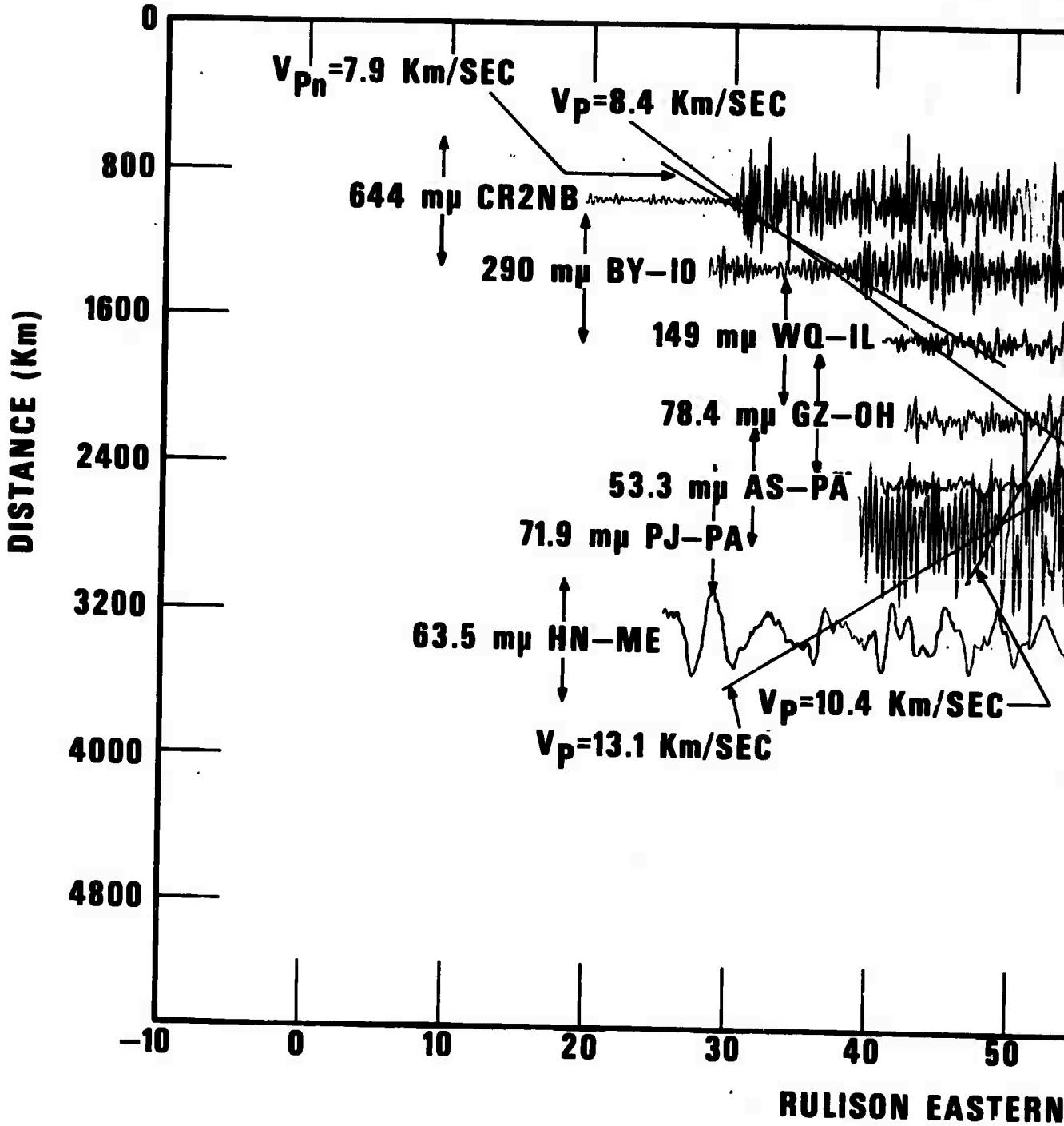

Figure 10. Short pe
profile.

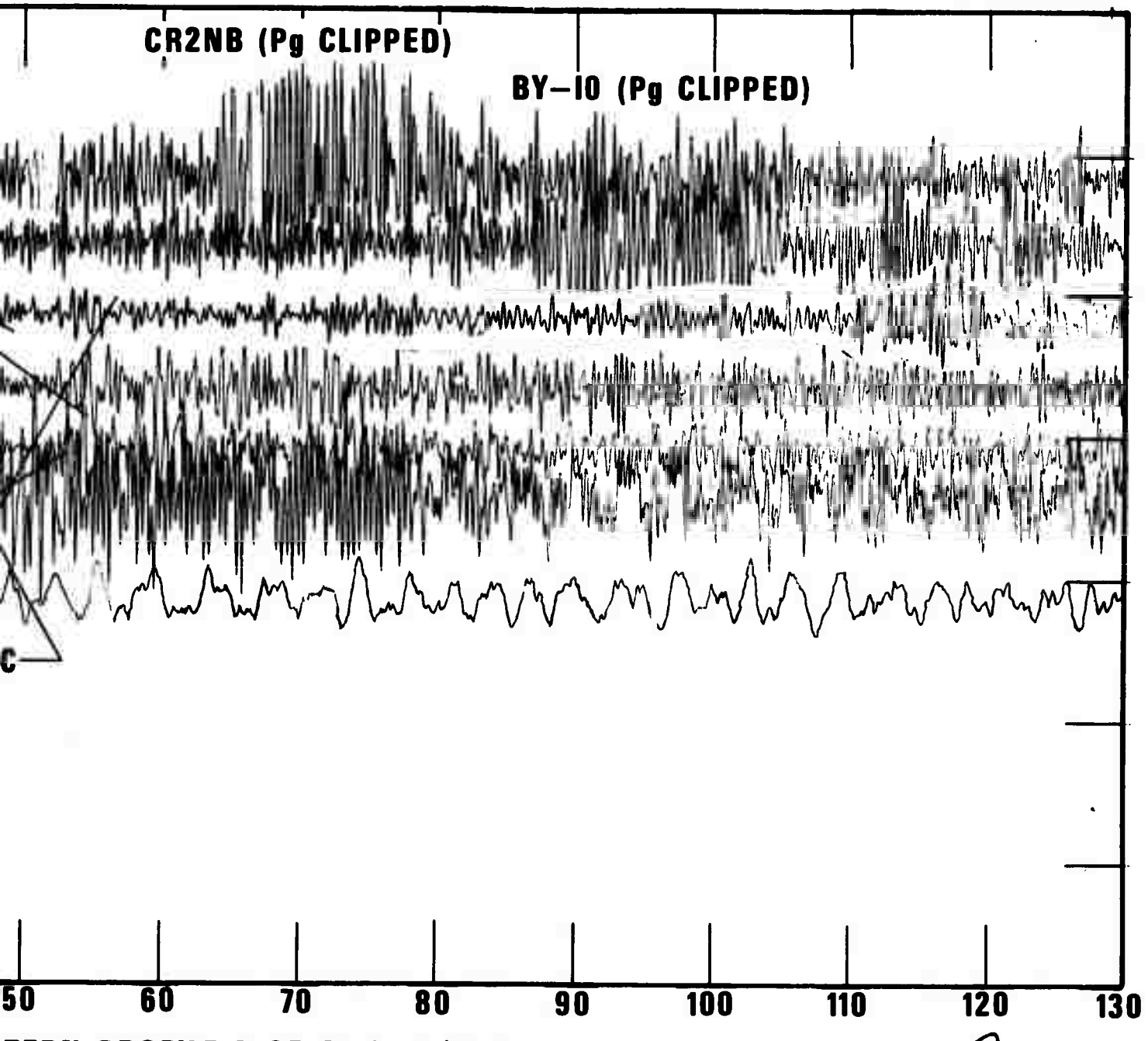

B

hort period vertical seismograms for the east
rofile.

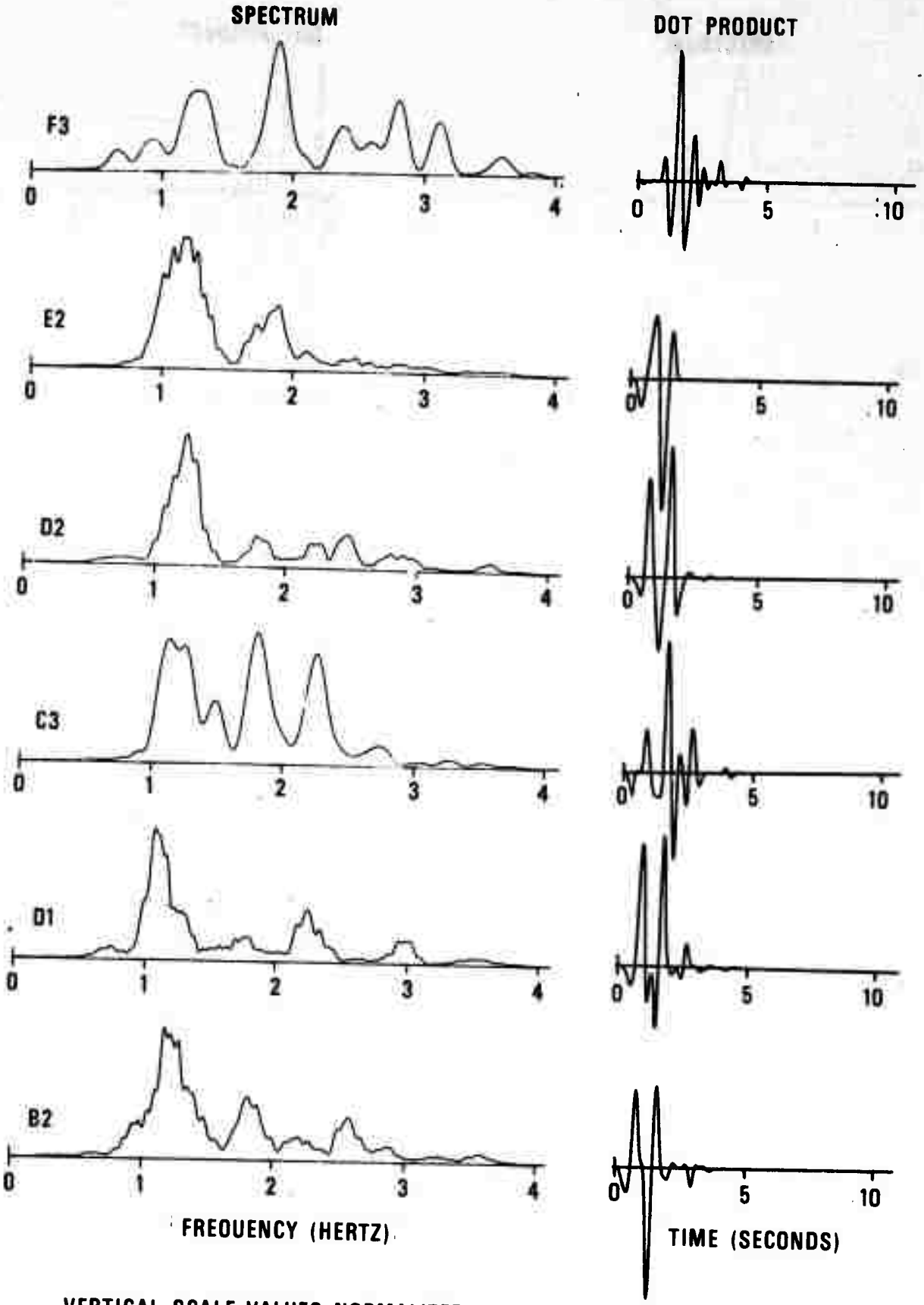

VERTICAL SCALE VALUES NORMALIZED TO PLOT SCALE OF 1 INCH

Figure 11a. Cepstrum analysis for RULISON at LASA sub-array centers.

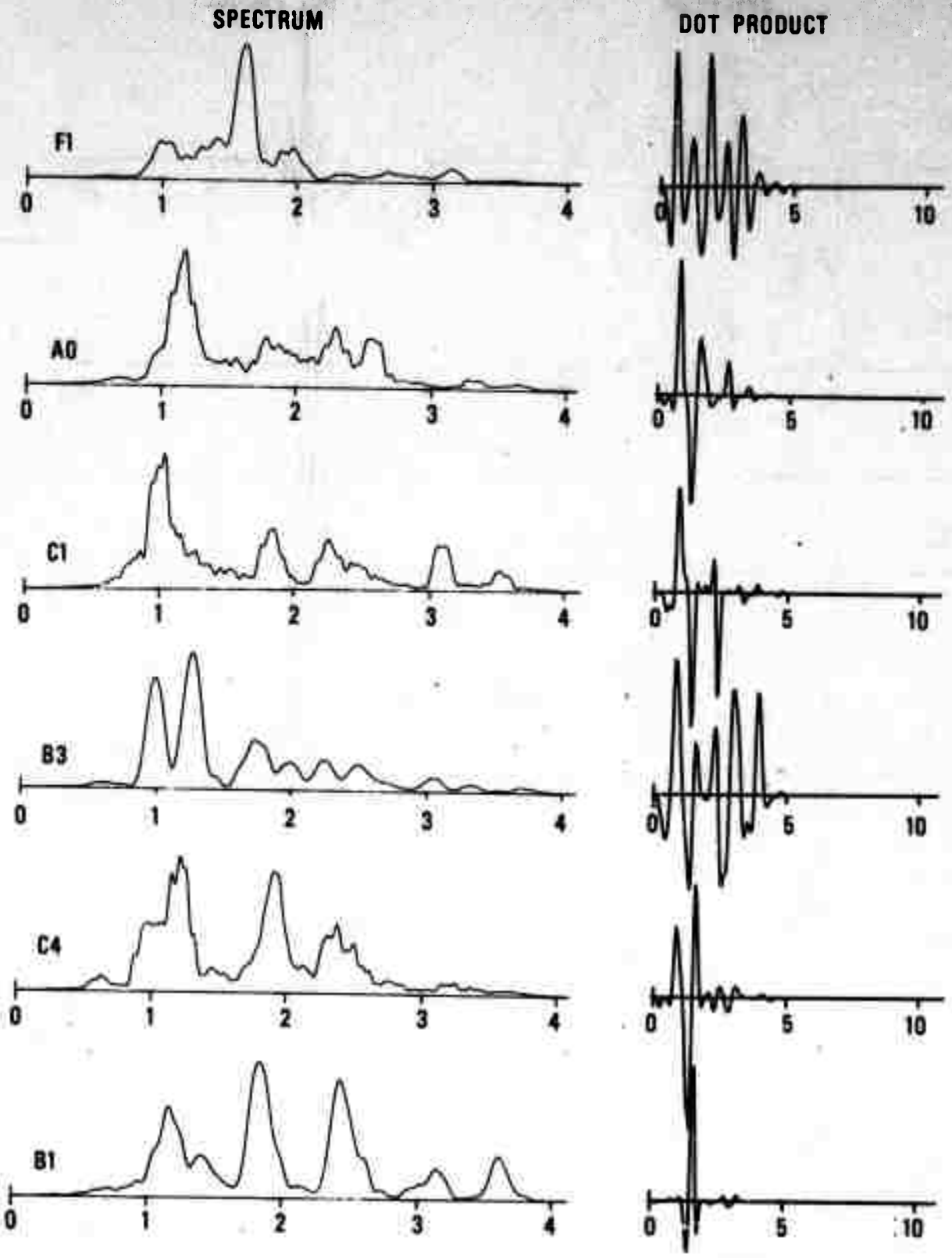

Figure 11b. Cepstrum analysis for RULISON at LASA sub-array centers.

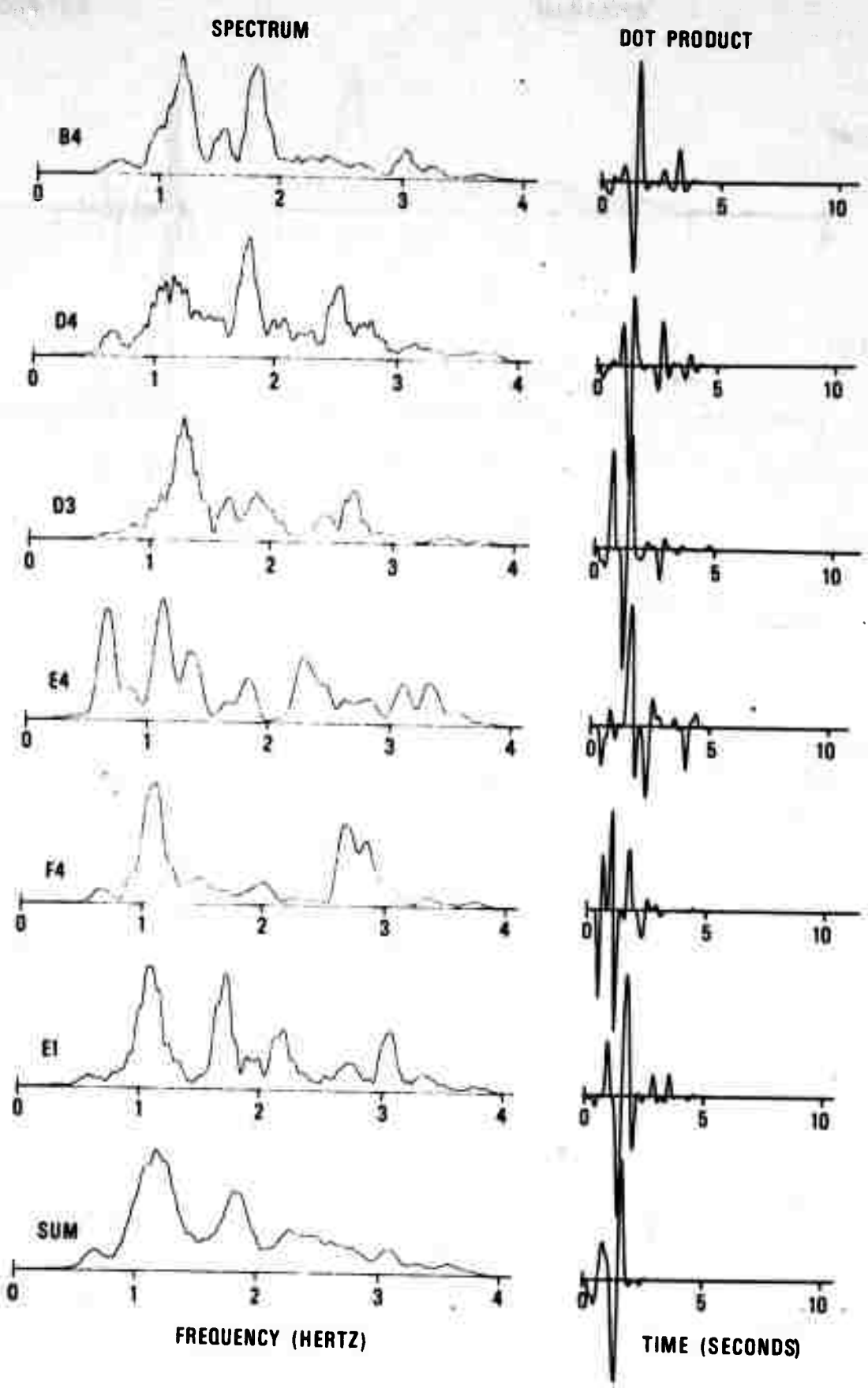

VERTICAL SCALE VALUES NORMALIZED TO PLOT SCALE OF 1 INCH

Figure 11c. Cepstrum analysis for RULISON at LASA sub-array centers.

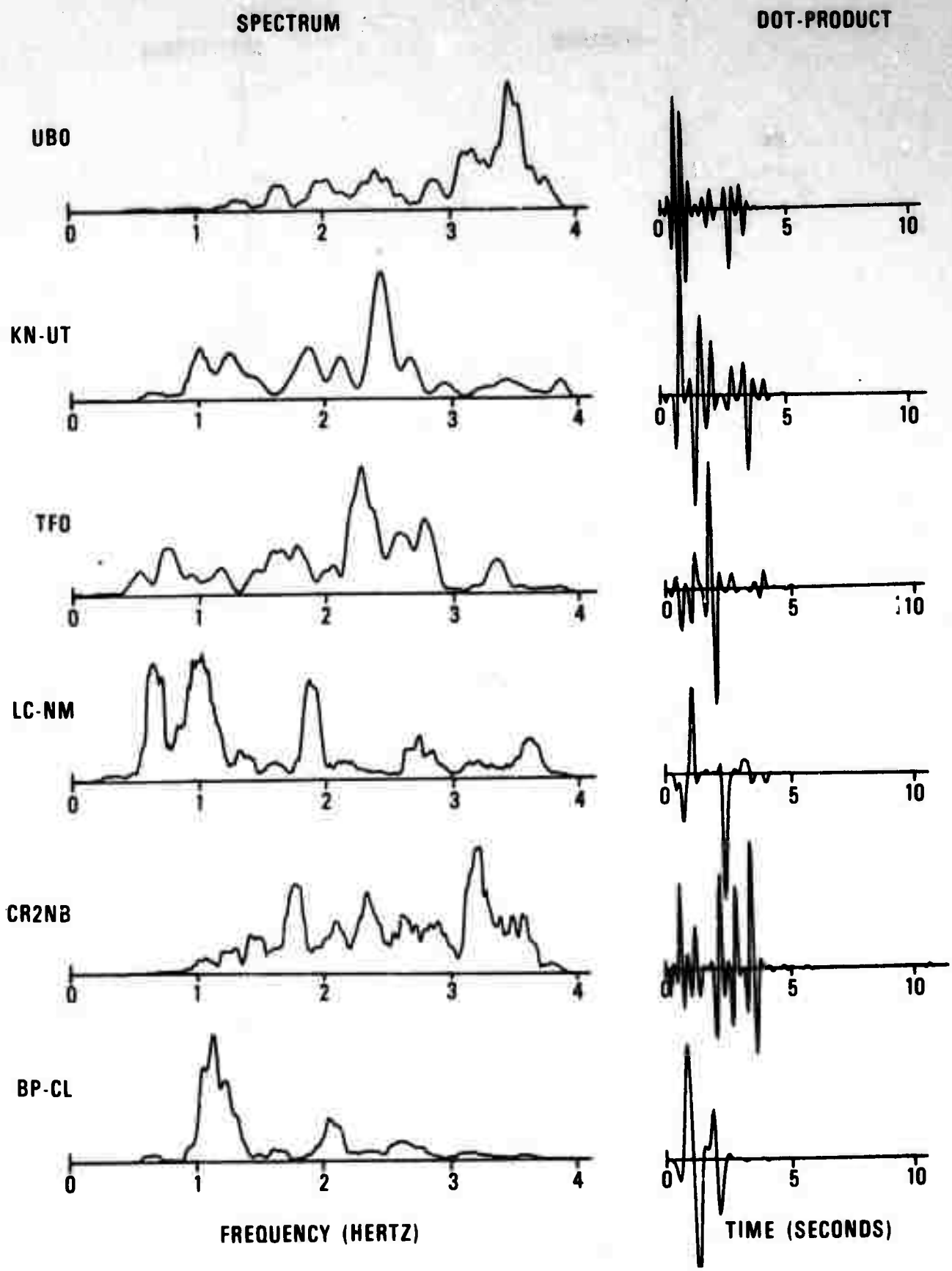

VERTICAL SCALE VALUES NORMALIZED TO PLOT SCALE OF 1 INCH

Figure 12a. Cepstrum analysis of Pn and P for RULISON.

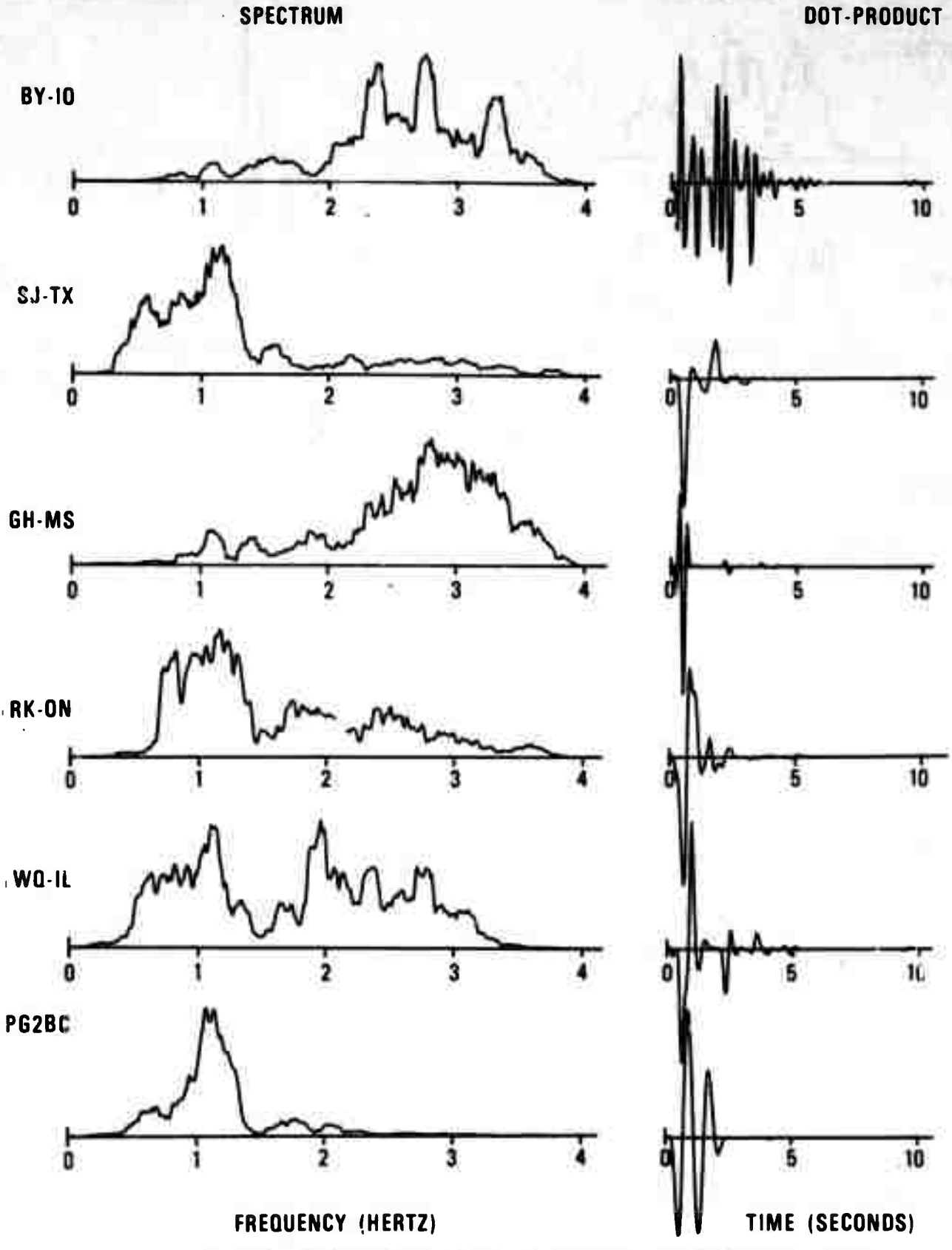

VERTICAL SCALE VALUES NORMALIZED TO PLOT SCALE OF 1 INCH

Figure 12b. Cepstrum analysis of Pn and P for RULISON.

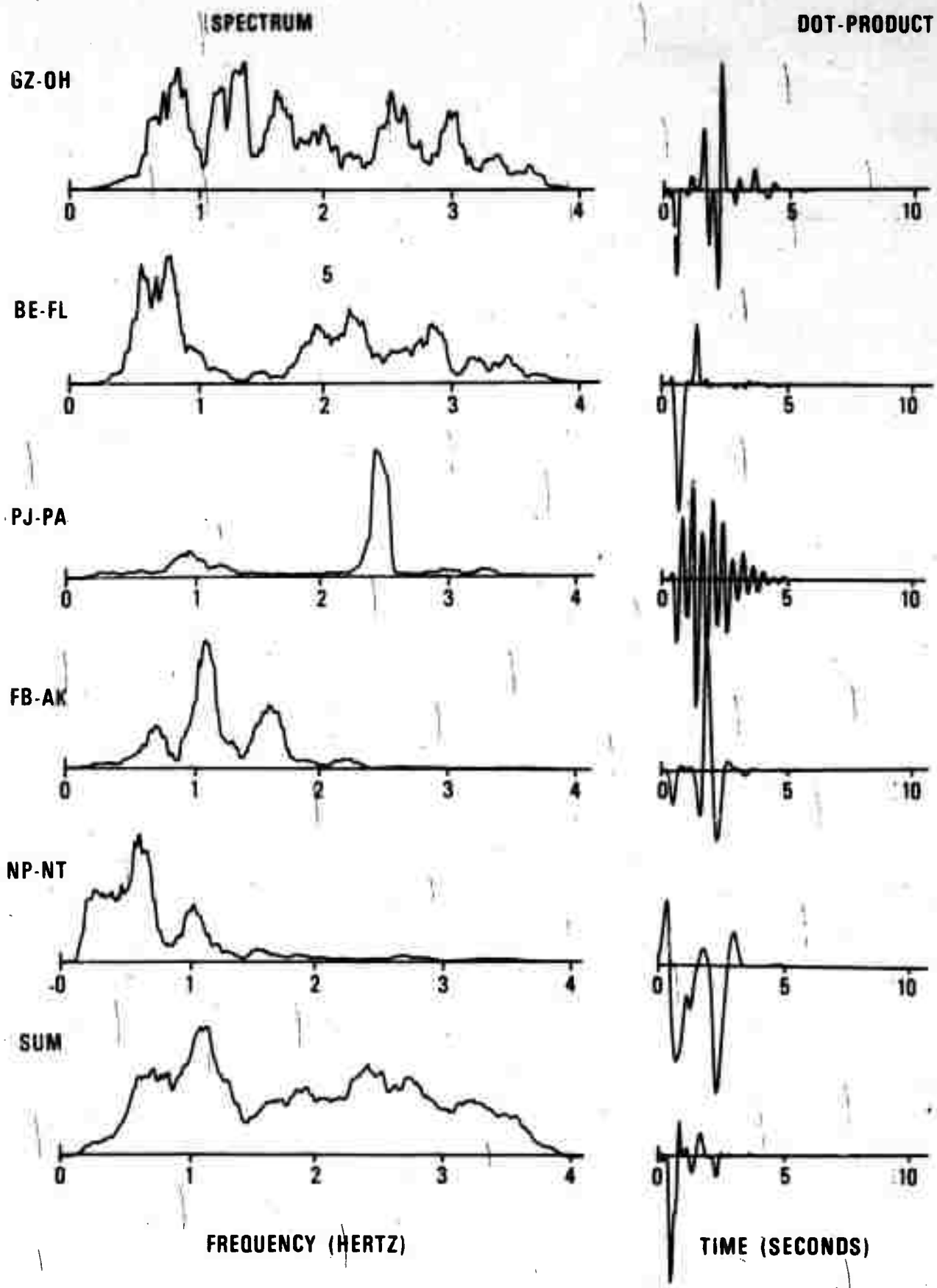

VERTICAL SCALE VALUES NORMALIZED TO PLOT SCALE OF 1 INCH

Figure 12c. Cepstrum analysis of Pn and P for RULISON.

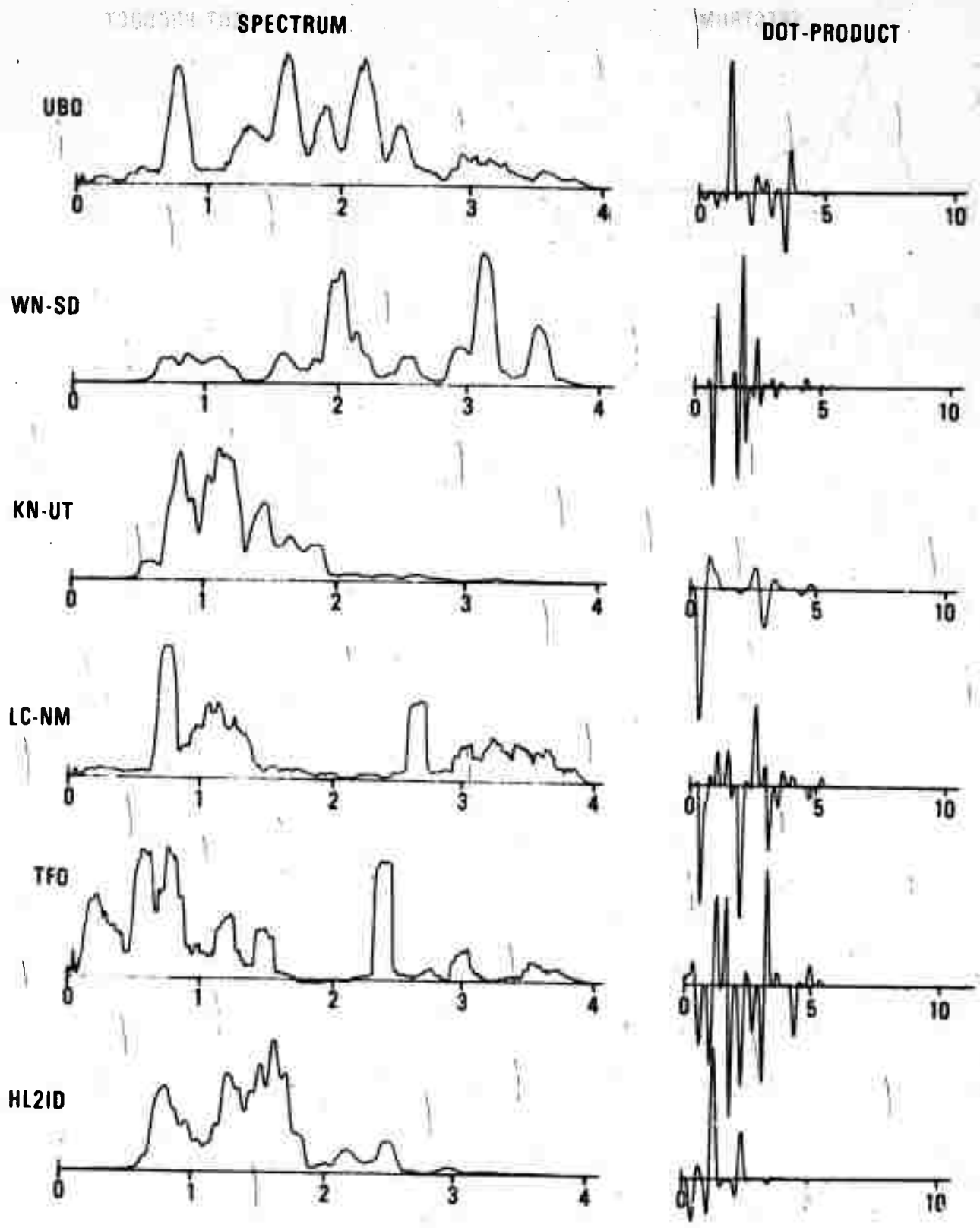

Figure 13a. Cepstrum analysis of Pn and P for the Colorado earthquake.

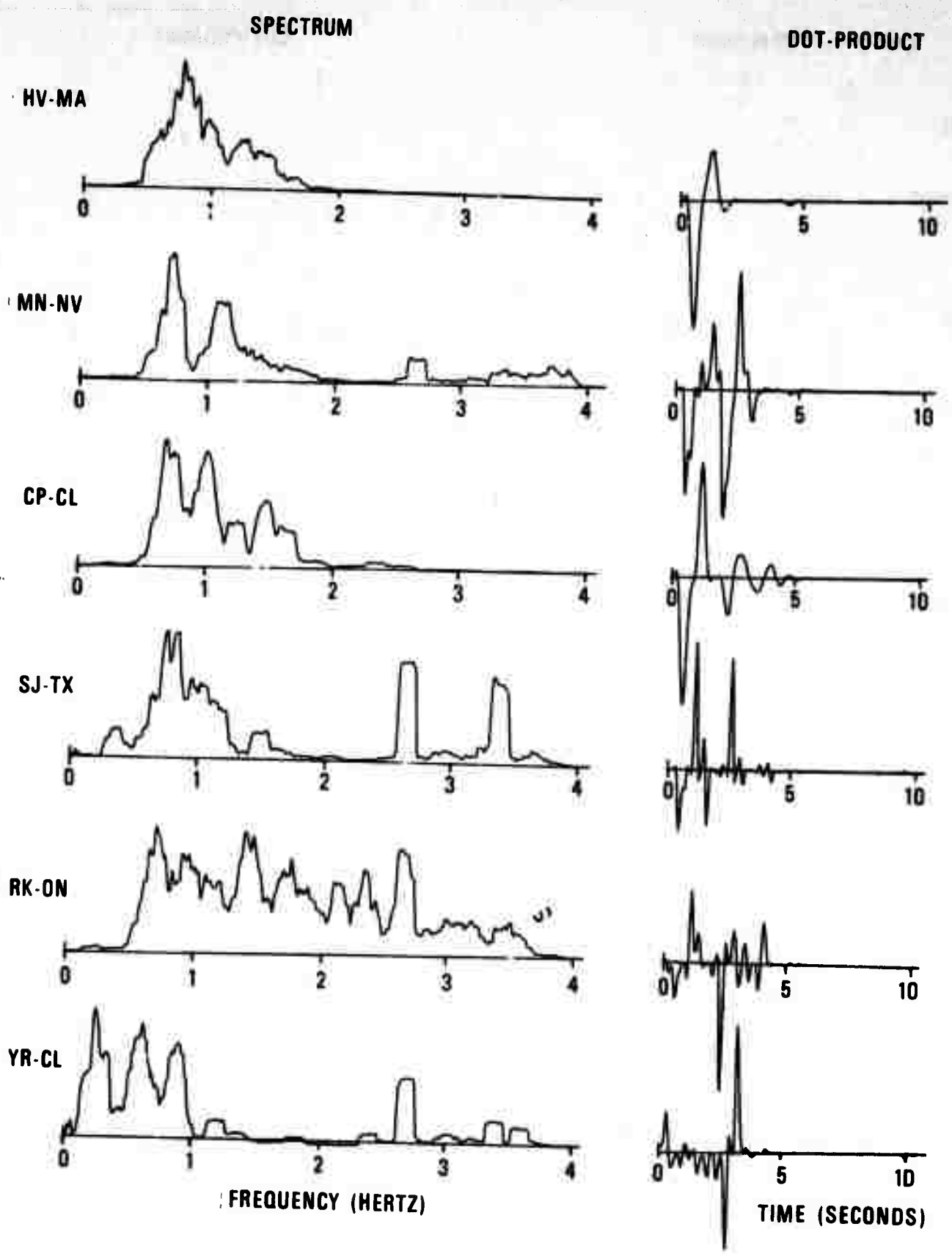

VERTICAL SCALE VALUES NORMALIZED TO PLOT SCALE OF 1 INCH

Figure 13b. Cepstrum analysis of Pn and P for the Colorado earthquake.

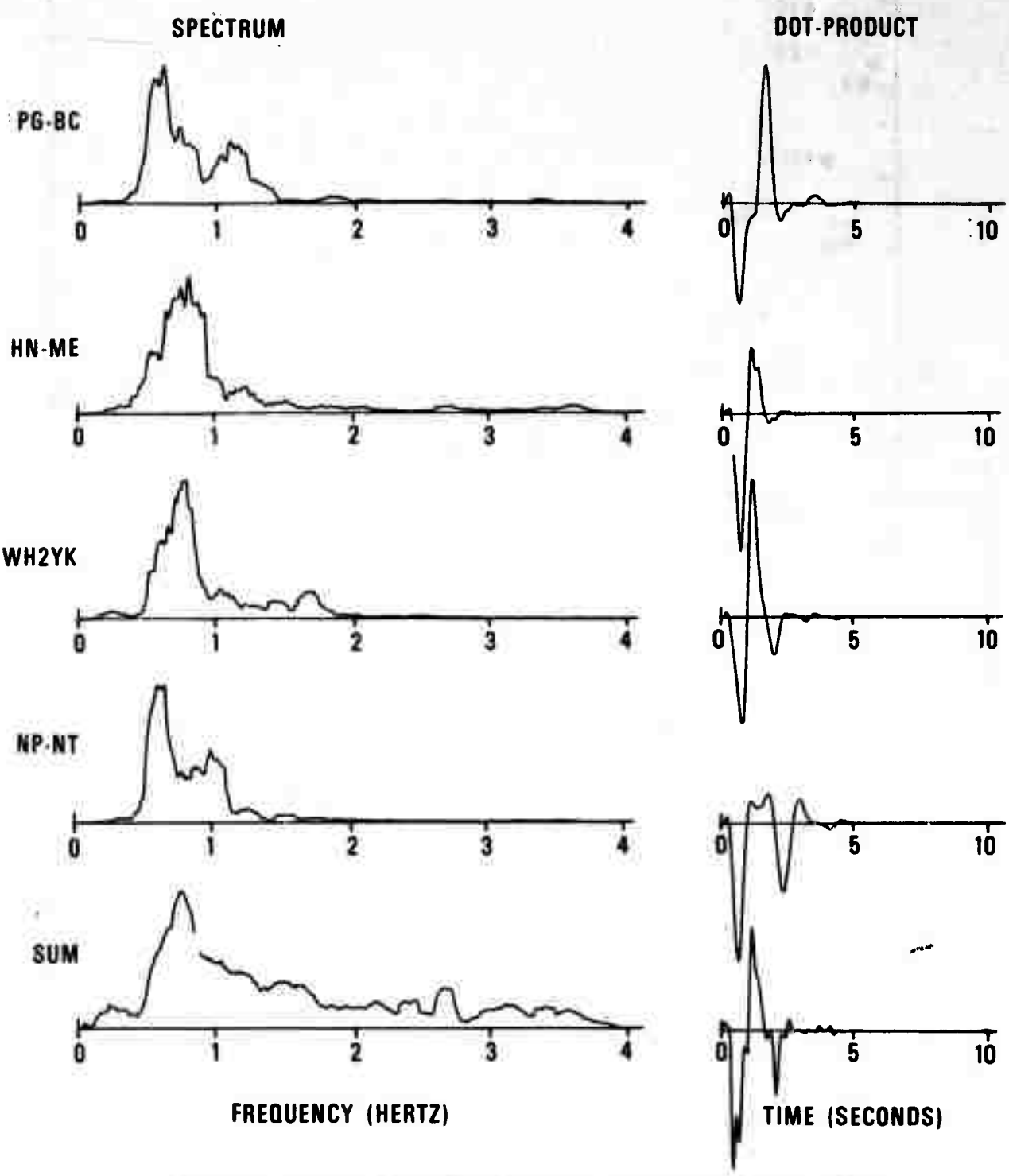

VERTICAL SCALE VALUES NORMALIZED TO PLOT SCALE OF 1 INCH

Figure 13c. Cepstrum analysis of Pn and P for the Colorado earthquake.

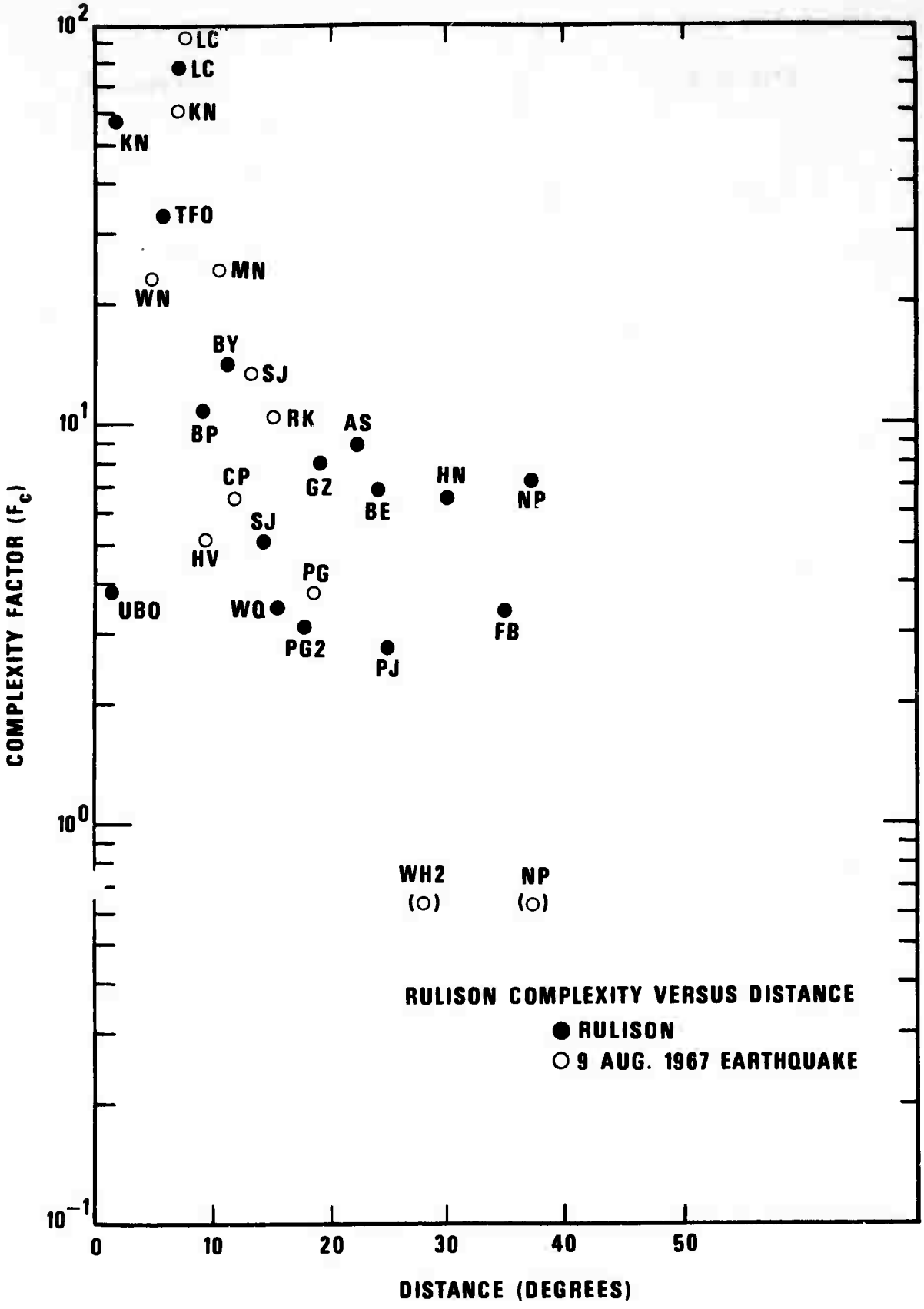

Figure 14. RULISON complexity versus distance.

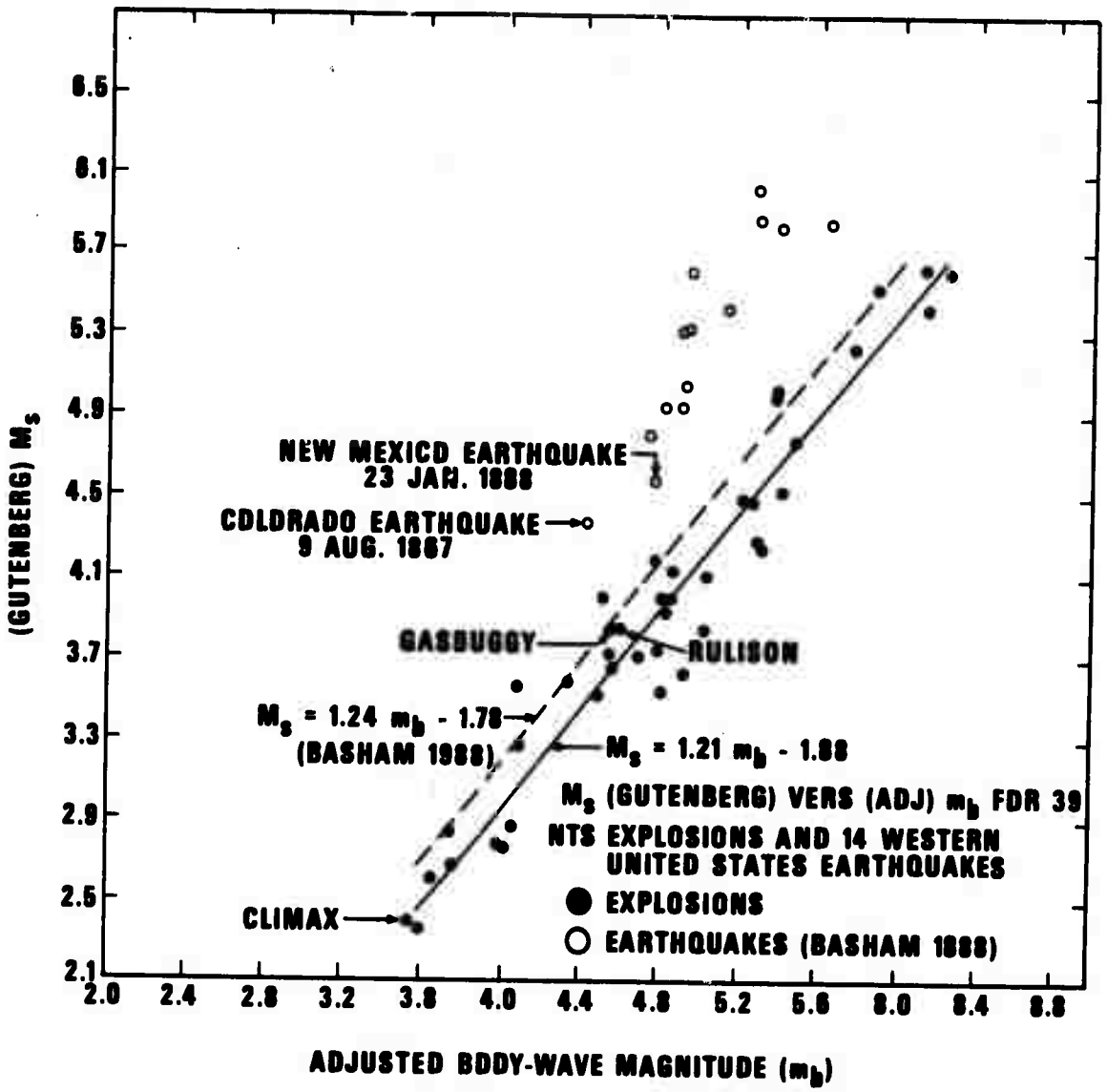

Figure 15. M_s (Gutenberg) versus m_b for 39 NTS explosions and 14 western United States explosions.

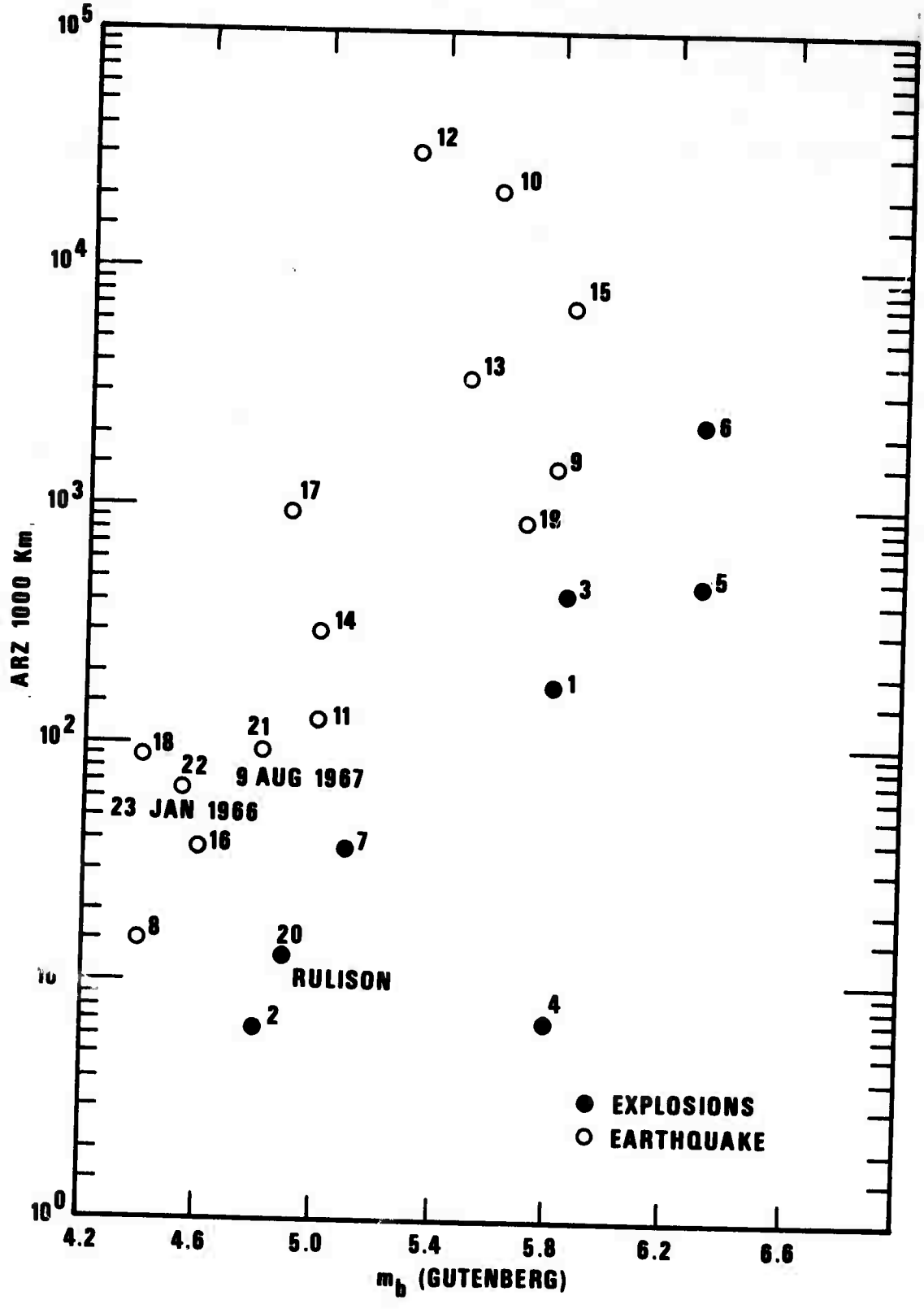

Figure 16. ARZ versus m_b.

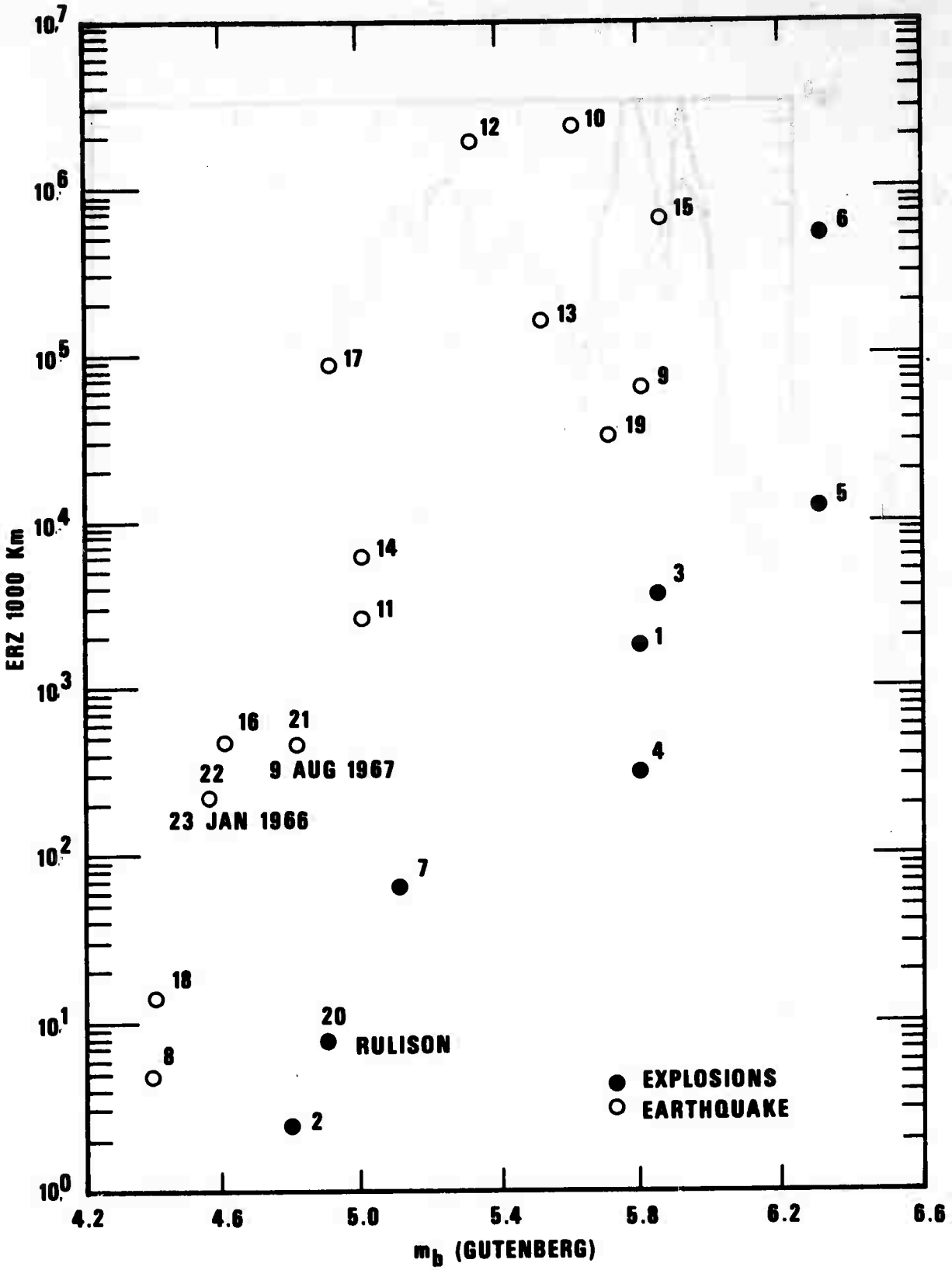

Figure 17. ERZ versus m_b.

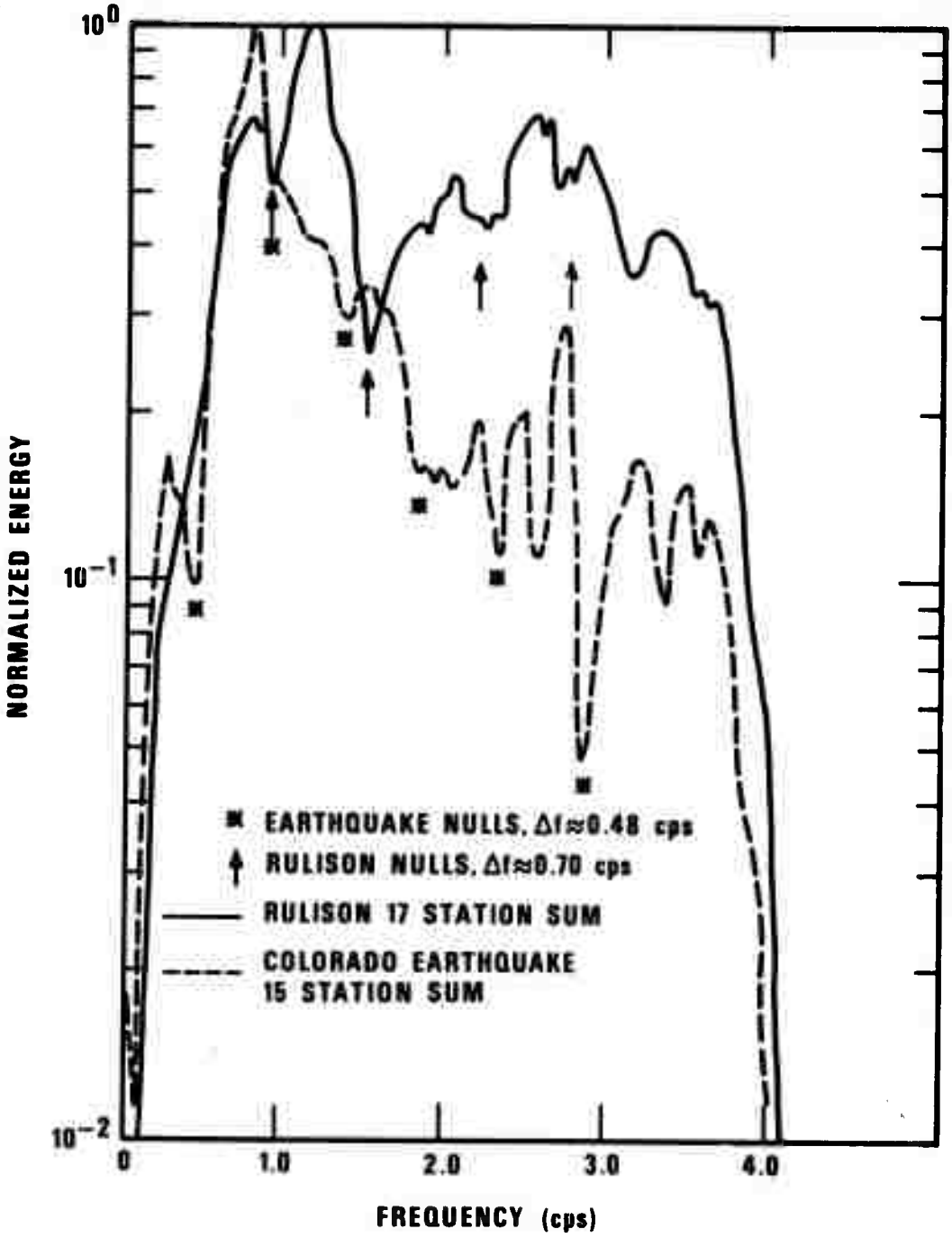

Figure 18. Comparative SP spectral energy summation for RULISON and 9 August 1967 earthquake.

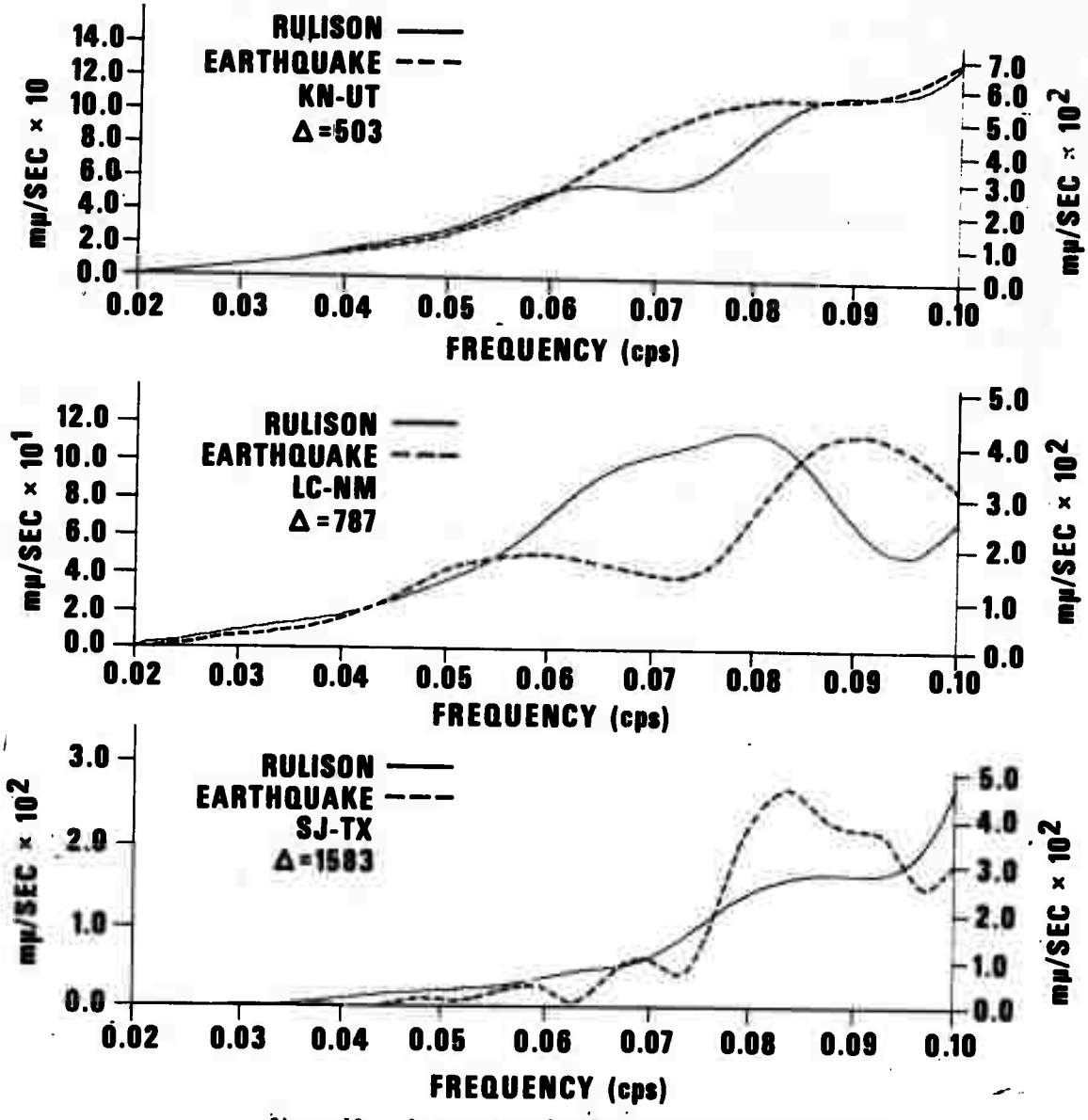

Figure 19a. Comparative LR amplitude spectra for RULISON and 9 August 1967 earthquake at KN-UT, LC-NM, SJ-TX, RK-ON, and NP-NT.

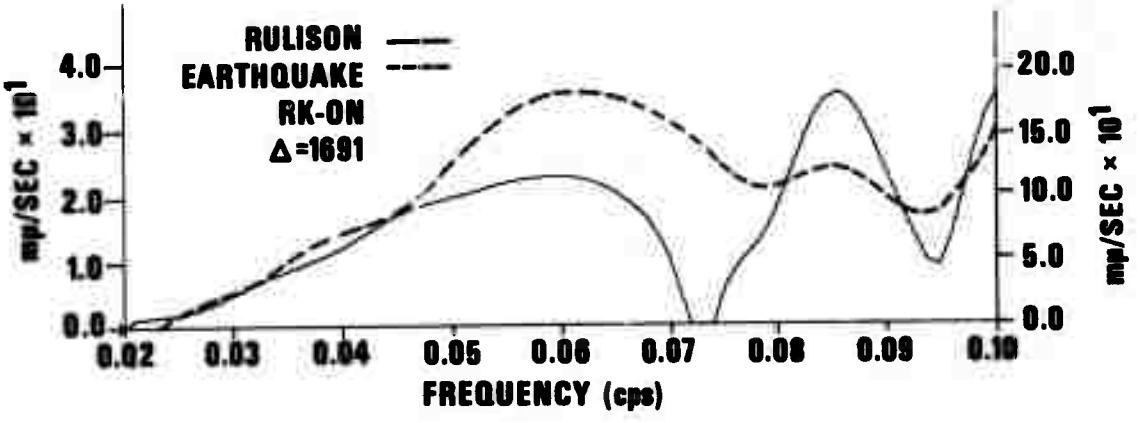

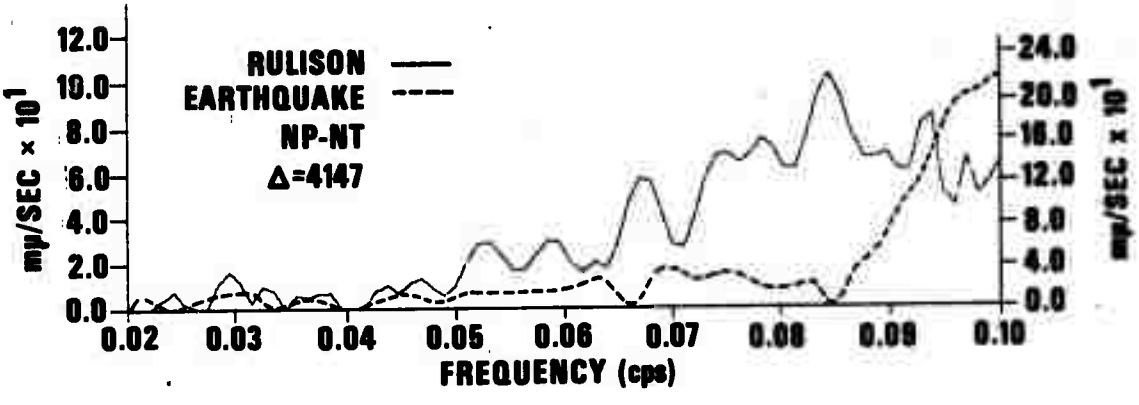

Figure 19b. Comparative LR amplitude spectra for RULISON and 9 August 1967 earthquake at KN-UT, LC-NM, SJ-TX, RK-ON, and NP-NT.

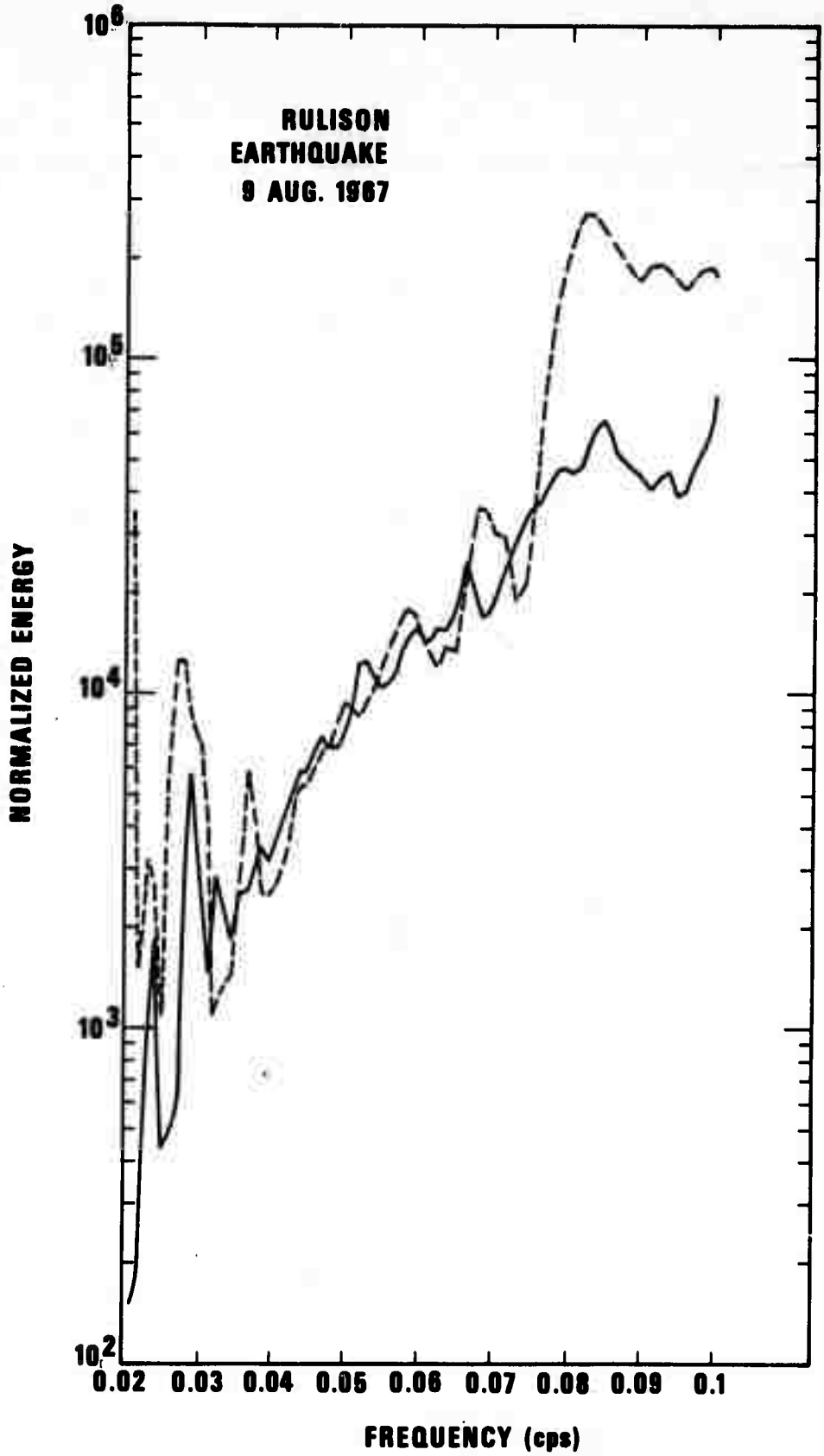

Figure 20. Comparative LR spectral energy summation for RULISON and 9 August 1967 earthquake.

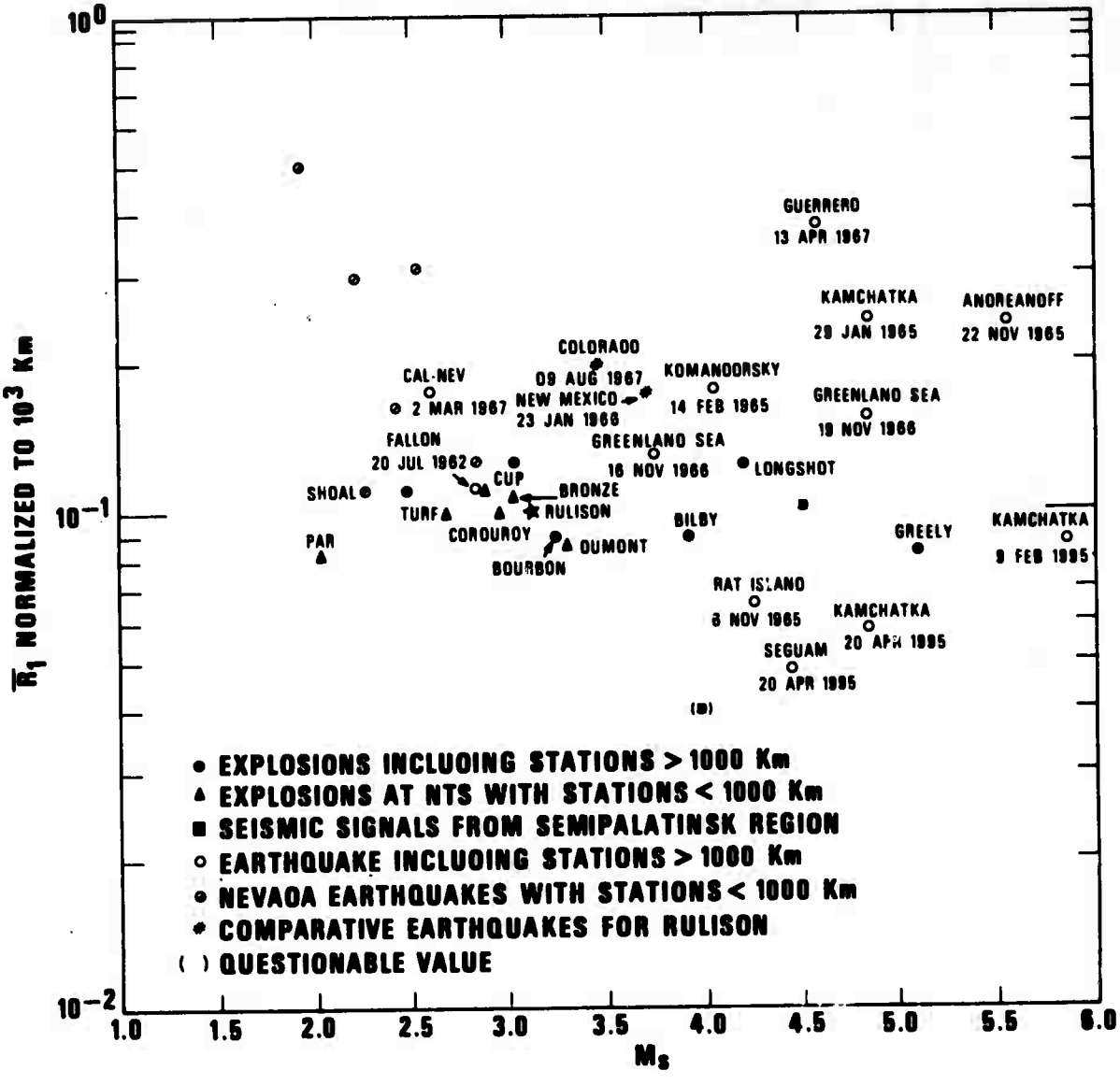

Figure 21. Normalized energy ratio $\bar{R}_1$ versus M_s.

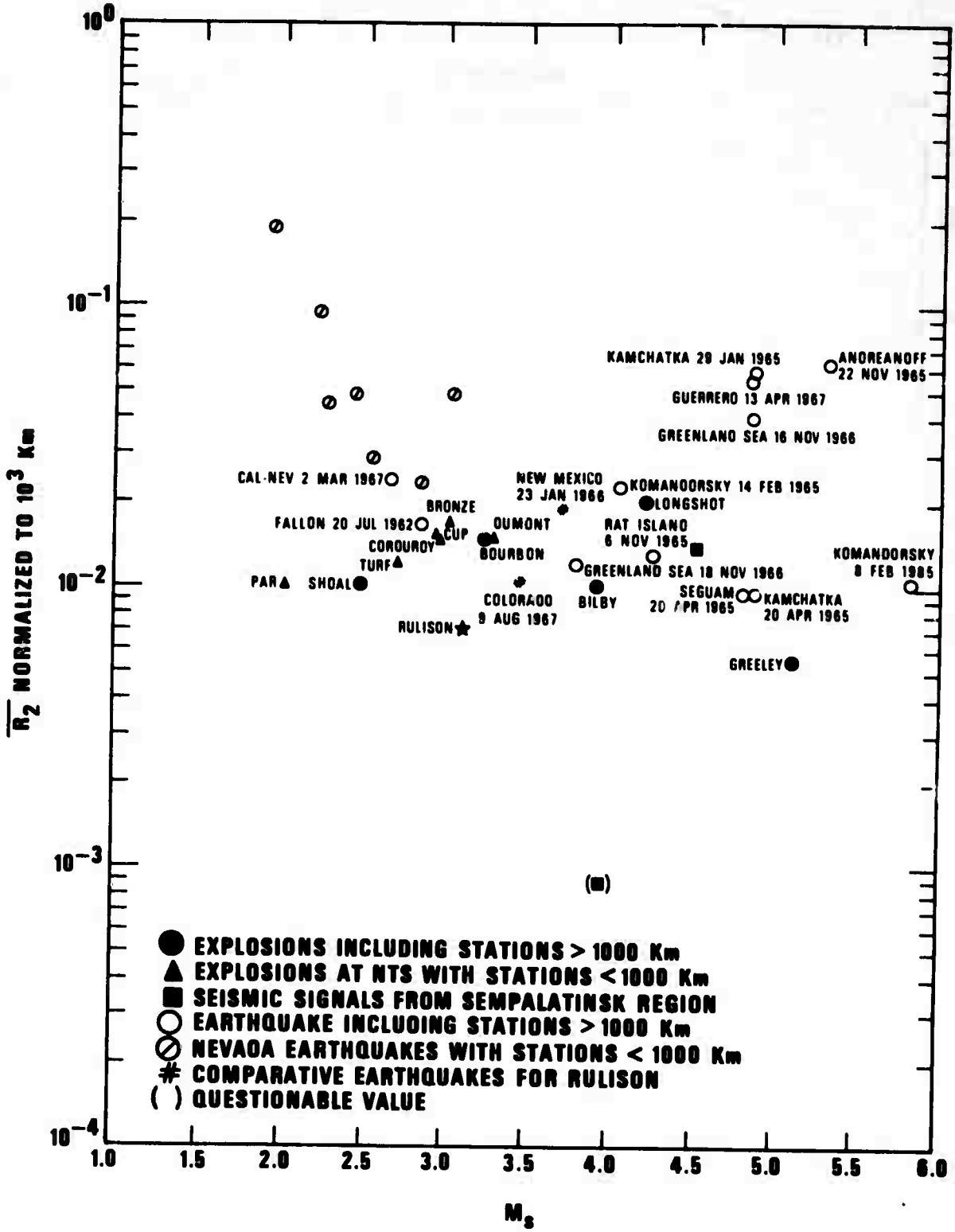

Figure 22. Normalized energy ratio $\overline{R}_2$ versus M_s.

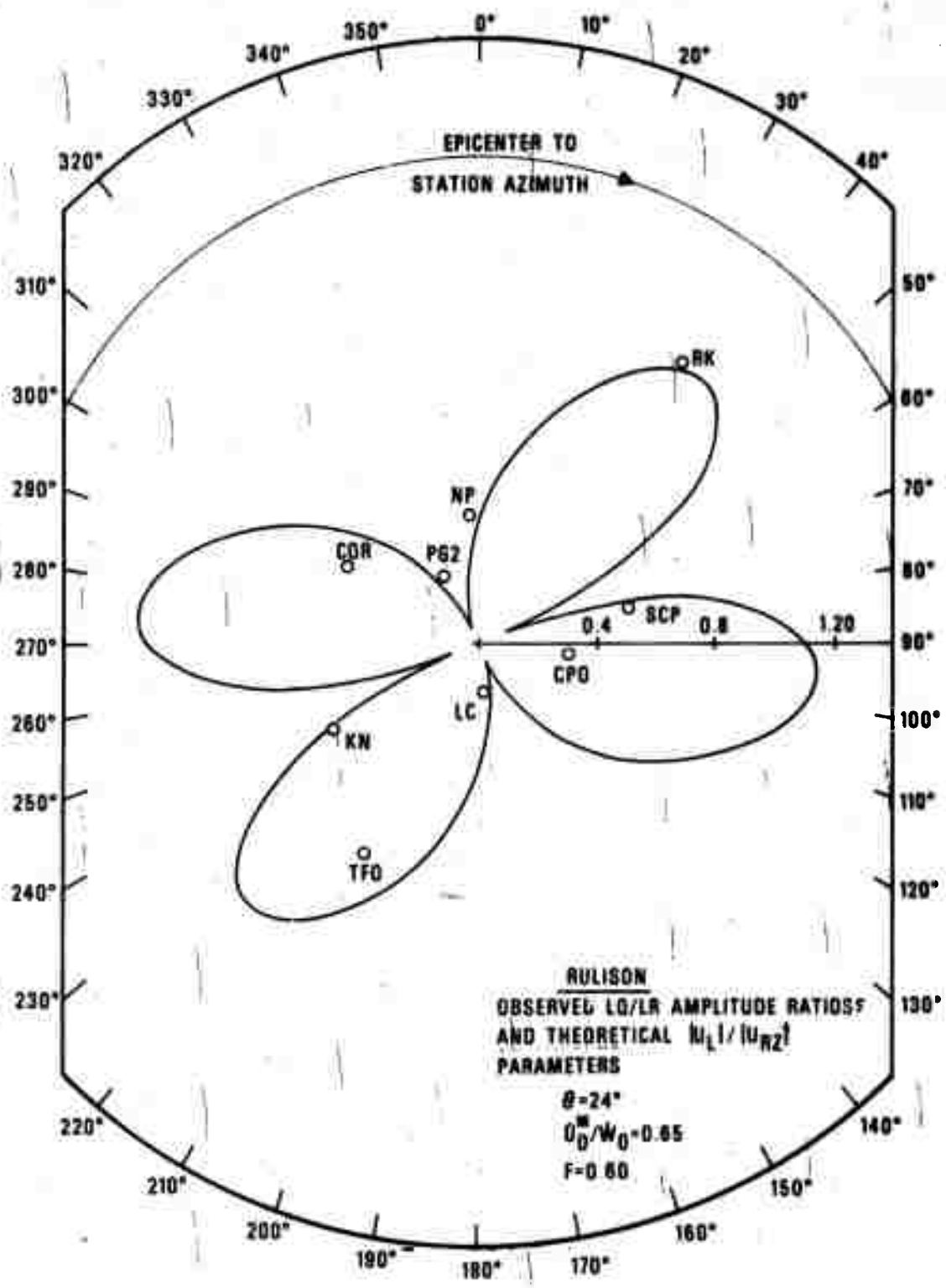

Figure 23. Observed LQ/LR amplitude ratios and theoretical $|U_L|/U_{Rz}|$ parameters for RULISON.

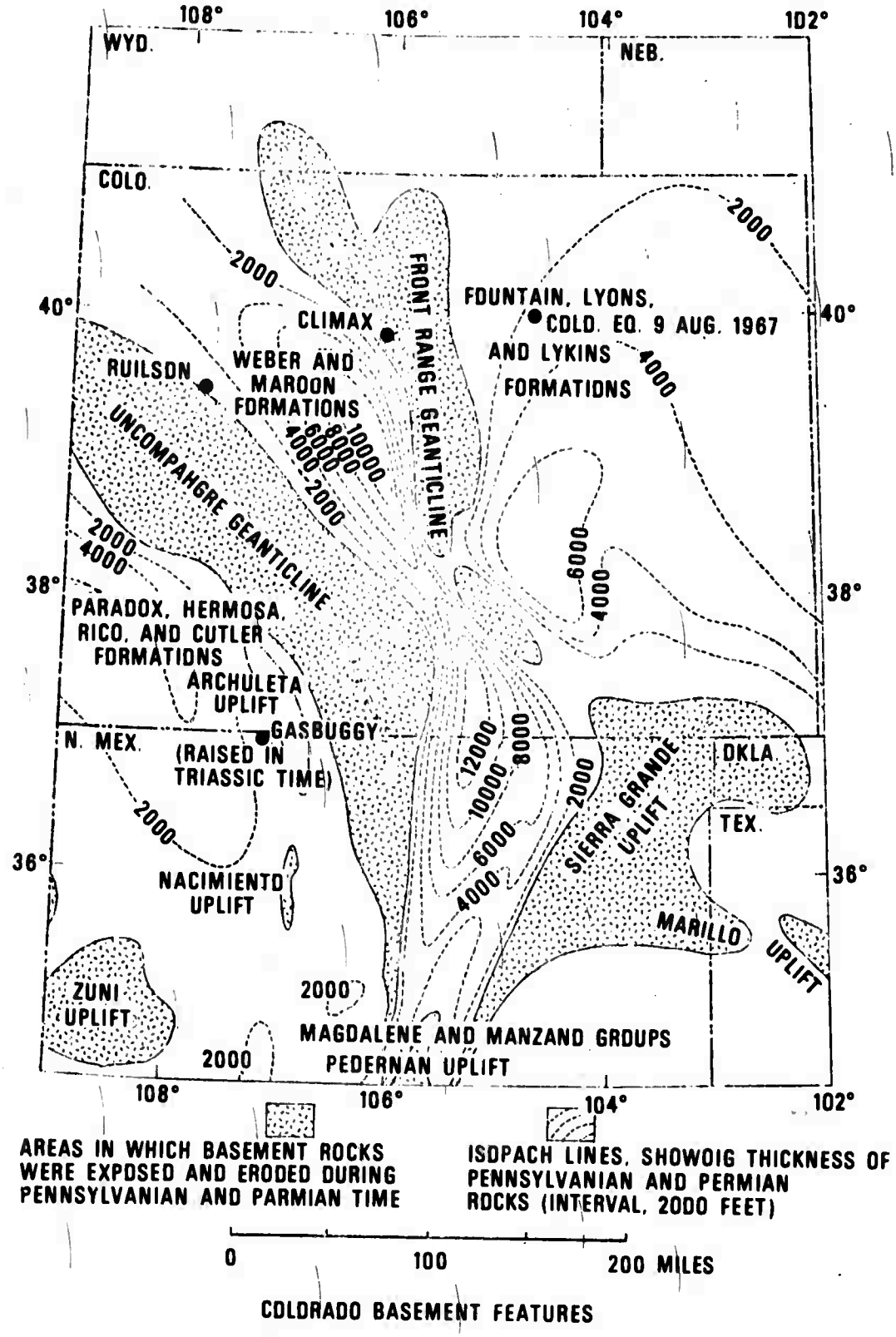

Figure 24. Map of the Colorado basement features.

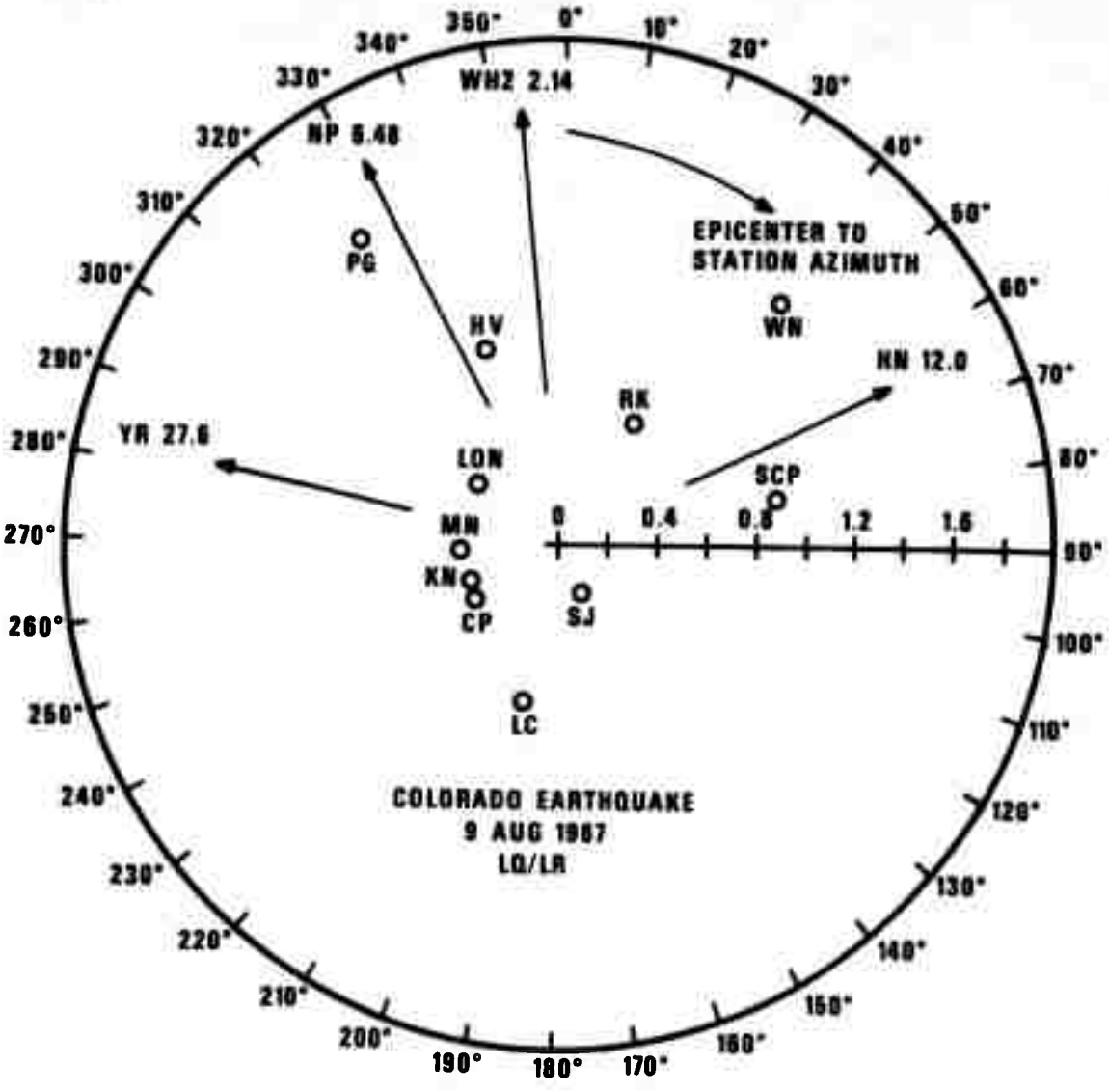

Figure 25. Observed LQ/LR amplitude ratios for the 9 August 1967 earthquake.

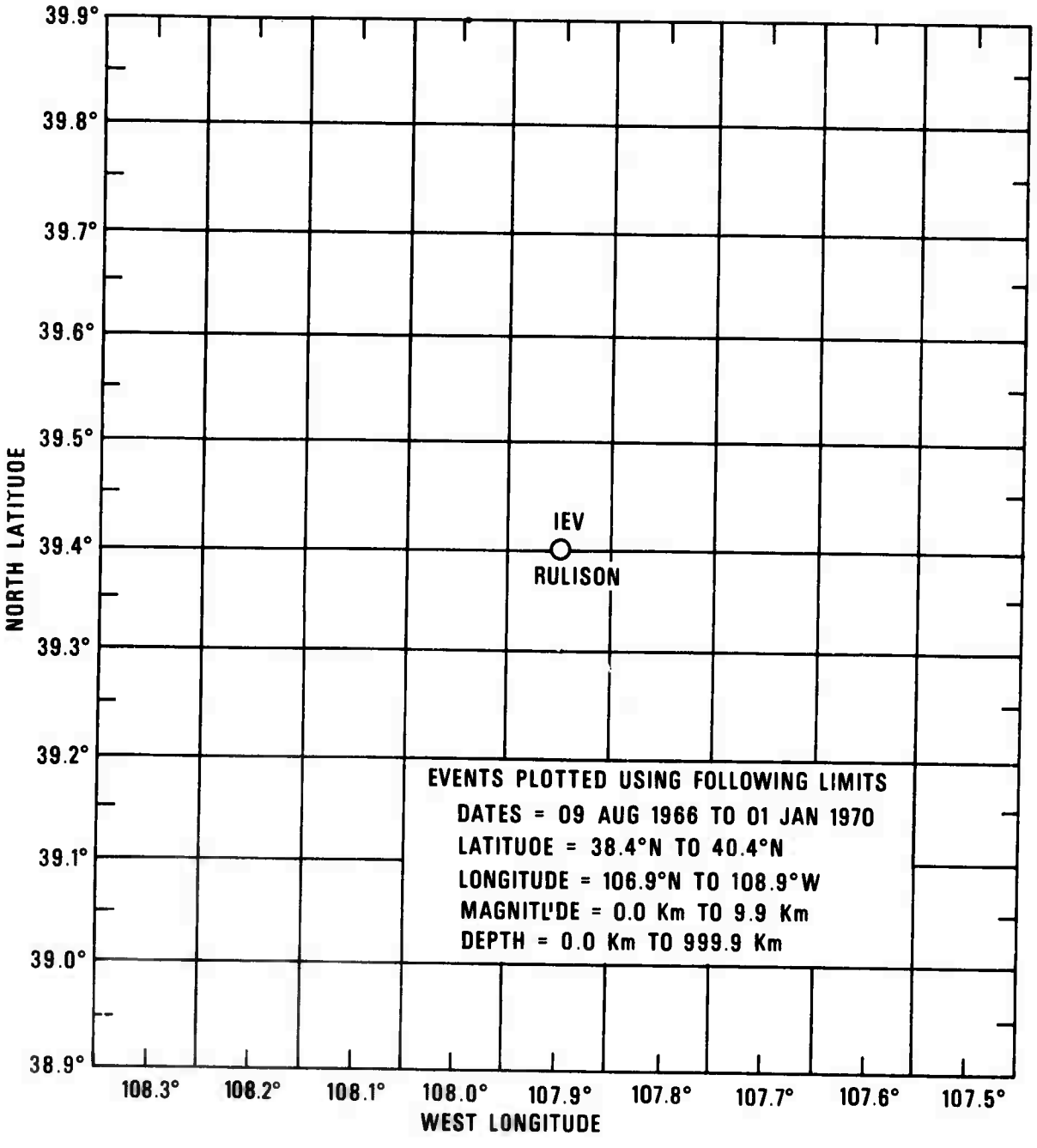

Figure 26. Seismicity of the RULISON source region.

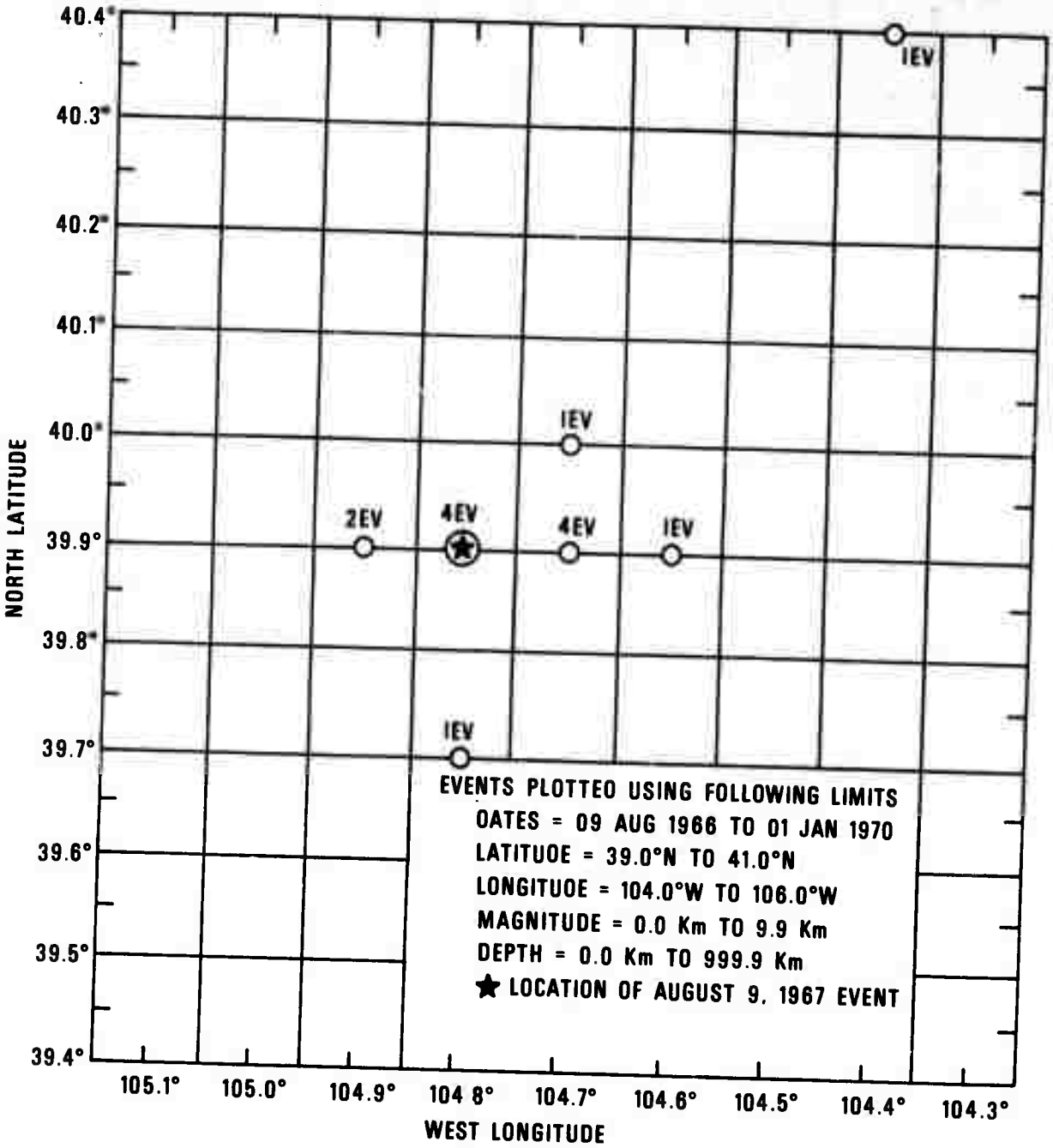

Figure 27. Seismicity of the 9 August 1967 Colorado earthquake region.

TABLE I

Event Description

For

RULISON

Date: 10 September 1969

Time of Origin: 21:00:00.1Z

Magnitude: 4.62 with standard deviation of ±0.36 (11 stations)

Location: Western Colorado situated between the White River uplift and the Uinta Basin

Coordinates:

Latitude: 39°24'21"N

Longitude: 107°56'53"W

Environment:

Geological Medium:	Mesa Verde Sandstone
Surface Elevation:	8154 feet above mean sea level
Shot Elevation:	277 feet below mean sea level
Shot Depth:	8431 feet below surface

TABLE II

Principal Phases for NULISON

CODE	STATION	DISTANCE (km)	DISTANCE (deg)	INST.	MAGNIFICATION (k) FILMx10	PHASE	TRAVEL TIME OBSERVED MIN	TRAVEL TIME OBSERVED SEC	PERIOD T SEC	MAXIMUM AMPLITUDE A/T	MAGNITUDES m_b	MAGNITUDES M_s	MAGNITUDES m_e	MAGNITUDES M_s^c
U80	Unita Basin, Utah	172.0	1.55	SPZ	0.54	P_n	00	29.4	0.3	1366.0	5.06		4.47 (7.9)	
				SP2	0.58	e	00	30.2	0.3	254.2				
				SPZ	0.58	P_g	00	31.3	0.4	972.2				
				SPZ	0.54	e	00	39.3	0.4	985.6				
				SPE	0.06	L_g	00	58.0	0.4	194.4				
KN-UT	Kanab, Utah	503.0	4.52	SPZ	23.8	P_n	01	11.3	0.4	116.0	5.31		4.89 (7.9)	
				SP2	23.8	e	01	12.0	0.4	106.0				
				SPZ	23.8	e	01	12.5	0.4	459.0				
				SPZ	7.75*	P_g	01	20.9	0.5	3270.0				
				SPR	24.7	e	03	12.5	0.8	643.0				
				SPT	8.75*	L_g			0.5	3435.0				
				LPT	15.5*	LQ			12.0	182.0				
				LP2	32.8	LR			12.0	320.0		3.73		4.31
ALQ	Albuquerque, New Mexico	512.8	4.61	SPZ	362.0	P_n	01	12.9	0.4	18.8	4.67		3.96 (7.9)	
				SPN	362.0	L_g	02	21.0	1.4	452.0				
				LPZ	5.4	LR			14.0	186.0		3.49		4.09
TFO	Tonto Forest, Arizona	641.0	5.76	SPZ	62.5	P_n	01	28.3	0.3	30.0	5.03		4.56 (7.9)	
				SPZ	7.50	e	01	29.8	0.3	25.0				
				SP2	32.6 *	P_g	01	43.4	0.4	768.0				
				SPE	7.50	L_g	03	03.0	0.6	975.0				
				LPE	2.50	LQ			11.5	125.0				
				LPZ	8.50	LR			14.0	157.0		3.58		4.12
LC-NM	Las Cruces, New Mexico	787.0	7.07	SPZ	76.5	P_n	01	46.7	0.5	7.60	4.69		4.17 (7.9)	
				SPZ	76.5	e	01	50.2	0.8	18.0				
				SPZ	76.5	e	02	03.4	0.6	28.7				
				SPZ	76.5	P_g	02	10.9	0.9	373.0				
				LPR	42.9	LQ			16.0	19.0				
				LPZ	5.20	LR			16.0	122.0		3.62		4.11
LAO	LA5A, Montana	822.0	7.39	SPZ	-	P_n	01	48.7	0.4	44.7	5.51		5.06 (7.9)	
				LPZ	-	LR			17.7	162.0		3.66		4.25
TUC	Tucson, Arizona	827.8	7.45	SPZ	362.0	P_n	01	48.7	0.5	4.88	4.59		4.03 (7.9)	
				SPN	362.0	L_g	03	42.0	1.3	394.0				
				LPZ	2.70	LR			9.0	329.0		4.08		4.57
CH2NB	Crete, Nebraska	957.0	8.61	SPZ	13.3	P_n	02	05.4	0.3	213.0	6.45		5.02 (8.5)	
				SP2	13.3	P_g	02	39.1	-	-				
				SPN	13.9	L_g	04	35.0	-	-				
				LPZ	2.39	LR			12.0	141.0		3.81		4.27
BP-CL	Bishop, Calif.	965.0	8.68	SPZ	148.0	P_n	02	(06.0)	0.8	9.00	5.09		4.58 (7.9)	
				SPZ	148.0		02	(07.0)	0.6	30.1				
				SP2	148.0	e	02	(11.0)	0.7	35.4				
				SPZ	148.0	P_g	02	(40.0)	0.6	24.9				
				LPZ	42.5	LR			12.0	79.1		3.58		4.03
BMO	Blue Mountain, Oregon	981.0	8.82	SPZ	830.0	P_n	02	11.3	0.4	7.08	5.01		4.48 (7.9)	
				SPZ	25.0	e	02	12.2	0.6	97.5				
				SPZ	25.0	e	02	29.3	0.6	87.8				
				SPZ	25.0	P_g	02	40.6	0.6	87.8				
				LPZ	25.0	LR			(19.0)	28.6		(3.16)		(3.60)
BY-IO	Bloomfield, Iowa	1329.0	11.95	SP2	72.0	P	02	(51.0)	0.4	44.9	5.75		4.63 (8.5)	
				SPZ	22.0	P_g	03	41.9	0.5	133.0				
				SPT	24.0	L_g	06	43.0	0.8	379.0				
				LPZ	12.3	LR			13 0	32.1		3.37		3.80
LON	Longmire, Washington	1390.2	12.50	SPZ	181.0	P_n	03	04.6	0.6	4.60	4.71		4.80 (7.9)	
				SPE	181.0	L_g	06	46 0	1.1	9.10				
				LPZ	2.70	LR			14.0	118.0		4.02		4.38
COR	Corvallis, Oregon	1394.0	12.54	SPZ	45.3	P	03	03.0	0.6	61.9	5.84		4.85 (8.5)	
				LPN	2.70	LQ			11.0	56.8				
				LPZ	2.70	LR			11.0	109.0		3.99		4.35
SJ-TX	San Jose, Texas	1583.0	14.23	SPZ	330.0	P	03	29.8	0.8	8.60	4.46		4.06 (8.5)	
				SPZ	60.0	P_g	04	31.3	1.0	62.5				
				SPR	321.0	L_g	08	04.0	1.3	59.9				
				LPZ	2.37	LR			15.0	84.5		3.97		4.31
GH-MS	Greenville, Mississippi	1658.0	14.91	LPZ	4.80	LR			12.0	84.0		3.98		4.33

TABLE II (Cont'd.)

Principal Phases for RULISON

CODE	STATION	DISTANCE (km)	DISTANCE (deg)	INST.	MAGNIFICATION (k) FILMx10	PHASE	TRAVEL TIME OBSERVED MIN	TRAVEL TIME OBSERVED SEC	PERIOD T SEC	MAXIMUM AMPLITUDE A/T	MAGNITUDES m_b	MAGNITUDES M_s	MAGNITUDES m_e	MAGNITUDES M_s^C
RK-ON	Nedleke, Onterio	1691.0	15.21	SPZ	288.0	P	03	32.2	0.5	39.0	4.89		4.78	
				5PZ	288.0	P_g	04	41.0	0.6	27.8			(8.5)	
				5PT	339.0	L_g	07	32.1	0.8	47.8				
				5PZ	288.0	e	07	49.7	0.8	32.5				
				LPT	58.1	LQ			14.0	28.9				
				LPZ	70.5	LR			19.0	25.1		3.48		
WQ-IL	Wateeke, Illinois	1740.0	15.64	5PZ	120.0	P	03	(44.9)	0.4	27.0	4.47		4.64	
				5PZ	22.0	P_g	04	52.2	0.4	56.0			(8.5)	
				5PT	22.0	L_g	08	23.0	0.7	127.0				
				LPZ	19.2	LR			13.0	79.6		3.99		
PG28C	Prince George, British Colombia	1960.0	17.63	5PZ	277.0	P	04	07.9	0.4	34.2	4.43			
				5PZ	277.0	a	04	09.7	0.6	23.4				
				5PZ	277.0	a	04	10.7	0.7	44.0				
				LPT	123.0	LQ			(16.0)	(11.6)				
				LPZ	96.6	LR			12.5	49.1		3.89		
CPU	Cumberlend Plateau, Tenn.	2018.0	18.15	5PZ	40.0	P	04	13.2	(0.8)	(33.6)	(4.45)			
				5PN	370.0	L_g			-	-				
				LPN	2.00	LQ			12.5	143.0				
				LPZ	1.90	LR			13.0	(363.0)		(4.77)		
GZ-UH	Galion, Ohio	2146.0	19.30	5PZ	162.0	P	04	(26.9)	0.6	17.1	4.23			
				5PT	158.0	L_g	10	30.0	0.8	37.2				
				LPZ	11.0	LR			(17.0)	(84.5)		(3.60)		
A5-PA	Altoone, Pennsylvania	2504.0	22.51	5PZ	265.0	P	05	01.2	0.6	12.8	4.36			
				5PZ	265.0	a	05	08.0	(0.7)	13.6				
				5PT	300.0	L_g			1.2	49.4				
				LPZ	27.3	LR			12.5	12.6		3.46		
SCP	Steta College, Pennsylvania	2558.1	23.01	5PZ	90.6	P	05	06.2	0.8	36.2	4.86			
				5PN	90.6	L_g	12	06.0	1.1	105.0				
				LPN	2.70	LQ			9.0	53.0				
				LPZ	2.70	LR			11.0	106.0		4.40		
BE-FL	Belleview, Fle.	2643.0	23.77	LPZ	4.34	LR			17.0	11.2		3.46		
PJ-PA	Pottstown, Pa.	2757.0	24.80	5PZ	117.0	P	05	24.4	0.6	9.20	4.42			
				5PT	227.0	L_g	13	17.9	1.4	33.1				
				LPZ	10.5	LR			14.0	25.5		3.85		
HN-ME	Houlton, Maine	3320.0	29.85	5PZ	98.5	P	06	07.1	1.0	15.2	4.78			
				LPZ	56.1	LR			15.0	46.1		4.22		
COL	College, Alaska	3819.7	34.35	5PZ	181.0	P	06	48.7	0.8	20.4	5.01			
FB-AK	Fairbanks, Alaska	3843.0	34.56	5PZ	162.0	P	06	50.4	0.6	17.9	4.95			
				5PZ	162.0	a	06	52.7	0.6	16.9				
				5PZ	162.0	e	07	16.2	0.6	6.30				
				LPZ	16.5	LR			15.0	44.5				
NP-NT	Mould Bay Northwest Terr.	4147.0	37.30	5PZ	226.0	P	07	13.3	0.4	3.72	4.07	4.32		
				5PZ	226.0	a	07	16.4	0.5	112.0				
				SPZ	226.0	PcP	09	32.5	0.4	124.0				
				LPT	16.4	LQ			(14.0)	(18.1)				
				LPZ	17.5	LR			16.0	42.7		4.40		
ARE	Arequipa, Peru	7247.0	65.17	5PZ	90.6	P	10	45.4	1.1	16.2	5.21			

A/T mu/sec
() Doubtful values or phases
- Not measureable due to clipping, etc.
* Measurements made from playouts
a Phases measured but not identified

TABLE III

Location Results

	ALL AVAILABLE STATIONS WITHOUT TRAVEL-TIME ANOMALIES			COMMON NETWORK WITHOUT TRAVEL-TIME ANOMALIES		COMMON NETWORK WITH TRAVEL-TIME ANOMALIES	
	RULISON Depth Restrained	DEPTH Free RULISON	Earthquake*	RULISON	Earthquake*	RULISON	Earthquake
Number of Stations	66	66	10	10	10	10	10
Azimuth Aperture (Deg)	200	200	179	170	179	170	179
Magnitude of Shift (km)	1.37	5.65	27.30	15.73	27.30	15.41	14.42
Azimuth of Shift (deg)	263.2	31.1	10.4	38.4	10.4	171.7	348.7
Standard deviation of errors (sec)	1.181	1.078	1.422	1.491	1.422	1.069	1.075
Area of 95% confidence ellipse (sq. km)	324	273	3767	4607	3767	2396	2166
Depth		41km					
Computed Origin Time	21:00:07.44	21:00:02.02	13:25:10.28	21:00:02.48	13:25:10.28	20:59:58.25	13:25:07.97

*All available stations for the earthquake were also used in the common network locations.

TABLE IV

List of Events Occurring in the 9 August 1967 Colorado Earthquake Source Region

DATE	ORIGIN TIME	LATITUDE	LONGITUDE	DEPTH KM	MAGNITUDE
14 Nov 66	20:02:35.8	39.9N	104.7W	5	4.1
03 Feb 67	05:27:58.0	39.7N	104.8W	5	4.3
10 Apr 67	19:00:25.6	39.9N	104.8W	5	4.8
10 Apr 67	20:11:14.1	39.9N	104.9W	5	4.8
10 Apr 67	23:58:40.7	39.9N	104.8W	5	0.0
27 Apr 67	17:24:41.7	39.9N	104.7W	5	4.4
19 Jun 67	15:39:22.0	39.9N	104.8W	5	0.0
09 Aug 67	13:25:06.2	39.9N	104.7W	5	5.3
15 Nov 67	07:10:12.1	39.9N	104.6W	5	3.7
27 Nov 67	05:09:22.7	40.0N	104.7W	5	5.2
27 Nov 67	05:35:00.7	39.9N	104.7W	5	4.4
27 Nov 67	05:42:53.3	39.9N	104.9W	5	0.0
15 Jul 68	18:33:12.1	39.9N	104.8W	5	0.0
26 May 69	01:30:08.6	40.4N	104.4W	33	4.2

LIMITS OF SEARCH

Dates: 9 August 66 to 1 Jan 70
Latitude: 39.0°N to 41.0°N
Longitude: 104.0°W to 106.0°W
Magnitude: 0.0 to 9.9

APPENDIX I

Station Locations and Elevations for RULISON

CODE	STATION	DISTANCE (km)	LATITUDE	LONGITUDE	ELEVATION (km)
UBO	Unita Basin Observatory, Utah	0172	40°19'18"N	109°34'07"W	1.596
KN-UT	Knab, Utah	0503	37°01'22"N	112°49'39"W	1.737
ALQ	Albuquerque, New Mexico	0513	34°56'30"N	106°27'30"W	1.853
TFO	Tonto Forest Observatory, Arizona	0641	34°17'12"N	111°16'03"W	1.609
LC-NM	Las Cruces, New Mexico	0787	32°24'08"N	106°35'58"W	1.585
(LAO)	LASA, AO-10	0822	46°41'19"N	106°13'20"W	0.744
TUC	Tucson, Arizona	0828	32°18'35"N	110°46'56"W	0.980
CR2NB	Crete, Nebraska	0957	40°39'52"N	092°51'15"W	0.442
BP-CL	Bishop, California	0965	37°21'36"N	118°41'25"W	2.317
BMO	Blue Mountain Observatory, Oregon	0981	44°50'56"N	117°18'20"W	1.189
BY-IO	Bloomfield, Iowa	1329	40°46'09"N	092°27'09"W	0.259
LON	Longmire, Washington	1390	46°45'00"N	121°48'36"W	0.854
COR	Corvallis, Oregon	1394	44°35'09"N	125°18'12"W	0.123
SJ-TX	San Jose, Texas	1583	27°36'43"N	098°18'46"W	0.114
GH-MS	Greenville, Mississippi	1658	33°19'45"N	091°02'07"W	0.030
RK-ON	Red Lake, Ontario	1691	50°50'20"N	093°20'40"W	0.366
WQ-IL	Watseka, Illinois	1740	40°51'56"N	087°35'11"W	0.198
PG2BC	Prince George, British Columbia	1960	53°59'50"N	122°31'23"W	0.914
CPO	Cumberland Plateau Observatory, Tenn.	2018	35°35'41"N	085°34'13"W	0.574
GZ-OH	Galion, Ohio	2146	40°39'36"N	082°47'00"W	0.372
A5-PA	Altoona, Pennsylvania	2504	40°43'59"N	078°31'26"W	0.469
SCP	State College, Pennsylvania	2558	40°47'42"N	077°51'54"W	0.352
BE-FL	Belleview, Florida	2643	28°54'19"N	082°03'52"W	0.021
PJ-PA	Pottstown, Pennsylvania	2757	40°16'58"N	075°35'01"W	0.091
WH2YK	Whitehorse, Yukon	3016	60°44'03"N	135°08'57"W	0.762
HN-ME	Houlton, Maine	3320	46°09'43"N	067°59'09"W	0.210
COL	College, Alaska	3820	64°53'08"N	147°48'04"W	*
FB-AK	Fairbanks, Alaska	3843	64°57'07"N	148°17'03"W	0.716
NP-NT	Mould Bay, Northwest Territories	4147	76°15'08"N	119°22'18"W	0.059
ARE	Arequipa, Peru	7247	16°27'43"S	071°29'29"W	2.452

*Elevation not known

APPENDIX 2

RULISON

Site Recording Information

STATION	DISTANCE (km)	EPI-STATION AZIMUTH	BACK AZIMUTH	R INSTALLED AZIMUTH	T INSTALLED AZIMUTH	SP INSTRUMENT	LP SPRENGNETHER
UBO	172.0	306.8	125.7	90°	0°	JM	x
KN-UT	502.6	239.8	56.8	95°	185°	Small Benioff	x
ALQ	513.0	164.6	345.5	90°	0°	Benioff	x
TFO	640.5	208.5	26.5	90°	0°	JM	x
LC-NM	786.6	170.7	351.5	133°	233°	Small Benioff	x
LAU	821.5	9.3	190.5	90°	0°	Hall-Sears	Geotech
TUC	828.0	198.9	17.2	90°	0°	Benioff	x
CR2NB	957.0	78.3	265.4	73°	163°	Geotech 18300	Geotech
BP-CL	965.2	259.8	73.1	274°	4°	Geotech 18300	Geotech
BMO	981.2	311.1	124.8	90°	0°	JM	X
BY-IO	1328.8	78.5	268.5	81°	177°	Small Benioff	x
LON	1390.0	310.4	121.0	90°	0°	Benioff	x
COR	1394.0	299.3	109.1	90°	0°	Benioff	x
SJ-TX	1582.7	142.8	328.2	127°	217°	Small Benioff	x
GH-MS	1658.0	108.8	298.8	107°	197°	Geotech 18300	Geotech
RK-ON	1690.9	36.6	226.8	58°	148°	Small Benioff	x
WQ-IL	1739.5	78.1	271.3	90°	180°	Geotech 18300	SL-210-220
PG2BC	1960.0	330.6	140.0	110°	20°	Small Benioff	x
CPO	2018.0	95.1	288.8	90°	0°	JM	x
GZ-OH	2145.7	78.2	274.5	93°	183°	Geotech 18300	SL-210-220
AS-PA	2503.5	77.2	276.3	96°	186°	Geotech 18300	Geotech
SCP	2558.0	76.9	276.4	90°	0°	Benioff	x
BE-FL	2642.8	108.2	302.9	115°	205°	Small Benioff	x
PJ-PA	2757.1	77.5	278.5	97°	187°	Geotech 18300	Geotech
WH2YK	3016.3	330.6	129.5	325°	055°	Benioff	x
HN-ME	3319.5	63.7	271.4	93°	183°	Small Benioff	x
COL	3820.0	331.0	118.4	90°	0°	Benioff	x
FB-AK	3843.2	330.9	117.9	0°	90°	Small Benioff	Geotech
NP-NT	4147.1	355.5	165.3	356°	86°	Small Benioff	x
ARE	7247.0	141.1	329.5	90°	0°	Benioff	x

JM: Johnson-Matheson

APPENDIX 3A.

System Response Curves WWSSS Network.

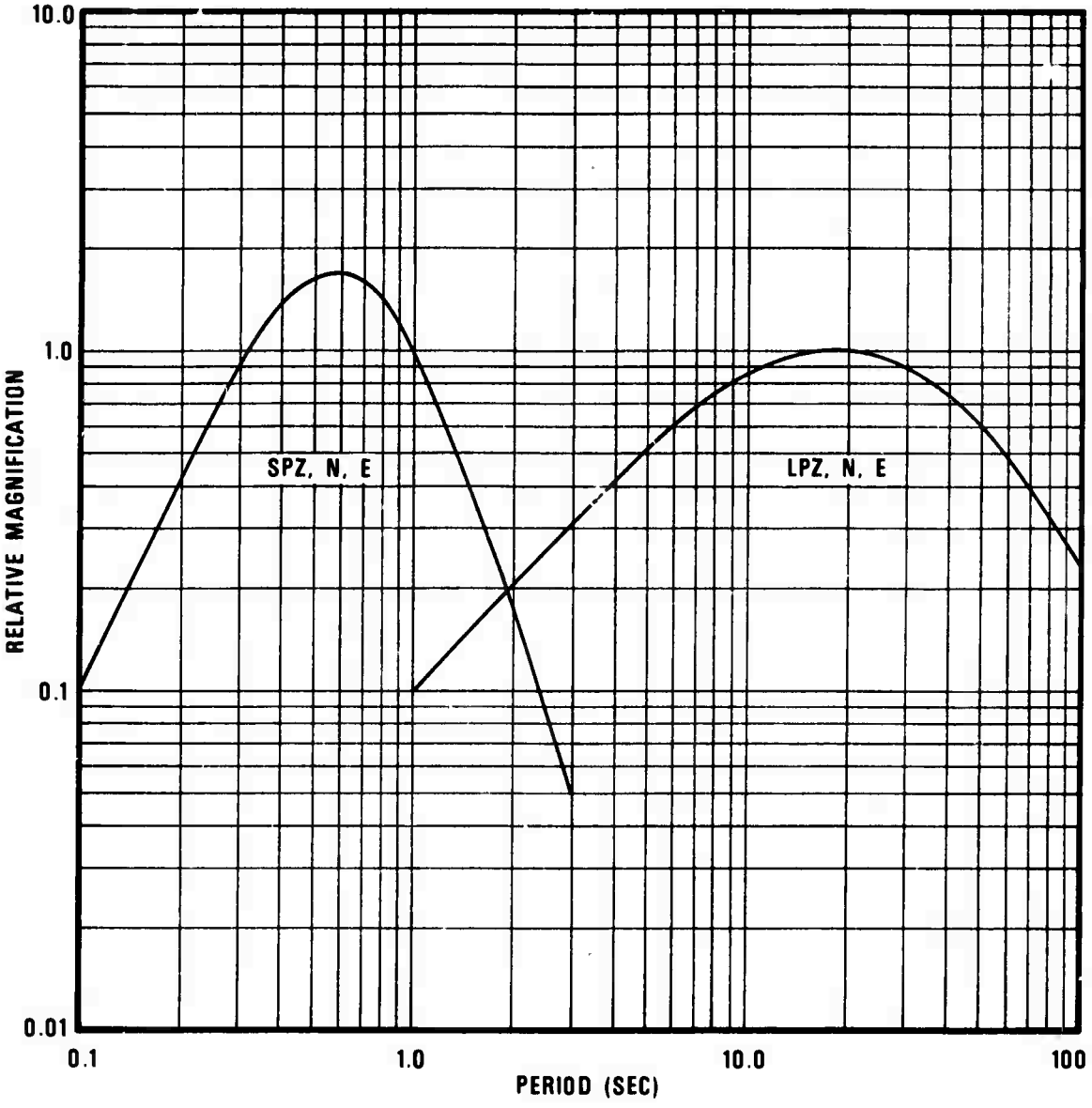

APPENDIX 3B.

LRSM Large or Small Benioff Short Period and Sprengnether Long Period.

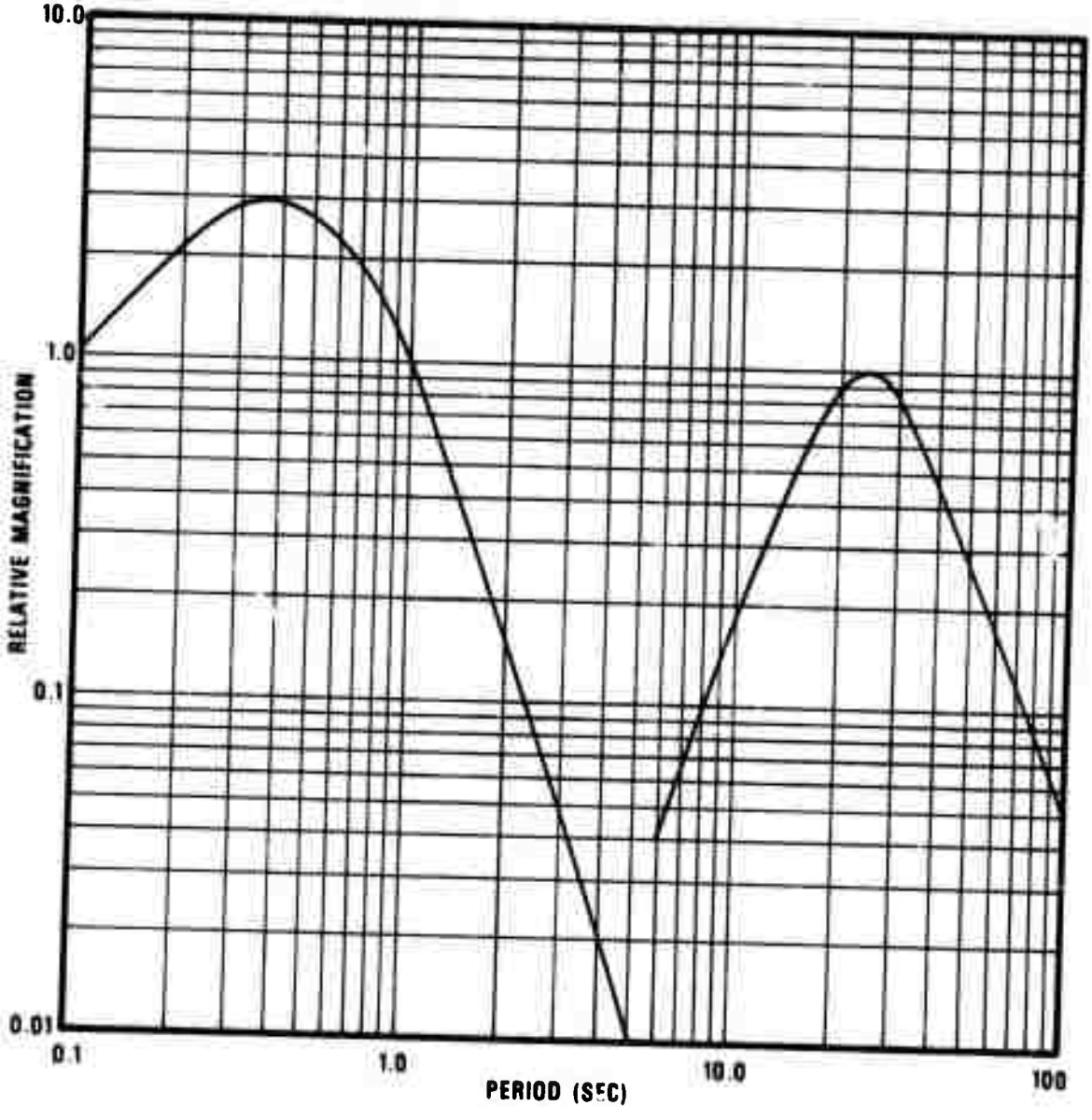

APPENDIX 3C.

LRSM Geotech 18300 Short Period.

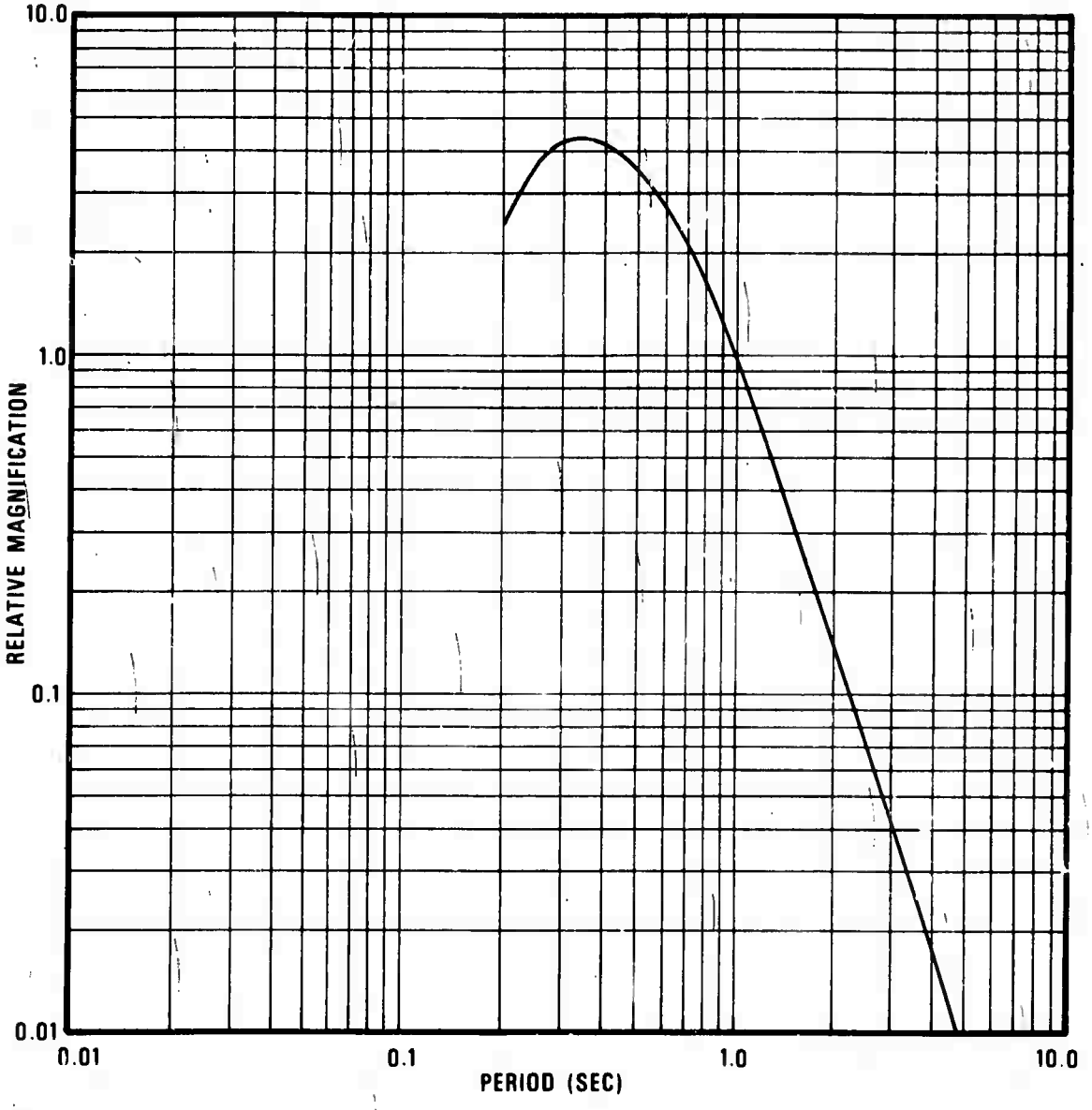

APPENDIX 3D.

VELA Johnson-Matheson Short Period.

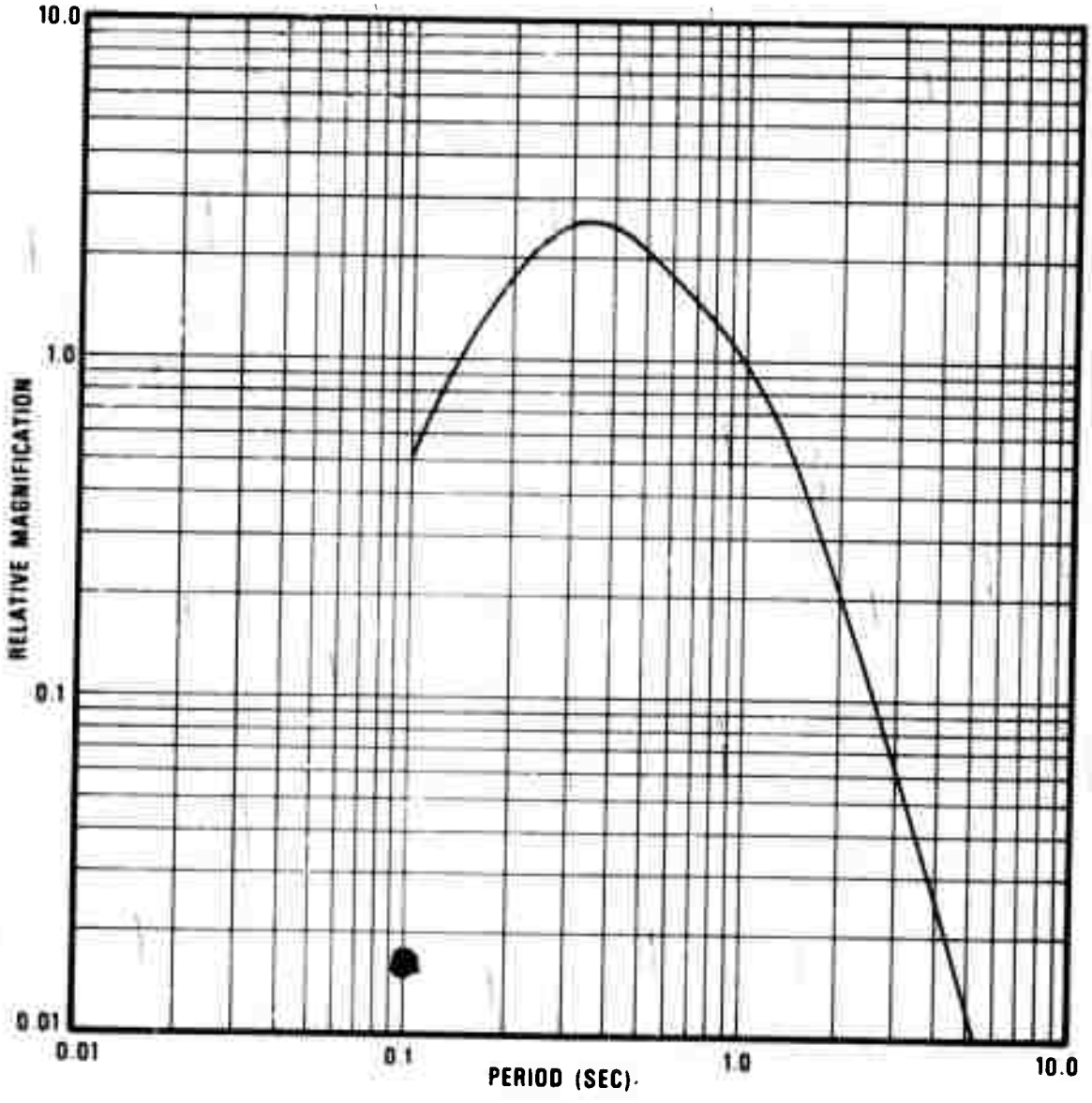

APPENDIX 4.

Distance Factors (B) for Surface Focus

DISTANCE (DEGREES)	B	DISTANCE (DEGREES)	B	DISTANCE (DEGREES)	B	DISTANCE (DEGREES)	B
1	-	26	3.4	51	3.7	76	3.9
2	2.2	27	3.5	52	3.7	77	3.9
3	2.7	28	3.6	53	3.7	78	3.9
4	3.1	29	3.6	54	3.8	79	3.8
5	3.4	30	3.6	55	3.8	80	3.7
6	3.6	31	3.7	56	3.8	81	3.8
7	3.8	32	3.7	57	3.8	82	3.9
8	4.0	33	3.7	58	3.8	83	4.0
9	4.2	34	3.7	59	3.8	84	4.0
10	4.3	35	3.7	60	3.8	85	4.0
11	4.2	36	3.6	61	3.9	86	3.9
12	4.1	37	3.5	62	4.0	87	4.0
13	4.0	38	3.5	63	3.9	88	4.1
14	3.6	39	3.4	64	4.0	89	4.0
15	3.3	40	3.4	65	4.0	90	4.0
16	2.9	41	3.5	66	4.0	91	4.1
17	2.9	42	3.5	67	4.0	92	4.1
18	2.9	43	3.5	68	4.0	93	4.2
19	3.0	44	3.5	69	4.0	94	4.1
20	3.0	45	3.7	70	3.9	95	4.2
21	3.1	46	3.8	71	3.9	96	4.3
22	3.2	47	3.9	72	3.9	97	4.4
23	3.3	48	3.9	73	3.9	98	4.5
24	3.3	49	3.8	74	3.8	99	4.5
25	3.5	50	3.7	75	3.8	100	4.4

APPENDIX 5

Description of Events for m_b versus ARZ and ERZ

No.	Date	Area/Event	Latitude	Longitude	Origin Time (Z)	Depth (km)	Body-Wave Magnitude	Rayleigh-Wave Magnitude
1	13 Sep 1963	Bilby - N.T.S.	37°03.633'N	116°01.30'W	17:00:00.1	0.76	5.80	3.92
2	26 Oct 1963	Shoal-Sand Springs Range, Nevada	39°12.017'N	118°22.817'W	17:00:00.1	0.37	4.80	2.48
3	29 Oct 1965	Long-Shot-Amchitka Island	51°26.294'N	179°10.950'E	21.00:00.1	0.70	5.85	4.06
4	21 Nov 1965	Test-Kazakh	49°48'N	73°06'E	04:57:57.9	----	*5.8	3.97
5	13 Feb 1966	Test-Kazakh	49°48'N	78°06'E	04:57:57.9	----	*6.3	4.51
6	20 Dec 1966	Greeley - N.T.S.	37°18.117'N	116°24.500'W	15:30:00.1	1.23	6.29	5.18
7	20 Jan 1967	Bourbon - N.T.S.	37°05.984'N	116°00.233'W	17:40:04.4	0.56	5.10	3.24
8	20 Jul 1962	Fallon, Nevada Eq.	39°38.833'N	118°12.667'W	09:02:08.3	20	4.40	2.85
9	29 Jan 1965	Kamchatka Eq.	54°48'N	161°42'W	09:35:25.7	33	*5.8	4.86
10	08 Feb 1965	Komandorsky Eq.	55°06'N	165°42'W	15:46:49.9	40	*5.6	5.82
11	14 Feb 1965	Komandorsky Eq.	55°06'N	165°36'W	17:01:13.9	20	*5.0	3.99
12	20 Apr 1965	Kamchatka Eq.	54°48'N	161°24'W	06:50:17.6	33	*5.3	4.85
13	20 Apr 1965	Seguam Eq.	52°24'N	172°00'E	06:43:08.8	35	*5.5	4.77
14	06 Nov 1965	Rat Island Eq.	51°24'N	176°42'E	22:30:20.5	40	*5.0	4.33
15	22 Nov 1966	Andreanoff Eq.	51°18'N	179°48'W	20:25:30.4	40	5.86	5.56
16	18 Nov 1966	Greenland Sea Eq.	73°24'N	06°48'E	18:07:54.0	33	*4.6	3.81
17	18 Nov 1966	Greenland Sea Eq.	73°24'N	06°48'E	18:48:43.9	33	*4.9	4.84
18	02 Mar 1967	California-Nevada Border Eq.	36°18'N	117°42'W	14:12:49.1	14	*4.4	2.66
19	13 Apr 1967	Guerrero, Mexico Eq.	18°30'N	100°12'W	19:59:51.9	86	*5.7	4.58
20	10 Sep 1969	Rulison-Colorado	39°24'N	107°57'W	21:00:00.1	2.5	4.90	3.13
21	09 Aug 1967	Colorado Eq.	39°54'N	104°42'W	13:25:06.2	5.0	4.81	3.47
22	23 Jan 1968	New Mexico Eq.	37°00'N	106°54'W	01:56:38.0	10.0	4.55	3.84

*USC&GS Magnitudes--all other magnitudes computed at SDL.

After Lambert et al (1969).

APPENDIX 6.

Additional Long Period Rayleigh-Wave Spectra

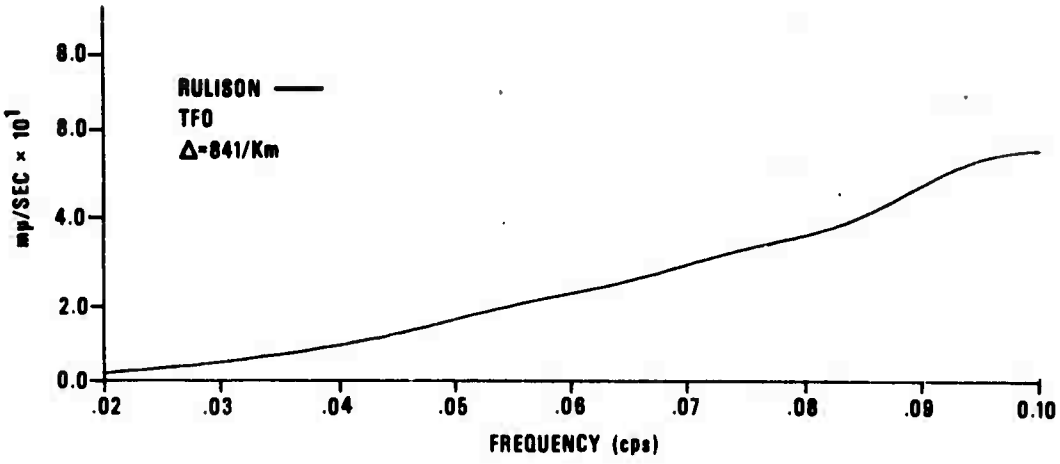

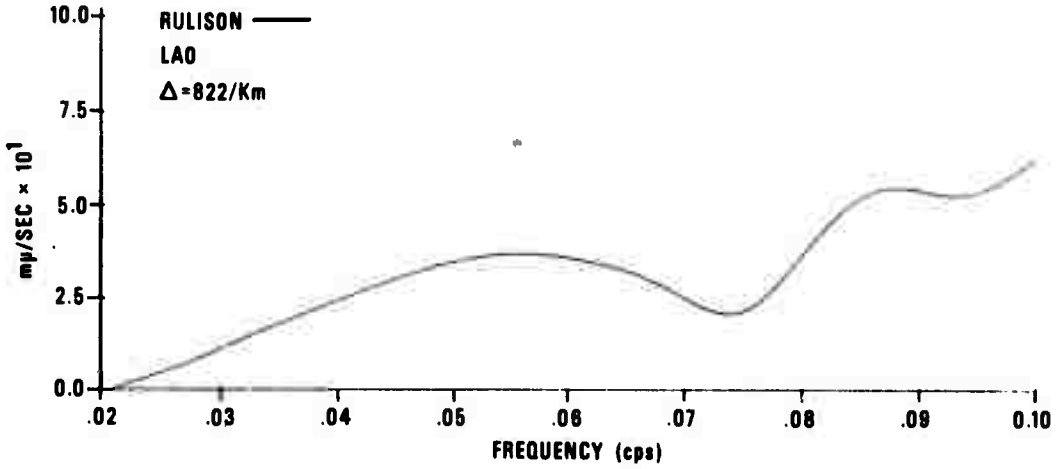

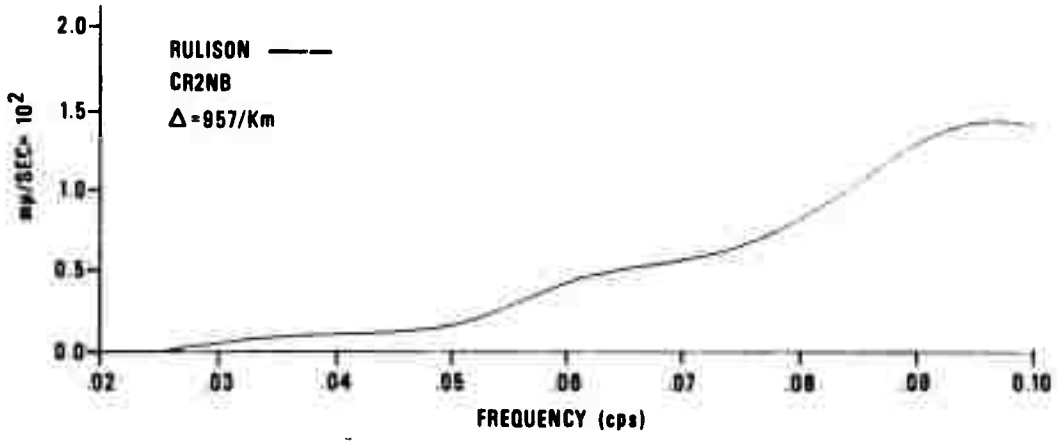

Additional Long Period Rayleigh-Wave Spectra

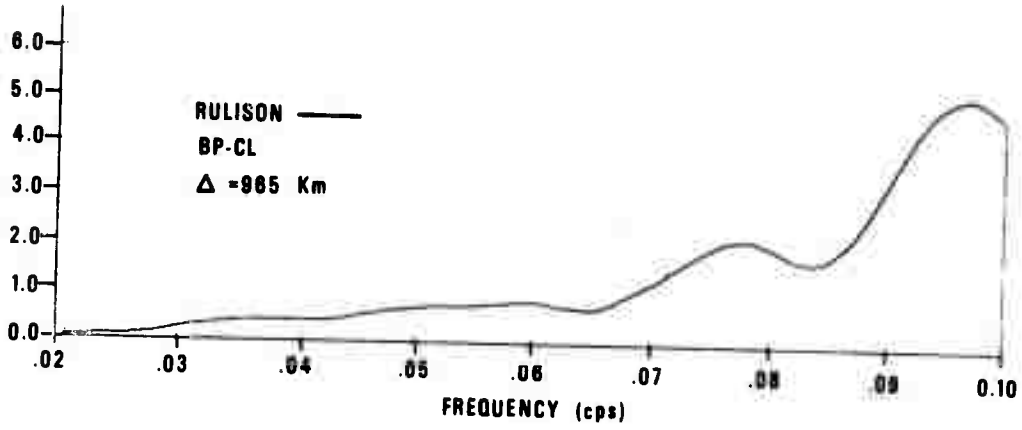

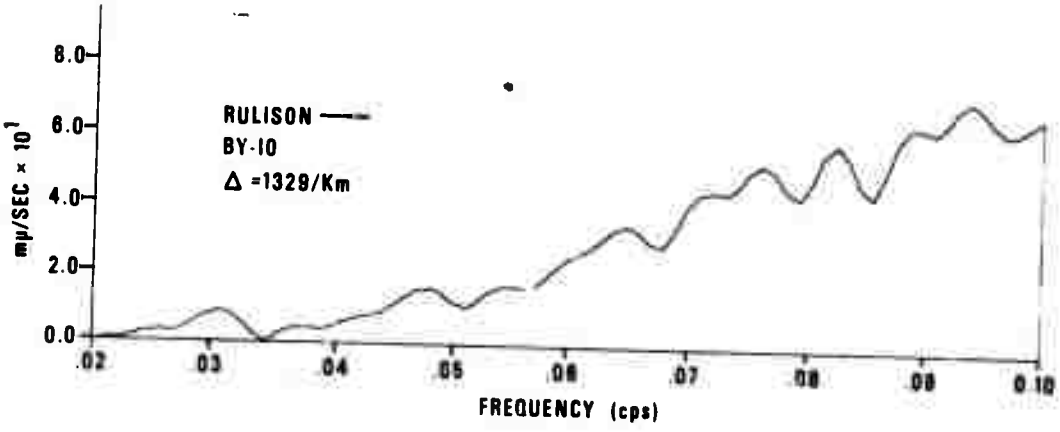

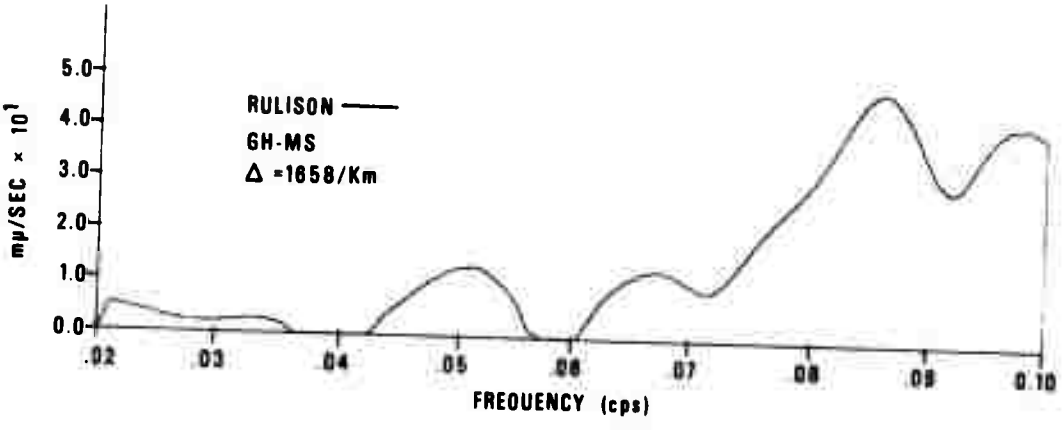

Additional Long Period Rayleigh-Wave Spectra

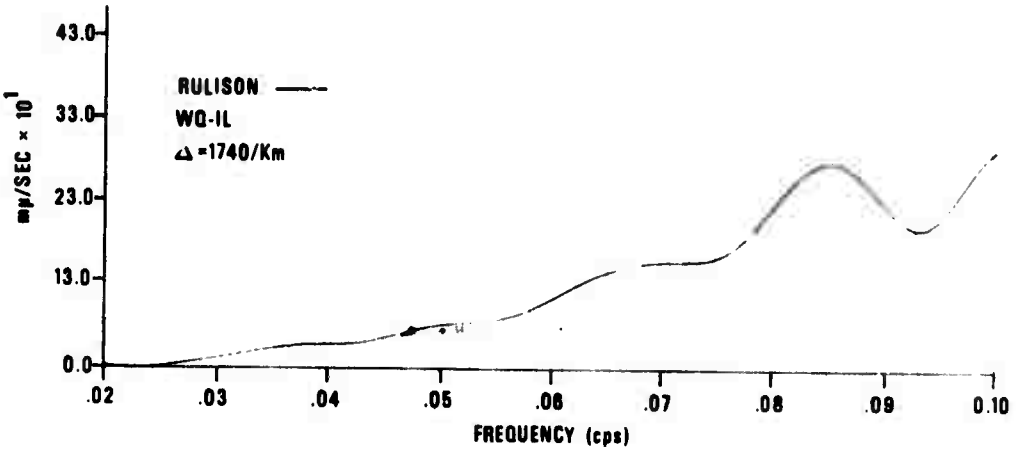

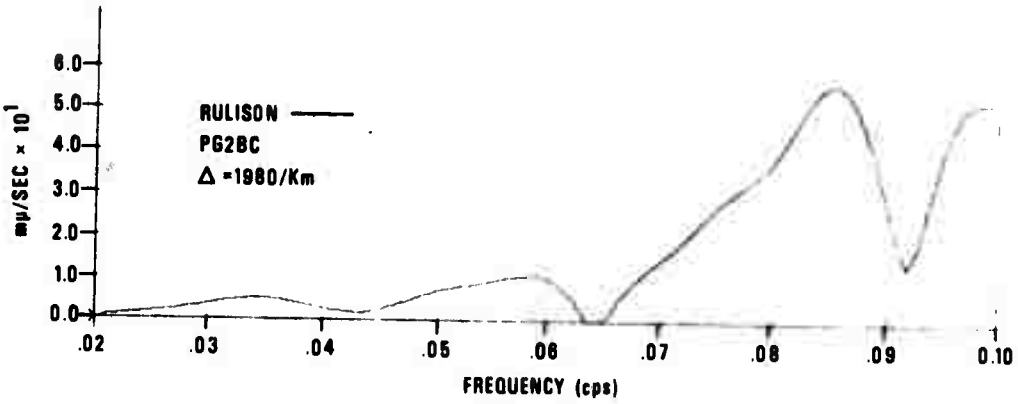

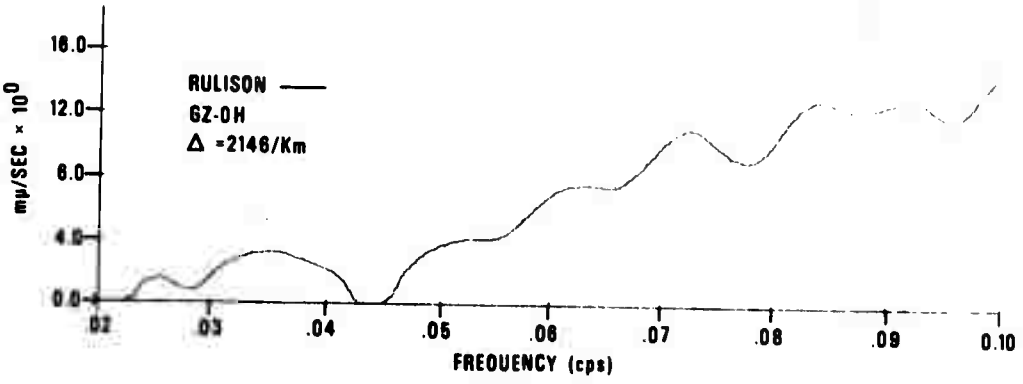

Additional Long Period Rayleigh-Wave Spectra

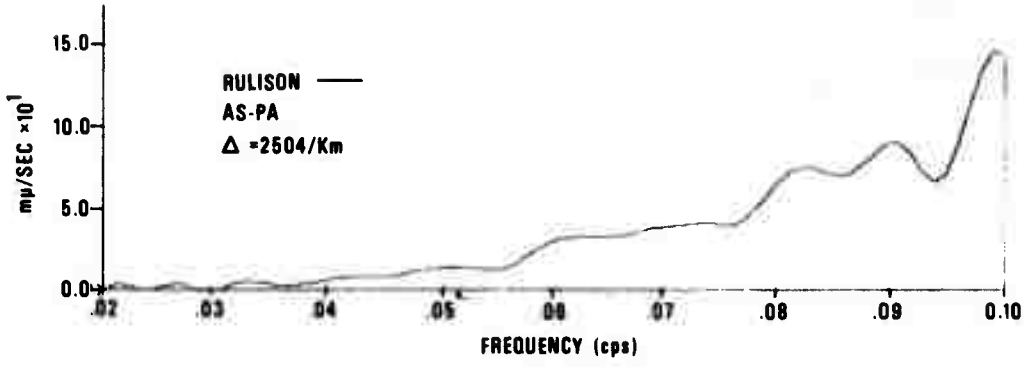

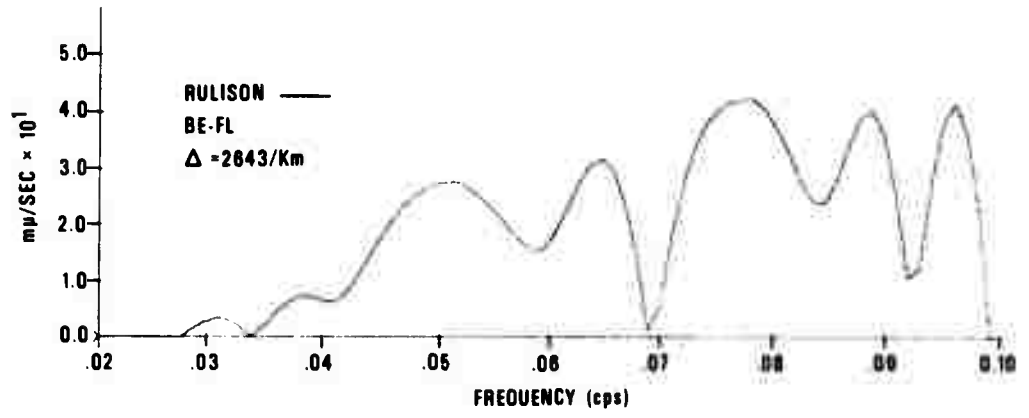

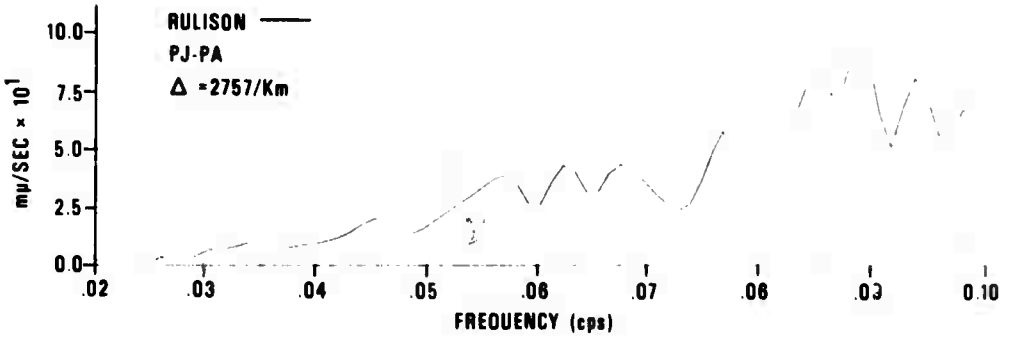

APPENDIX 6. (Cont'd.)

Additional Long Period Rayleigh-Wave Spectra

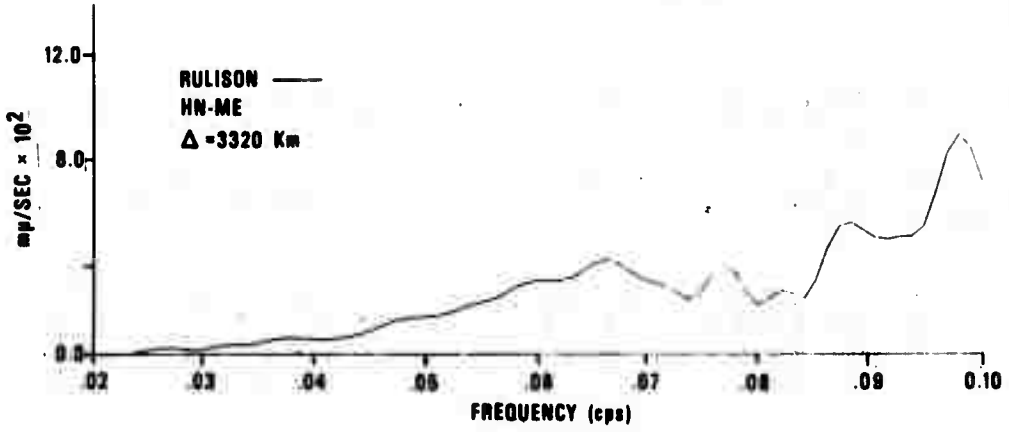

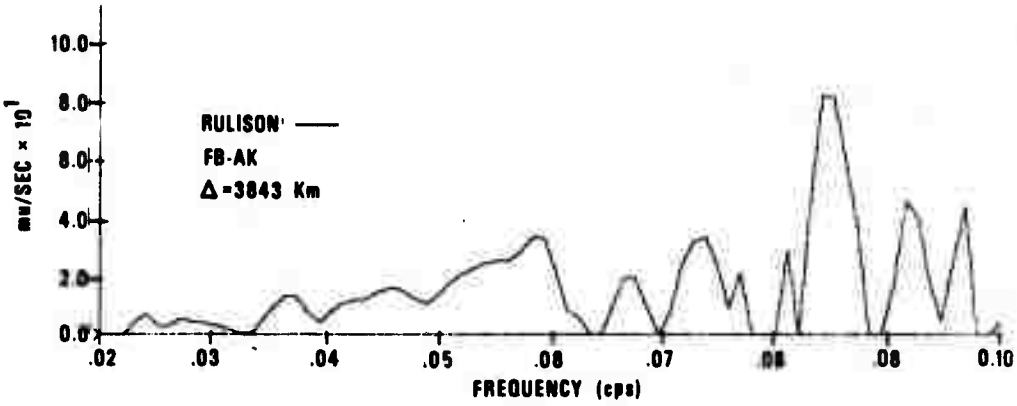

Description of Events for R_1 and R_2

Figure Symbol	Date	Area/Event	Latitude	Longitude	Origin Time (Z)	Depth (km)	Body-Wave Magnitude	Rayleigh-Wave Magnitude	Geologic Medium
●	13 Sep 1963	Bilby - N.T.S.	37°03.633'N	116°01.30'W	17:00:00.1	0.76	5.80	3.92	Tuff
●	26 Oct 1963	Shoal-Sand Springs Range, Nevada	39°12.017'N	118°22.817'W	17:00:00.1	0.37	4.80	2.48	Granite
●	29 Oct 1963	Long Shot-Amchitka Island	51°26.294'N	179°10.950'E	21.00:00.1	0.70	5.85	4.21	Andesite
●	20 Dec 1964	Greeley-N.T.S.	37°18.117'N	116°34.500'W	15:30:00.1	1.23	6.29	5.12	Tuff
●	20 Jan 1967	Benham - N.T.S.	37°05.984'N	116°00.233'W	17:40:04.4	0.56	5.10	3.24	Tuff
✱	18 Sep 1967	Rulison-Colorado	39°24.398'N	107°56.883'W	21:00:00.1	2.57	4.90	3.13	Sandstone
■	21 Nov 1965	Test-Kazakh	49°48'N	79°06'E	04:57:57.9	----	*5.8	3.97	----
■	13 Feb 1966	Test-Kazakh	49°48'N	79°06'E	04:57:57.9	----	*6.3	4.51	----
▲	24 Apr 1964	Turf - N.T.S.	37°08.983'N	116°03.317'W	21:10:00.2	0.49	4.95	+2.70	
▲	09 Oct 1964	Par - N.T.S.	37°09.083'N	116°04.617'W	14:00:00.1	0.92	4.78	+2.02	Alluvium
▲	26 Mar 1965	Cup - N.T.S.	37°08.850'N	116°02.563'W	15:34:08.2	0.75	5.25	+2.89	Tuff
▲	23 Jul 1965	Broca - N.T.S.	37°0.9847'N	116°01.983'W	17:00:00.0	0.53	5.22	+3.03	Tuff
▲	03 Dec 1965	Corduroy - N.T.S.	37°09.867'N	116°03.013'W	15;13:02.1	0.68	5.62	+2.97	Tuff
▲	19 May 1966	Dumont - N.T.S.	37°06.647'N	116°03.483'W	13:56:28.1	0.67	5.48	+3.30	Tuff
○	20 Jul 1962	Fallon, Nevada, Eq.	39°38.833'N	118°12.667'W	09:02:08.3	20	4.40	2.85	Tuff
○	29 Jan 1965	Kamchatka Eq.	54°48'N	161°42'W	09:35:25.7	33	*5.8	4.86	
○	08 Feb 1965	Komandorsky Eq.	55°06'N	165°42'W	15:46:49.9	40	*5.6	5.82	
○	14 Feb 1965	Komandorsky Eq	55°06'N	165°36'W	17:01:13.9	20	*5.0	3.99	
○	20 Apr 1965	Kamchatke Eq.	54°48'N	161°36'W	06:50:17.6	33	*5.3	4.85	
○	20 Apr 1965	Seguam Eq.	52°24'N	172°00'E	06:43:08.8	35	*5.5	4.77	
○	06 Nov 1965	Rat Island Eq.	51°24'N	176°42'E	22:30:20.5	40	*5.0	4.33	
○	22 Nov 1965	Andreanoff Eq.	51°18'N	179°48'W	20:25:30.4	40	5.86	5.56	
✱	23 Jan 1966	New Mexico	37°00'N	106°54'E	01:56:38.8	10	4.56	3.84	
○	18 May 1966	Greenland Sea Eq.	73°24'N	04°48'E	18:07:54.0	33	*4.6	3.81	
○	18 Nov 1966	Greenland Sea Eq.	73°24'N	06°48'E	18:48:43.9	33	*4.9	4.84	
○	02 Mar 1967	California-Nevada Border Eq.	36°18'N	117°42'W	14:12:49.1	14	*4.4	2.66	
○	13 Apr 1967	Guerrero, Mexico, Eq.	18°30'N	100°12'W	19:59:51.9	86	*5.7	4.56	
✱	09 Aug 1967	Colorado Eq.	39°54'N	104°42'W	13:25:06.2	5	4.81	3.47	
⊘	17 Aug 1966	S. Nevada Eq.	37°18'N	116°06'W	23:07:58.9	33	*5.2	+2.53	
⊘	18 Aug 1966	S. Nevade Eq.	37°24'N	116°06'W	06:14:58.6	9	*4.7	+1.93	
⊘	18 Aug 1966	S. Nevada Eq.	37°24'N	116°12'W	17:35:06.4	33	*5.2	+3.03	
⊘	19 Aug 1966	S. Nevada Eq.	37°18'N	116°18'W	00:18:55.8	33	*4.7	+2.27	
⊘	19 Aug 1966	S. Nevada Eq.	37°24'N	116°06'W	10:51:38.5	11	*4.5	+2.84	
⊘	22 Aug 1966	S. Nevada Eq.	37°18'N	116°12'W	06:27:30.2	33	*4.8	+2.43	
⊘	23 Sep 1966	S. Nevada Eq.	37°18'N	116°12'W	11:56:09.7	33	*4.5	+2.22	

* USCGS Magnitudes -- all other magnitudes computed at SDL.
+ Determined at distances < 1000 km

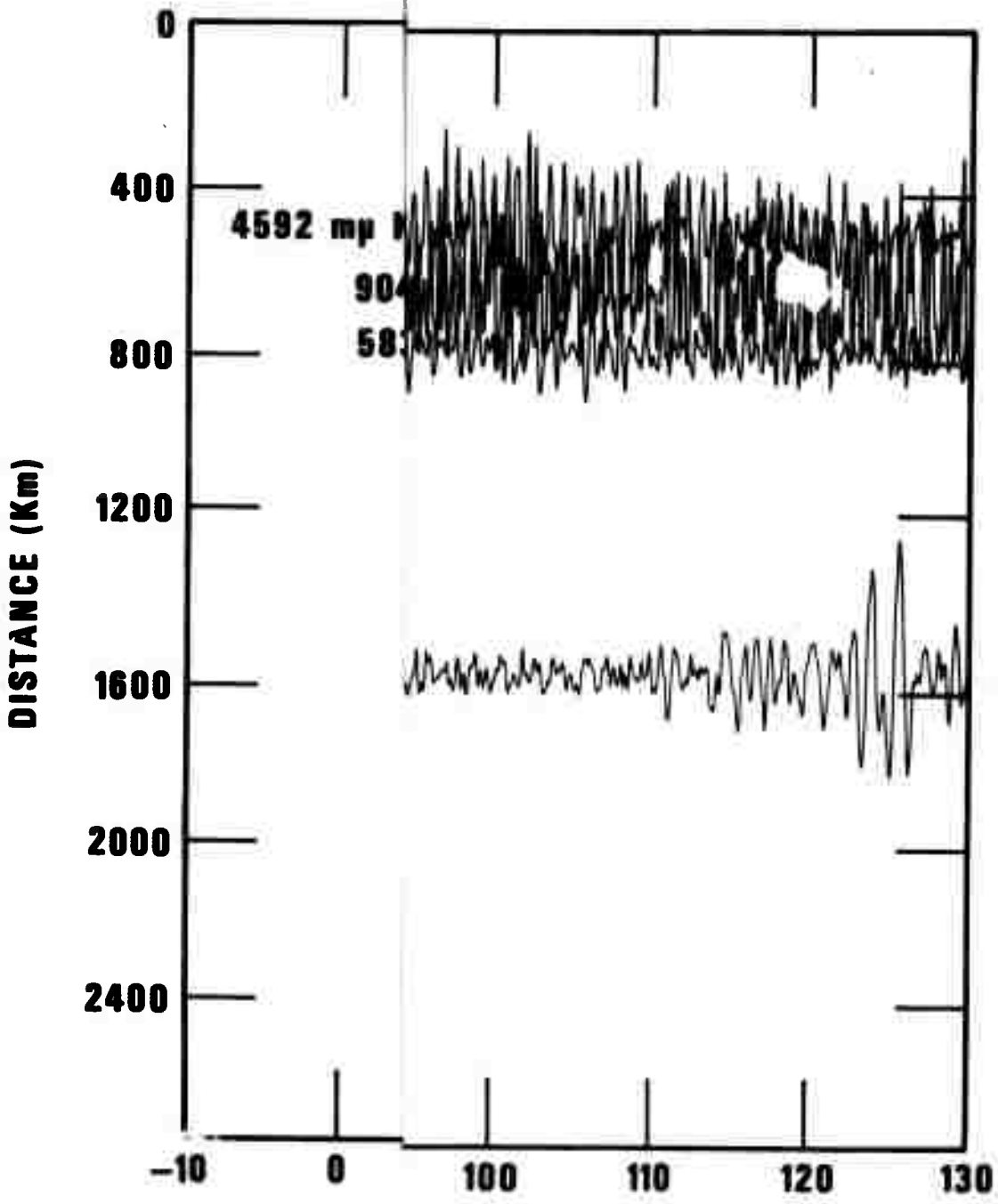

RULISON Seismograms

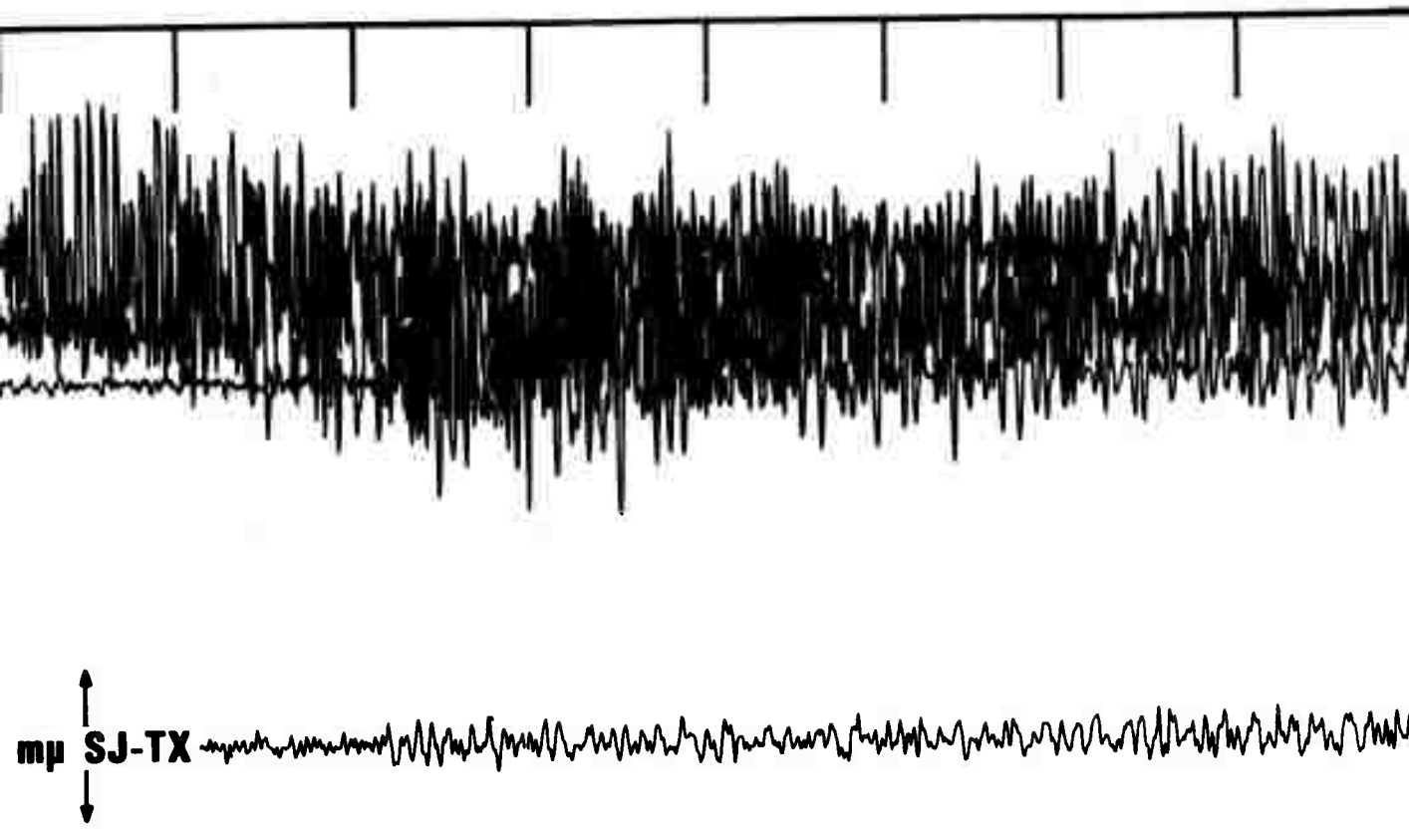

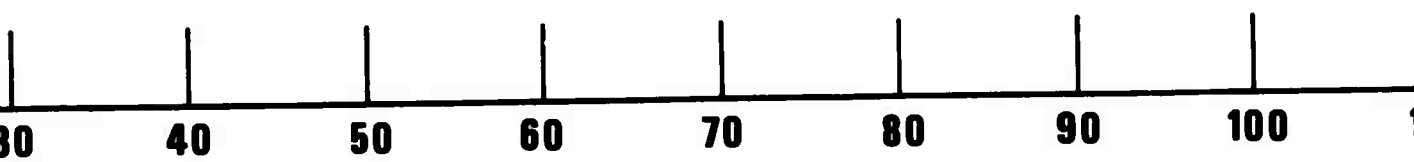

RULISON SOUTHEAST PROFILE P OR Pn
T–DIST/10.00 (SEC)

B

APPENDIX 8. RULISON Seismogr

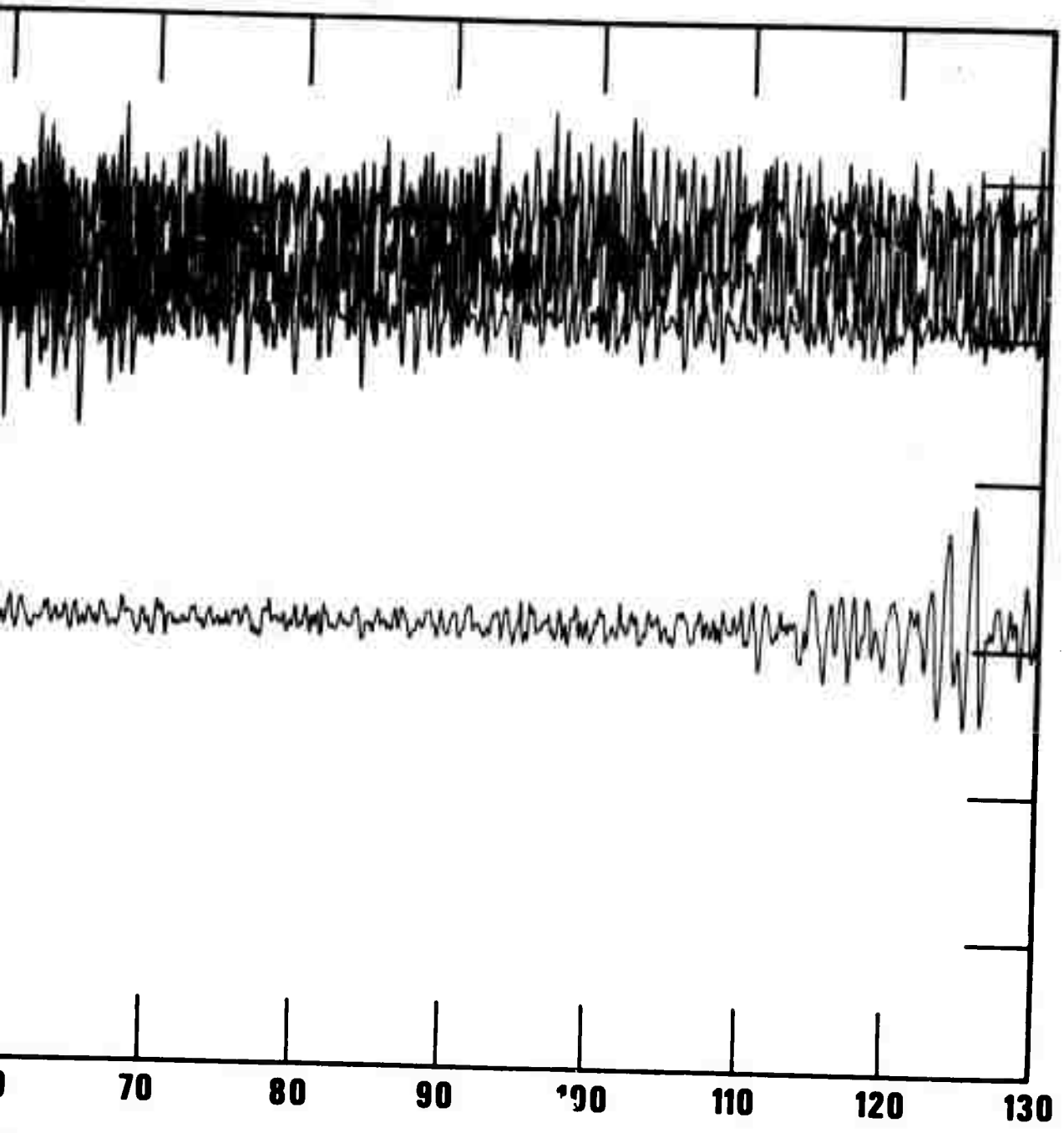

APPENDIX 8. RULISON Seismograms

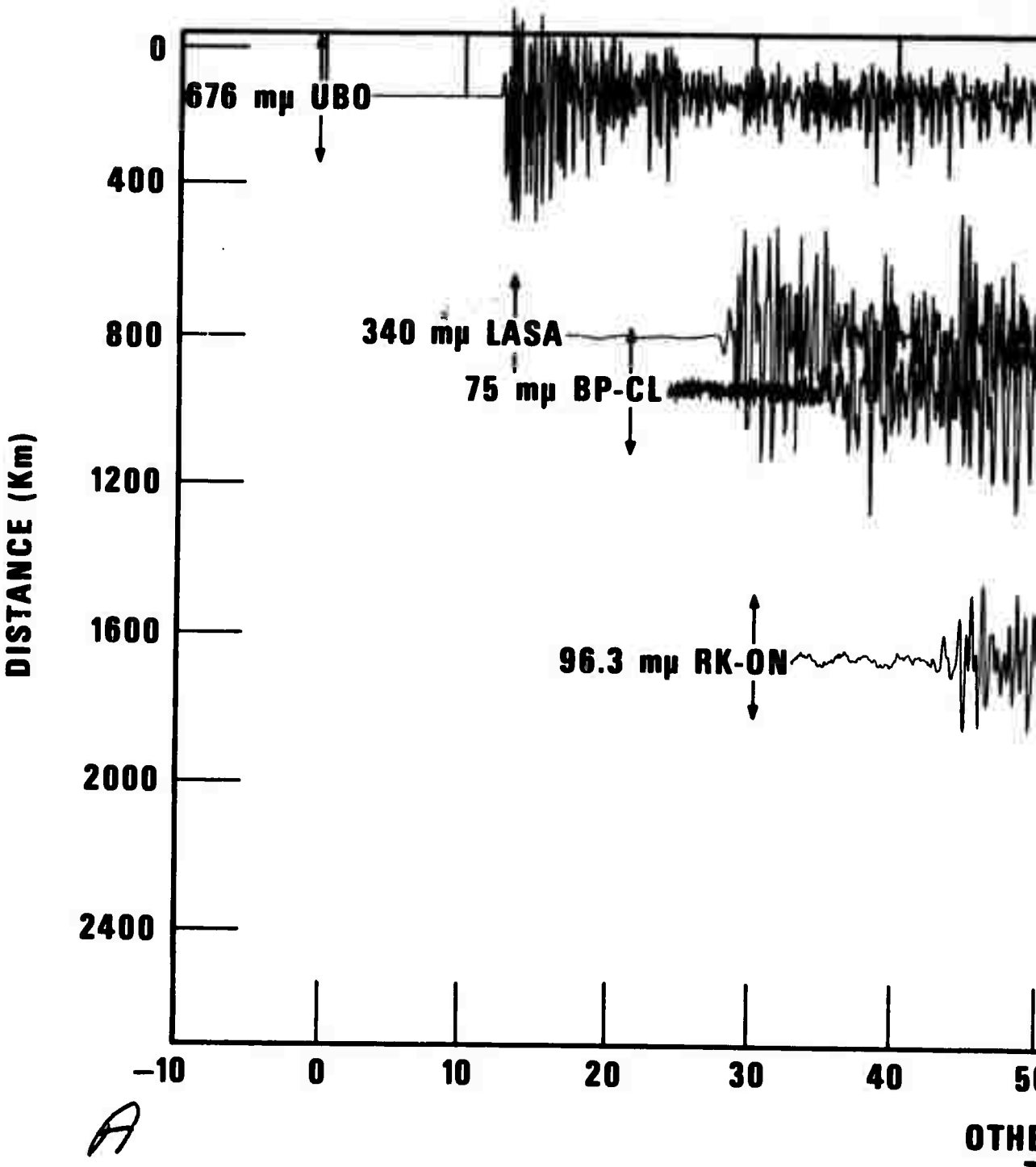
0
400
800
1200
1600
2000
2400
DISTANCE (Km)
676 mμ UBO
340 mμ LASA
75 mμ BP-CL
96.3 mμ RK-ON
−10
0
10
20
30
40
A
OTHE

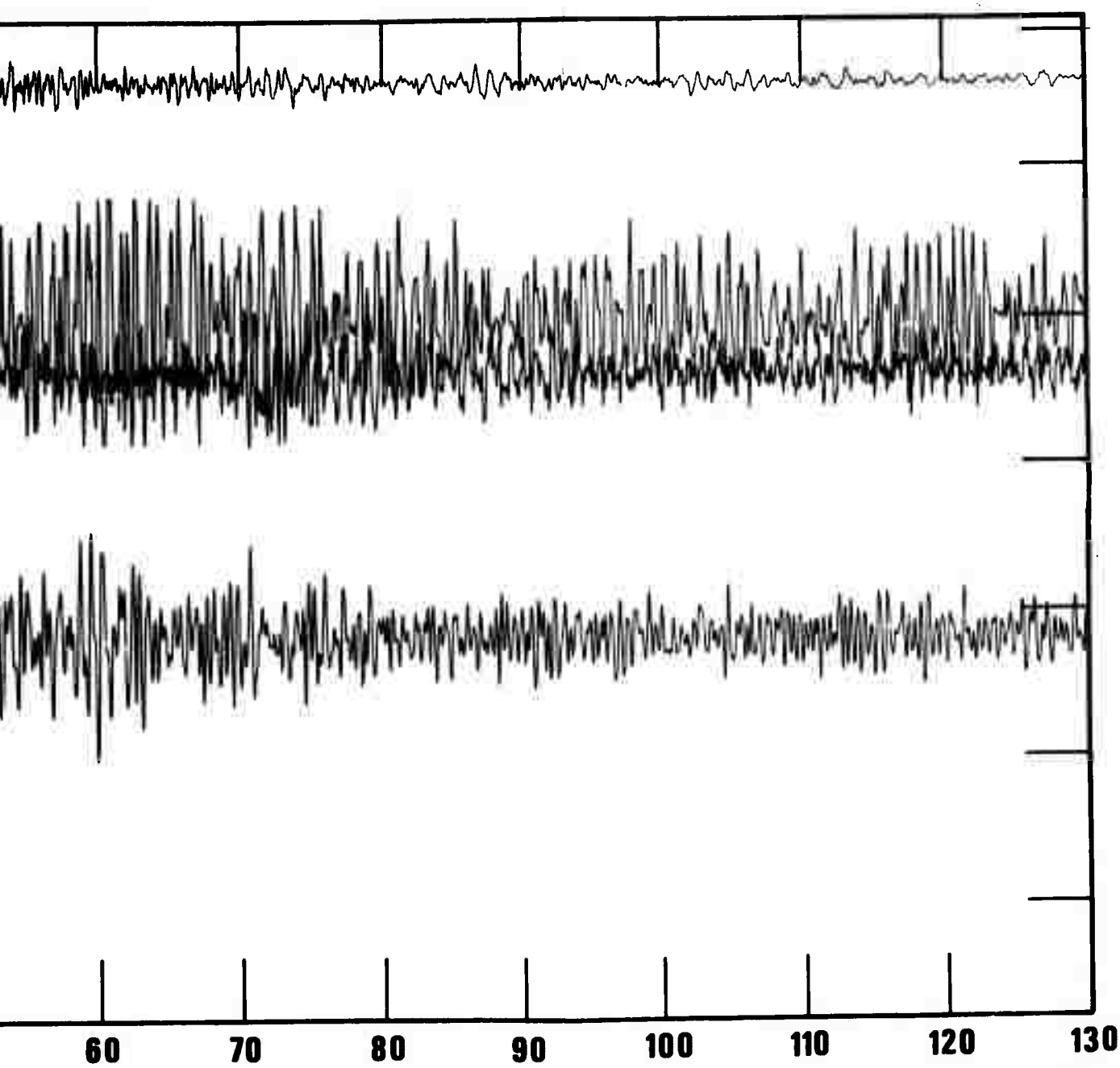

APPENDIX 8. (Cont'd.)

RULISON Seismograms

B

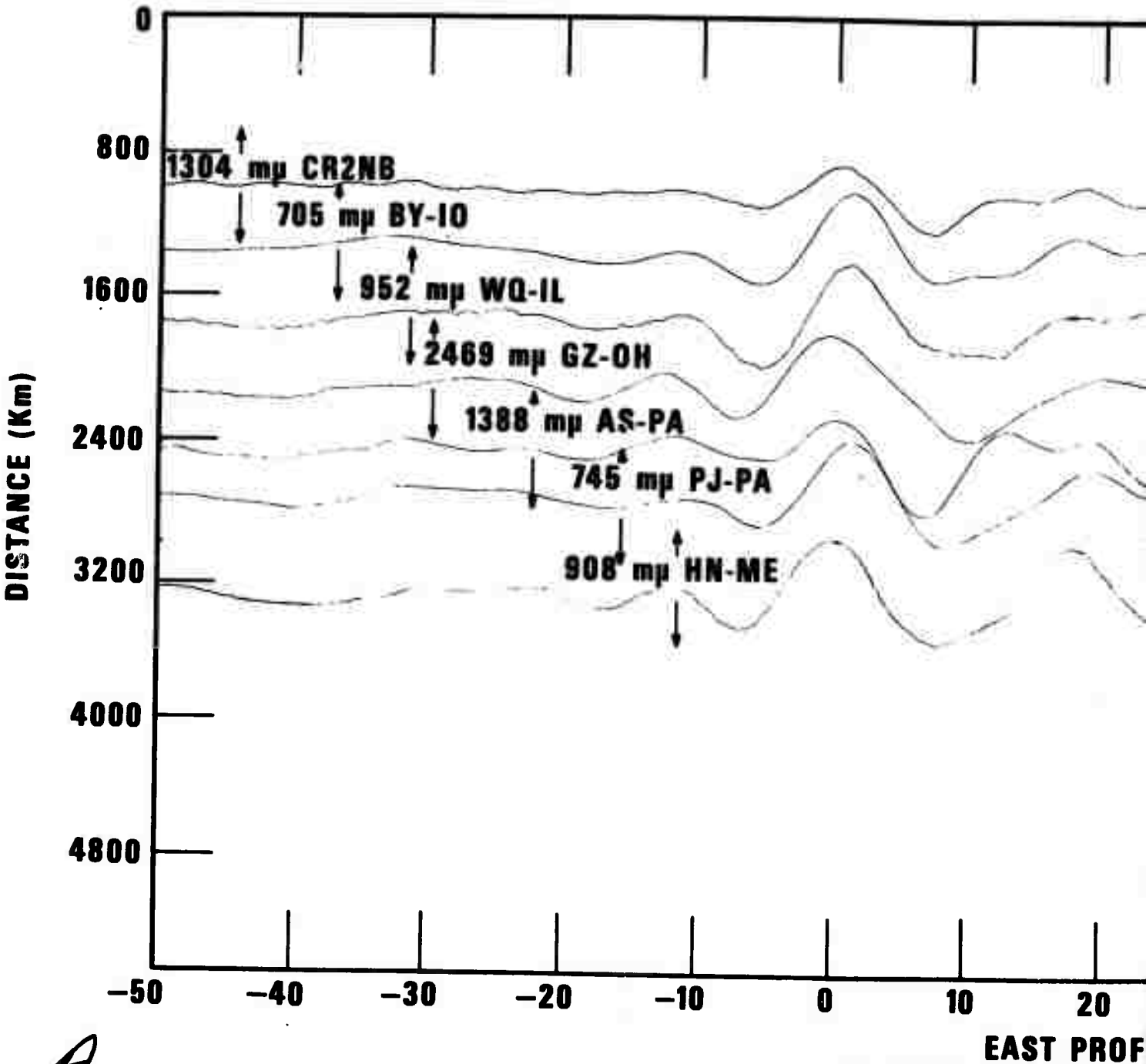
0
800
1600
2400
3200
4000
4800
DISTANCE (Km)
1304 mμ CR2NB
705 mμ BY-IO
952 mμ WQ-IL
2469 mμ GZ-OH
1388 mμ AS-PA
745 mμ PJ-PA
908 mμ HN-ME
−50
−40
−30
−20
−10
0
10
20
A
EAST PROF
RULISON RAYLEIGH W
T−DIST/3.00

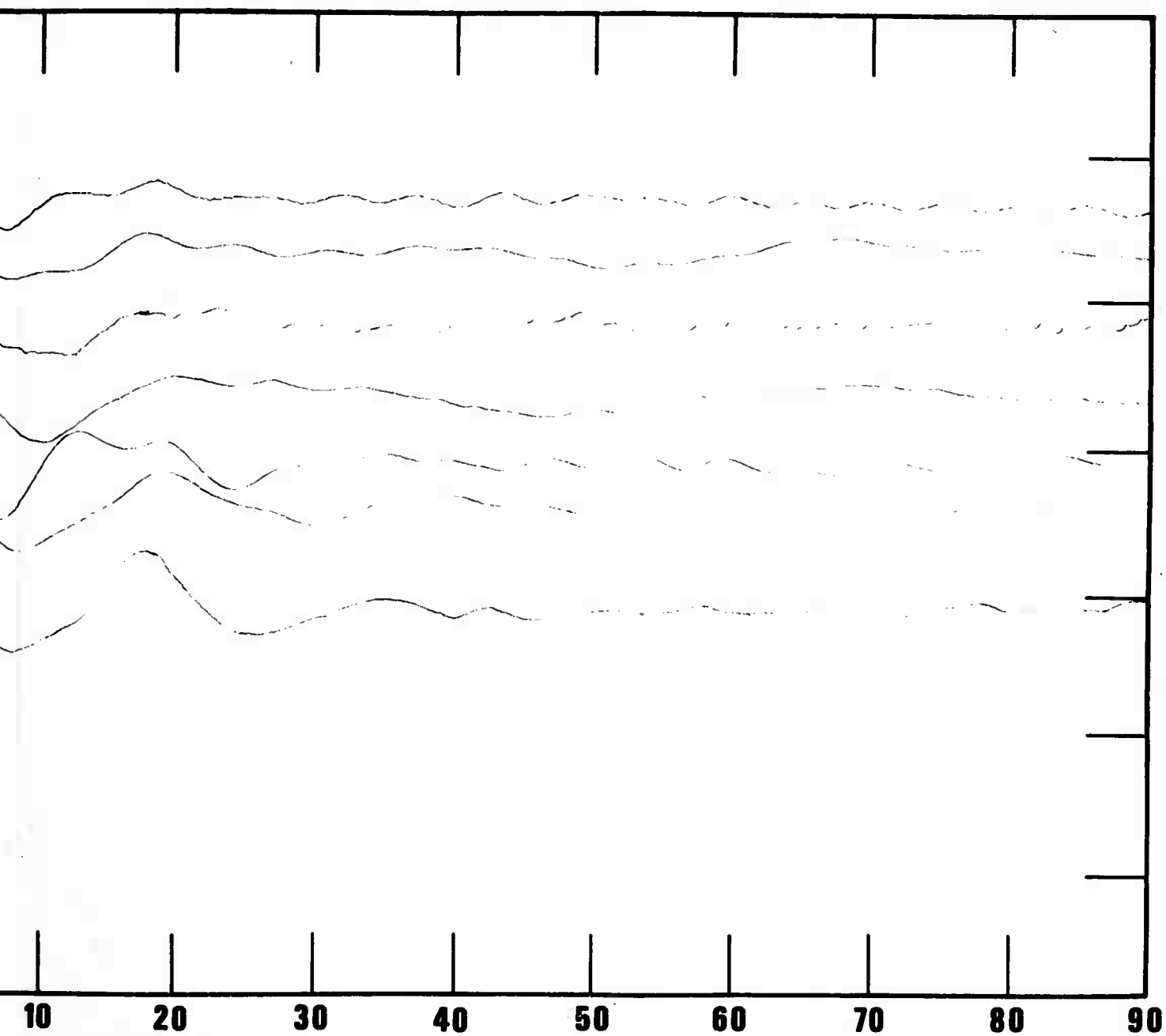

EAST PROFILE
ON RAYLEIGH WAVE PROFILE
T–DIST/3.00 (SEC)

APPENDIX 8. (Cont'd.)

RULISON Seismograms

B

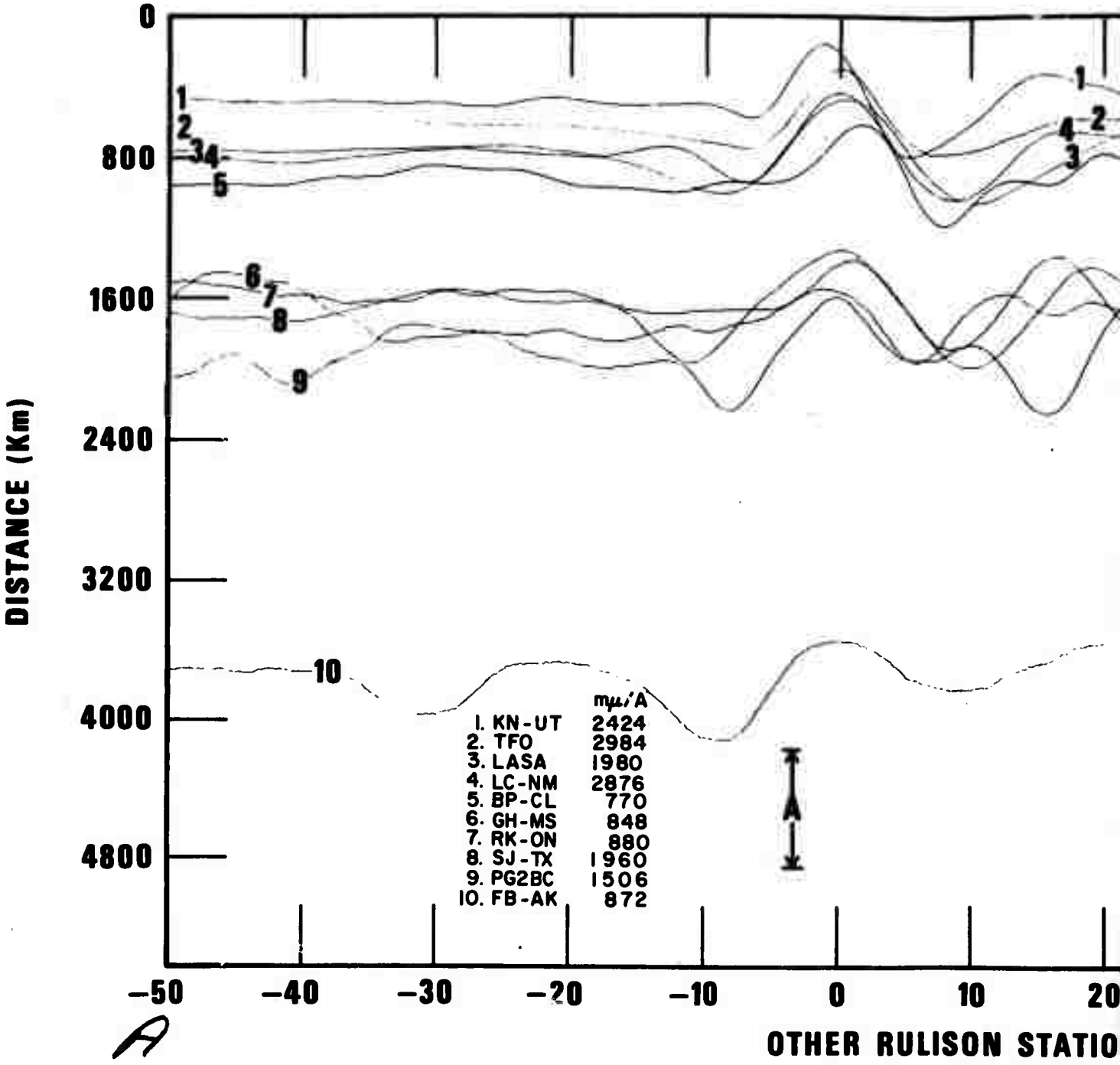
DISTANCE (Km)
0
800
1600
2400
3200
4000
4800
1
2
3
4
5
6
7
8
9
10
mμ/A
1. KN-UT 2424
2. TFO 2984
3. LASA 1980
4. LC-NM 2876
5. BP-CL 770
6. GH-MS 848
7. RK-ON 880
8. SJ-TX 1960
9. PG2BC 1506
10. FB-AK 872
A
−50
−40
−30
−20
−10
0
10
20
A
OTHER RULISON STATIO
T−DIST/3.

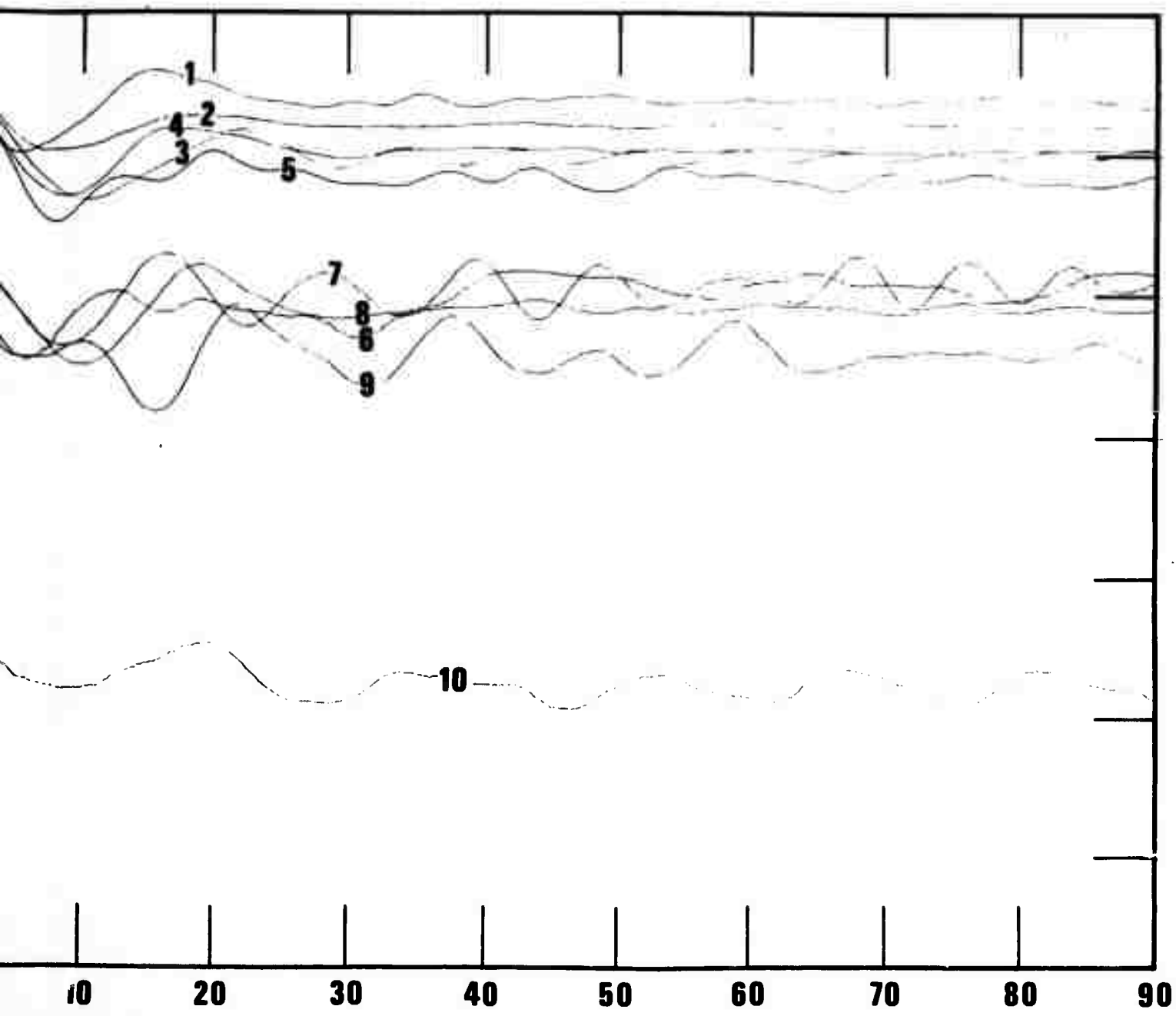

APPENDIX 8. (Cont'd.)

RULISON Seismograms